

COLORING OF FLUORITES AND PROBLEMS
RELATED TO THEIR ORIGIN

by

Rezan Birsoy

New Mexico Bureau
of
Geology and Mineral Resources

Submitted in partial fulfillment
of the requirements for the Degree of
Doctor of Philosophy
in Geoscience

NEW MEXICO INSTITUTE OF MINING AND TECHNOLOGY

Socorro, New Mexico

May 1977

TABLE OF CONTENTS

	Page
ACKNOWLEDGEMENTS	iii
ABSTRACT	iv
LIST OF FIGURES	v
LIST OF TABLES	ix
I. INTRODUCTION	1
I.1. General features of fluorite in terms of lattice and electronic structure	1
I.2. Previous studies and models on coloration of fluorite	4
I.2.1. Studied properties of naturally colored fluorites.	4
I.2.2. Properties of artificially colored fluorites	6
I.2.3. Review of coloration models	14
I.3. Use of the natural coloration of fluorite for geo- logical age determination	21
II. EXPERIMENTAL METHODS	23
II.1. The scope of this study	23
II.2. Sample preparation and instrumentation	25
III. EXPERIMENTAL RESULTS	28
III.1. Experiments on synthetic fluorites	28
III.1.1. Chemical analyses	28
III.1.2. Results of irradiation and absorption spectrum measurements	29
III.1.3. Results of thermal bleaching experiments	43

	Page
III.2. Studies of natural fluorites	48
III.2.1. Geological occurrences of natural fluorites subjected to this study	48
III.2.2. Chemical analyses	51
III.2.3. Absorption spectrum measurements	55
III.3. Transmission electron microscopy (TEM) studies of natural and synthetic fluorites	77
IV. DISCUSSION AND CONCLUSIONS	84
IV.1. Discussion of experimental results	84
IV.1.1. Natural fluorites	84
IV.1.2. Artificially colored synthetic fluorites	87
IV.2. Discussion of the use of the coloration and the 3050A° absorption band of fluorite for geological age dating	92
IV.3. Possible causes of the coloration of fluorites	93
IV.4. Conclusions	103
APPENDIX A	105
REFERENCES	111

ACKNOWLEDGEMENTS

The author wishes to express her sincere thanks and appreciation to her advisor Dr. Richard E. Beane for his guidance and encouragement throughout this study. The help, advice and constructive suggestions of Drs. Lawrence E. Murr and Carl J. Popp are sincerely appreciated.

A special thanks is due to Mr. Dan J. Sasmor of Sandia Laboratories, Albuquerque, New Mexico for his cooperation and for providing the irradiations of synthetic fluorites for this study. Sincere appreciation is extended to Drs. A. W. Laughlin and Glenn R. Waterbury of Los Alamos Scientific Laboratory, Los Alamos, New Mexico who analyzed for Uranium and Yttrium in the samples of this study respectively.

The author would like to thank all her fellow students and her friends, particularly Lisa Cole and Richard L. Naff for help and encouragement, and to Mrs. Pat Valentine for typing the thesis.

In addition, the author wishes to give special thanks to Mrs. Nancy Meyer for her exceptional consideration during this period of intense effort.

Finally the author expresses her appreciation to her husband, Yüksel K. Birsoy for his understanding and encouragement.

ABSTRACT

The present study was conducted to determine the contribution of trivalent ions (rare-earth elements, Yttrium), monovalent sodium and radioactive materials to the coloration of fluorites, to investigate the possibilities of using the 3050A° absorption band for geological age dating, and to establish possible models for coloration. For this purpose, synthetic fluorite and a variety of differently colored natural fluorites were analyzed for the rare earth elements, yttrium, radioactive materials and sodium. Synthetic fluorite samples were irradiated with x-rays, gamma rays, neutrons, electrons, protons and alpha particles at different energy levels. The absorption spectra of the natural fluorites were determined and their resulting colorations and absorption bands compared. The chemical impurities were evaluated and correlated as to their effects on each absorption band of the natural fluorites. Examination of the natural and synthetic fluorites with a transmission electron microscope provided evidence that the coloration of natural fluorites is related mainly to their impurities, while the coloration of synthetic fluorites is governed mainly by radiation-generated lattice defects. Although chemical impurities in the fluorites and the type and intensities of radiation to which they have been exposed were found to play a part in both systems, evidence was also found to dismiss the possible use of color centers of fluorites for geological age dating. Following the detailed investigation and comparison of the various natural and synthetic fluorites and their absorption spectra, proposed models for the coloration of fluorite were described.

LIST OF FIGURES

	Page
1. The structure of the fluorite lattice.	3
2. Schematic band structure along the [100] axis of calcium fluorite.	3
3. 78 K° absorption curves for 0.6 mm thick additively colored sample of calcium fluoride doped with 0.5 mole % Ce.	13
4. Schematic representation of F-aggregate centers. a) M-center. b) Models, in a (100) plane, of F-aggregate centers with D _{2d} point symmetry.	16
5. Optical density at 77 K° of an additively colored calcium fluoride crystal.	16
6. Absorption spectra of blue colored natural fluorite (F-N-2), before, and after heating and x-radiation treatment. F-N-2 sample spectrum without any treatment, a) spectrum after heating the sample to 200°C b) same sample, the spectrum, after irradiating with x-ray.	32
7. Gamma irradiated synthetic fluorites and their absorption spectra.	34
8. Growth of color center concentration of the various absorption bands with radiation dose.	36
9. Absorption spectra of alpha irradiated synthetic fluorites.	37
10. Absorption spectra of proton irradiated synthetic fluorites.	39
11. Absorption spectra of neutron irradiated synthetic fluorites.	41
12. Absorption spectra of the electron irradiated synthetic fluorites. a) Results of absorption spectrum measurements taken by Rao and Bose (1970).	42
13. Absorption spectra and bleaching experiment results of synthetic fluorite F-S-4, after exposure to 5.2 x 10 ⁶ R gamma ray. a) After heating to 100°C. b) After heating to 200°C. c) after heating to 400°C.	44

	Page
14. Absorption spectra of proton irradiated fluorite, F-S-2 (10^{17}H^+ / cm^2 at 250 KV), before and after heating experiments.	46
15. Absorption spectra of alpha irradiated ($10^{18}\text{He}^{+2}/\text{cm}^2$ at 250 KV) and thermally bleached F-S-1 synthetic fluorite.	47
16. Absorption spectra of synthetic fluorite irradiated with neutrons ($7.02 \times 10^{13} \text{ n}/\text{cm}^2$, 3.0 MeV) before and after heating experiments.	49
17. Absorption spectra of the electron irradiated sample, F-S-3, ex- posed to $10^{16} \text{ e}/\text{cm}^2$ at 1.4 MeV.	50
18. Plotting of rare-earth normalize abundances versus atomic numbers of rare-earths.	56
19. Absorption spectra of colorless natural fluorites.	58
20. Absorption spectra of purple colored natural fluorites.	59
21. Absorption spectra of purple-colorless banded natural fluorite.	60
22. Absorption spectra of blue and blue-colorless banded natural fluorites.	61
23. Absorption spectra of green colored natural fluorites.	63
24. Absorption spectra of green colored natural fluorites.	64
25. Absorption spectra of yellow colored natural fluorites	65
26. Absorption spectra of yellow and purple banded natural fluorites.	66
27. Plot showing the relation between color center concentration ($n_c f$) of 3050A° absorption band as a function of La, Ce concentrations in natural fluorites.	69
27a. Enlargement of lower left corner of Fig. 27.	70

	Page
27a. Enlargement of lower left corner of Fig. 27.	70
28. Plot showing the relation between color center concentration ($n_c f$) of 3050A° absorption band as a function of Sm concentration.	71
29. A plot showing the relation between color center concentration ($n_c f$) of the 5600-5900A° absorption band as a function of La, Ce concentrations.	72
30. Plot showing the relation between the color center concentration of the 5600-5900A° absorption bands as a function of Sm concentration.	73
31. Plot of total rare earth element concentration versus the color center concentration ($n_c f$) of 3050A° and 5800A° absorption bands.	75
32a. Plot of sodium concentrations versus the color center concentrations ($n_c f$) of the 3050A° and 5800A° absorption bands.	76a
32b. Plot of the 3900-4700A° absorption band versus Na concentration.	76b
33. Ordered defect aggregates of synthetic fluorite, and their development in (111) plane a) initial bright field electron transmission image of ordered defect aggregates; b) the same area of Fig. 33a, after electron-irradiation saturation; c) magnified portion of Fig. 33b showing the hexagonal arrangement of individual defect aggregates.	78
34. a) Ordered arrangement of defect aggregates in the (111) plane of synthetic fluorite and associated selected-area-electron diffraction pattern after 3 min. exposure. b) Defect aggregates in the (111) plane of synthetic fluorite and associated selected area diffraction pattern, with superlattice diffraction pattern development after electron irradiation saturation has been reached.	80

35. (111) plane of purple colored natural fluorite a) Dislocation loops with defect aggregate mosaic structures in the background with associated selected area diffraction patterns, loops lying along [110] direction. b) The same dislocation loops with hexagonal arrangement of defect aggregates after an addition of 5 min. of exposure. 81
36. a) Initial bright field electron transmission image of hexagonal defect aggregates of purple colored natural fluorites. b) Approximately the same area of Fig. 36a after 5 additional minutes of exposure. c) Fig. 36b, after 5 min. more exposure; defect aggregates which reached electron-irradiation saturation are associated with a selected-area diffraction pattern. 83
37. a) Color center model for the 3050Å absorption band of natural fluorites. Region I has tetragonal symmetry in which the compensating ion is local. Region II has cubic symmetry and the compensating ion is remote. b) Color center model for the visible region absorption and at 5600-5900Å. 96
38. a) Color center model for 5400-5500Å absorption bands, on the (100) plane in natural fluorite. b) Color center model for 3750-4750Å absorption band on the same plane. 99
39. a) Color center model for the 3800Å absorption band; the synthetic fluorites are mainly aggregates of F-centers, and have little contribution from impurities. b) Color center models of the 5450Å absorption band (region I), the 5030Å absorption band (region II) and the 3240Å absorption band (region III). 102

LIST OF TABLES

	Page
1. EPR and optical measurements of fluorites.	7
2. Coloration of synthetic fluorites obtained after different radiation and/or energy and flux	30
3. Geological features of fluorites used in this study.	52
4. Approximate locations and Munsell color designations of natural fluorites.	53
5. Analyses of rare-earth elements, Y, Na, Th and U which present in natural fluorites.	54

CHAPTER I

INTRODUCTION

Fluorite, one of the gangue minerals, found abundantly in hydrothermal ore deposits, has many industrial purposes. It is used in the production of fluorine chemicals such as hydrofluoric acid, as a flux in the production of steel, and in enamels and opaque and opalescent glass. It also has a use in optical instrumentation. Because it readily accepts rare-earth dopants, and because traces of rare-earth metal ions can efficiently change ultraviolet radiation into visible radiation, fluorite became one of the more convenient anhydrous hosts. After the discovery of the solid state laser, fluorite was one of the first materials intensively examined for possible use in the new lasers. For a while it was important as a laser material, but in time more convenient materials were found. However, spectroscopic studies of fluorites have been continued in terms of their defects, color centers and impurities. Defects, color centers and impurities of fluorite present a challenging theoretical problem for solid state physicists; fluorite studies may help to provide answers to many unsolved problems in geology such as age determination, and help further the metallurgists understanding of defect structures in natural minerals.

I.1. General features of fluorite in terms of lattice and electronic structure

Calcium fluoride is a RX_2 compound in which R is a calcium ion and X is a fluorine ion. Each ion of calcium is surrounded by eight

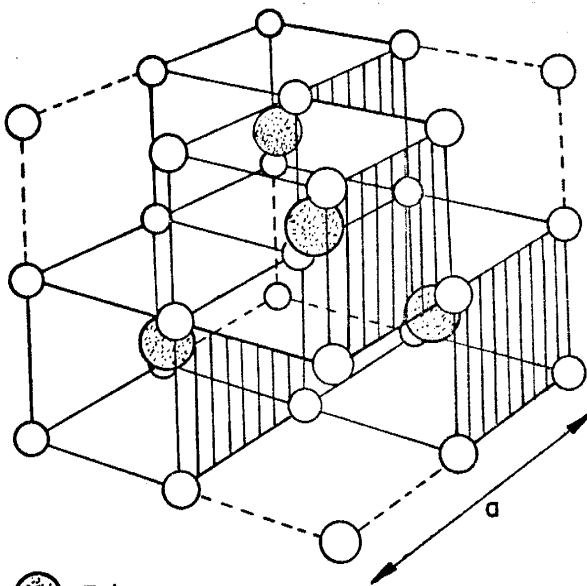
equivalent nearest neighbour fluorine ions forming the corners of a cube containing calcium at the center. Each fluorine ion is surrounded by a tetrahedron of four equivalent calcium ions. The structure has a face centered cubic translation group and space lattice symmetry of O_h^5 (Fig. 1). It comprises three inter-penetrating face-centered cubic lattices. The first lattice is the cube of side a ; calcium is originated at point $(0,0,0)$ with primitive translational vectors of $(0, 1/2 a, 1/2 a)$, $(1/2 a, 0, 1/2 a)$, $(1/2 a, 1/2 a, 0)$. Fluorine ions are located on two further lattices with similar translational vectors but with origins at $(1/4 a, 1/4 a, 1/4 a)$ and at $(3/4 a, 3/4 a, 3/4 a)$. The site of the calcium ion has O_h symmetry and the site of the fluorine ion has T_d symmetry. Interstitial sites also have O_h symmetry. Therefore the calcium ion has a coordination number of eight and the fluorine ion has a coordination number of four. The crystal radius of calcium is $0.95A^\circ$ and that of fluorine is $1.33A^\circ$.



There has been no systematic study of the bonding character of fluorite, but Phillips (1970) suggested that calcium fluoride has a large forbidden energy gap between the valence and the conduction bands, and thus bonding should be ionic in character. With a melting point of $1360^\circ C$ and heat of formation of -286.26 Kcal/mole, the calcium fluorite structure has a considerable thermal stability which is in keeping with its ionic character.

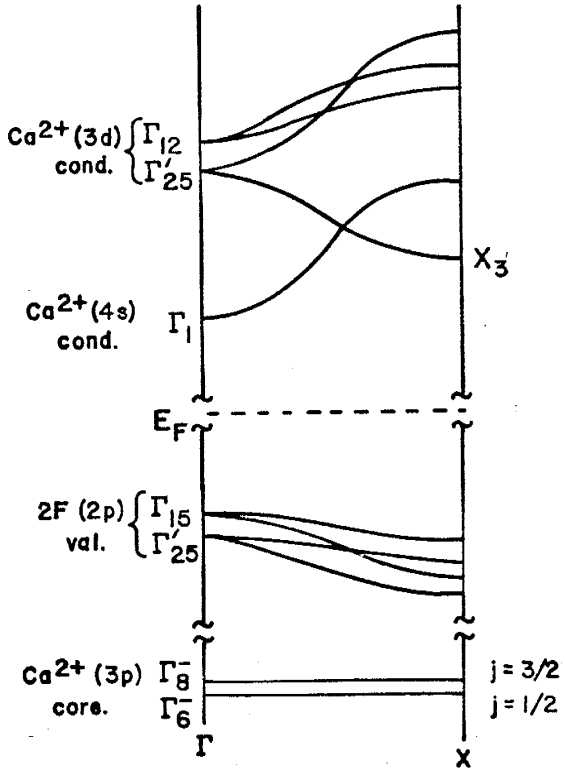
A detailed study of the electronic energy band structure of a solid requires a high degree of chemical purity and crystalline perfection. Because producing such a calcium fluoride is presently very difficult, no detailed calculations of the energy levels of the crystal have been

Fig. 1. The structure of the fluorite lattice a is the lattice parameter of the conventional cubic unit cell. For clarity the fluorine ions are drawn smaller than the Ca ions (After, Hayes, W., 1974).

Fig. 2. Schematic band structure along the $[100]$ axis of a CaF_2 (After, Rubloff, 1972).



 R ion
 X ion



made. However, Rubloff (1972) explains that in order to form the ionic solid, electrons are transferred from the s states of the metal ion (calcium) to the p states of the fluoride ion. This process gives positive (calcium) and negative (fluoride) ions, each having completely filled p states as their outermost electron shells. Then, electrons from the top of the valence bands, which are the filled p states of the fluoride ions, are excited to the bottom of the conduction band. Below the valence bands, the p core bands from the calcium ions are flat. The excited states of the calcium ions form the basis for a set of conduction bands. The excited d states of the calcium ion are very close to the energy of the s states, and therefore originate a second set of conduction bands in the crystal. The schematic band structure of calcium fluoride is illustrated in Fig. 2.

I.2. Previous studies and models on coloration of fluorite

I.2.1. Studied properties of naturally colored fluorites

Natural fluorites exhibit a variety of colors from deposit to deposit, and often within a single deposit (e.g. both blue and green colored fluorites are found in the same deposit in Hansonburg, N.M.). Even some single fluorite crystals show color bands (green-purple-white banded fluorites of Gila, N.M.). The nature of this coloration has attracted the attention of many scientists.

Colored natural fluorites are not desirable for optical instrumentation. Even if they are flawless, their coloring and display of ultraviolet and visible region absorption bands render them unsuitable for optical instrumentation. An early decoloration experiment of

natural fluorite was conducted by Herman and Silverman (1947). They demonstrated that the purple colored fluorite showed 5800Å, 3950Å and 3350Å absorption bands which, upon heating to 300°C, were reduced to one broad absorption band at about 4300Å, while the color changed to amber. However when the discolored fluorite was irradiated with 150 kV x-rays, it regained its original purple color. They recommended that if the fluorite is flawless but colored it can be decolorized and used for optical instrumentation.

Since then, physical and chemical properties of colored natural fluorites have been studied by many scientists to determine what causes color variation. Various colored fluorites show no difference in unit cell dimensions (Allen, 1952) indicating that coloration is not related with unit cell dimensions. Fluorites with principal light absorption at long wave lengths are characterized by abnormally low refractive indices, while those with principal absorption at short wavelengths are characterized by abnormally high refractive indices (Allen, 1952). Heating the Blue John's fluorite (purple) at constant rate causes the position of the major absorption band (initially at 5730Å) to shift to shorter wavelengths (Braithwaite et al, 1973). At temperatures above 300°C, the color is increasingly bleached (Berman, 1957; Braithwaite et al, 1973). Also upon heating, thermal expansion results in a decrease in specific gravity accompanied by an increase in index of refraction (Berman, 1957). Irradiation of natural fluorites with x-rays can produce color changes or much stronger coloration, but does not change the index of refraction (Allen, 1952). Variations of the composition of natural fluorites have not been related to color

variations in any way (Allen, 1952; Berman, 1957; and Braithwaite et al., 1973).

Studies of naturally colored red, yellow and green fluorites in terms of electron paramagnetic resonance (EPR) and optical measurements by spectrophotometry have been carried out by Bill et al. (1967). The corresponding results are given in Table 1.

Under the transmission electron microscope naturally colored and uncolored fluorites show a development of aggregates of color centers (color center is any unit in the crystal structure which causes the absorption of light) (Murr, 1973). Colored samples exhibit a mosaic contrast feature which intensifies and develops with increasing exposure to the electron beam. The associated selected area electron diffraction patterns contain regular super lattice refractions in addition to the (111) surface orientation of CaF_2 refractions. With long enough exposure to electrons the regular defect structures grow to form defect aggregates which are small hexagonal aggregates associated with a single (111) plane (Murr, 1974a).

I.2.2. Properties of artificially colored fluorites

Investigation of naturally colored fluorites to obtain a better understanding of the mechanism of coloration was difficult and caused much disagreement among investigators. Their study was hindered by the large number of variables involved. Fluorites contain many different organic and inorganic impurities including various amounts of radioactive materials, because they are crystallized under a diversity of thermodynamic conditions depending upon different geological settings.

Table 1. EPR and optical measurements of fluorites (after Bill et al., 1967)

No. of group	Colour	Origin	Treatment	EPR results	Optical Results (Wavelengths in μ)
1	red	Goescheneralp, Juchli, Grimsel, Grimselschollen +6 different crystals of unknown origin in Switzerland.	None X irradiated at room temp.	R center, sometimes Gd^{3+} in tetragonal symmetry. ^{a, b, e}	483/272/263. Often some weak suppl. lines in IR and UV. The above absorptions together with four new bands ^e at 570/400/330/225.
2	green-violet	Weardale.	Bleached	R center disappears also Gd^{3+} .	Absorption at 483 and the four bands at 570/400/330/225 disappear.
3	pale green	Dürschrennenhöhle am Säntis.	None	$Eu^{2+}Gd^{3+}$ in cubic symmetry ^d (about 90% of Gd^{3+}) and Gd^{3+} in tetrag. symmetry (about 10%). Concentration of both elements in the order of 0.01%.	690/609/440/442/353/333/305.2/277/255/217: intensity of absorption growing with diminishing wavelength in UV.
				Gd^{3+7} in cubic and in tetragonal symmetry (about same intensity of both spectra).	690/605/442/422/360/305/281/258: intensity of absorption growing with diminishing wavelength in UV.

Table 1. (Continued).

No. of group	Colour	Origin	Treatment	EPR results	Optical Results (Wavelengths in μ)
4	yellow	Cavin Rock, Wölsendorf, Puy de Dôme, Baslerjura	None	Yellow center; Gd^{3+} in cubic symmetry in very varying concentration ($<0.01\%$).	433/294
			Bleached	Yellow center destroyed irreversibly; most of the Gd^{2+} resonance disappears.	Absorption at 433 has disappeared irreversibly.
Artificial	green	$CaF_2:SmF_3$ (0.01%)	Bleached and X-rayed at room temperature	V_F center ^f appears, center not stable at room temperature	Crystal is colored blue, color not stable at room temperature
			X irradiated		680/610/440/422/396/355/305.5/281/255/240/(218)
			Hydrolysed and X irradiated		691/612/440/370/355/305.5/:strong absorption in UV, intensity growing with diminishing wavelength.

EPR measurements all at X-band. When not otherwise stated results given were measured at room temperature.

^aBill, Lacroix (1966)

^bBaker, Bleaney and Hayes (1958)

^cO'Connor, Chen (1963)

^dSierro (1963)

^fSierro (1965)

However, methods have been discovered for coloring the crystal artificially, thereby decreasing the number of unknown variables.

Early studies by Molwo (1934) produced color in fluorites by introducing electrons from a pointed cathode at 1500°C; Kellerman (1937) produced yellow coloration by radium irradiation at low temperatures; Doelter and Leitmeir (1931) used cathode rays, and Cork (1942) colored with deuteron bombardment. Wohler and Kasornowski (Doelter and Leitmeir, 1931) achieved a stable coloration using an additive coloration technique in which fluorite was heated with calcium vapor (in Allen, 1952). But these early investigators all used natural fluorites, and thus compositional variables were still present. But by 1950, techniques for growing relatively pure synthetic fluorite were developed for commercial use (Stockbarger, 1949).

Radiation effects

Color production in fluorites by hard x-radiation (200 kV, 10 mA) was first carried out by Smakula (1950) with 0.5 to 1 cm thick synthetic and natural fluorites. The crystals exhibited three absorption bands at 5800Å°, 6000Å° and 3350Å°, and showed color saturation with increasing exposure time; these same absorption bands were observed after irradiation at 40 kVP and 15 mA. When the crystals were heated with NaF at 1200°C and irradiated with x-rays, four absorption bands developed with even more intensity than the sample which was only x-ray irradiated (Schulman et al, 1952); 3300Å° and 3800Å° absorption bands were also developed. Exposure to 90 kV, 3 mA x-rays produced four absorption bands, but these were affected very little by visible light at room temperature (Barile, 1952), and they bleached after thermal treatment

(Barile, 1952; Smakula, 1953).

The x-ray induced four band spectrum can be bleached by light. For example, while 5800Å light does not effect any absorption band, 4000Å light decreases the intensity of the 4000Å band, creating a new one at 4850Å. Heat and light will restore these bleached absorption bands (Smakula, 1953). 40 kV, 20 mA x-radiation and the introduction of $8.8 \cdot 10^7$ flux neutrons produced practically the same four band absorption spectrum, although the neutrons caused more intense coloration and there was some shifting of the spectrum toward a longer wavelength (Bontinck, 1958). X-radiation produced a four band absorption spectrum (bands are at 2250Å, 3350Å, 4000Å and 5800Å), while strong additive coloration with subsequent quenching (Luty, 1953; in Messner and Smakula, 1960) and additive coloration at 700°C with Ca vapor generated only a two band spectrum at 3750Å and 5250Å. After irradiation with light of 3750Å, the 3750Å and 5250Å bands decreased slightly and at the same time a slight growth of a band at 2200Å and in the visible region was observed (Bontinck, 1958).

Irradiation of pure fluorite with high energy electrons (2.5 MeV) (Scouler and Smakula, 1960) and with both x-rays (150 kV) and high energy electrons (2.5 MeV) (Messner and Smakula, 1960) resulted in bands at 2250Å, 3350Å, 4000Å and 5800Å which increased in intensity with decreasing temperature during irradiation. However, when YF₃-doped fluorite (fluorite grown with YF₃ impurities) was irradiated with the same source at room temperature, the same absorption bands appeared with intensities which varied with concentrations of Yttrium in the fluorite. NaF-doped fluorite showed even more drastic changes when

irradiated under the same conditions; the resulting bands were at 3300A°, 3850A° and 6050A° and their intensity increased with a decrease in temperature during irradiation (Scouler and Smakula, 1960).

Synthetic fluorites from the Harshaw chemical company were found to contain impurities, especially Yttrium (O'Connor and Chen, 1963; Sashital and Vedam, 1973; Rao and Bose, 1970). When Harshaw fluorites and other synthetic fluorites of higher purity were irradiated with 5×10^6 rad of 2.5 MeV electrons at room temperature the pure fluorites exhibited absorption bands at 2250A°, 3350A°, 4000A° and 5800A°, while the Harshaw fluorites produced more intense bands at the same positions (O'Connor and Chen, 1973). After gamma irradiation, Yttrium-doped fluorites revealed that the intensity of the absorption bands in the visible region is roughly proportional to the Yttrium concentration (Theissing et al, 1969). Two pieces of the same single crystal (not Harshaw fluorite) were irradiated, one with x-rays and the other with low energy electrons (10 kV) at room temperature. The electrons did not produce any coloration, while the x-rays produced the usual four band spectrum (Rao and Bose, 1970). When temperatures during the electron irradiation were increased to the 100°C-400°C range, the produced coloration yielded absorption bands at 3780A° and 5600A°. Studies of the growth of color centers and the accompanying changes in the mechanical properties (flow stress, Vicker's micro hardness and dislocation mobilities) after gamma radiation at room temperature indicate that the 3350A° band (color center concentration of the 3350A° absorption band) shows a different growth trend than the 2250, 4000 and 5800A° absorption bands. These mechanical properties also increase

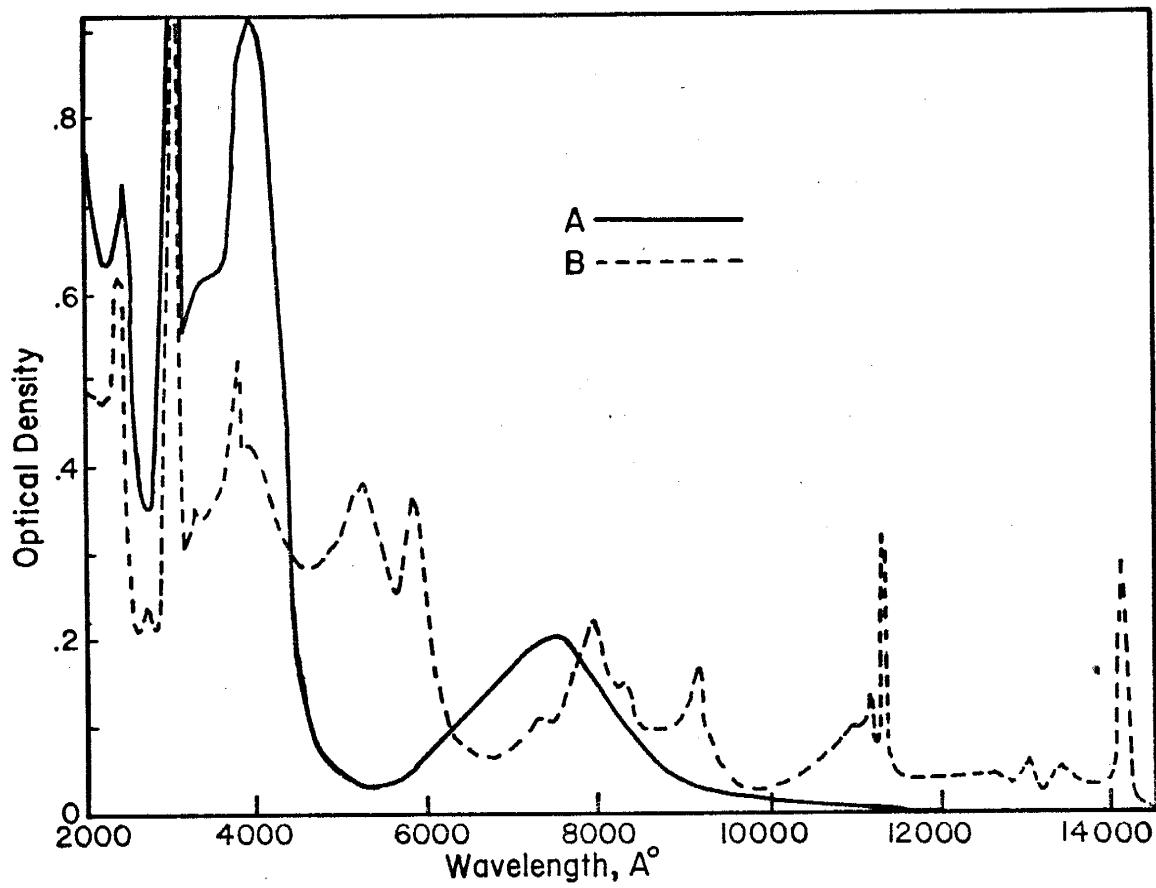
with increasing gamma radiation dose up to a level of 9×10^5 R. Flow stress and the 3350\AA band follow the same trend with increasing dosage (Sashital and Vedam, 1973).

X-irradiated fluorites exhibit a 4000\AA absorption band, and additively colored fluorites (Heating the fluorite with Ca vapor at a definite temperature) exhibit a 3750\AA band. Harshaw fluorite irradiated with 3 MeV electrons at Liquid Helium temperature gave results similar to additive coloration, with a band at 3750\AA (Kamikawa et al, 1966). Ratnam (1966) also produced the 3750\AA band with x-radiation at temperatures ranging between 180°C and 250°C .

Compositional effects

The study of color centers in fluorite has been complicated by the presence of impurities (Scouler and Smakula, 1960; O'Connor and Chen, 1963). Staebler and Kiss (1969) noted that photo reversible absorption changes had been found in La, Ce, Gd, or Tb doped fluorite after additive coloration with Ca vapor. Additive coloration of Ce doped fluorite resulted in a four band spectrum (2250 , 3000 , 4000 , and 7400\AA absorption bands) similar to that of Yttrium doped fluorite, and was thermally stable (Fig. 3, curve A); but when this fluorite was irradiated with ultraviolet light (3100 - 4000\AA) at room temperature it gave another spectrum (Fig. 3, curve B) which, either within a few days at room temperature, or as a result of optical absorption by the visible bands of curve B, reversed to curve A. Staebler and Schnalterly (1971) studied the La, Ce, Gd, Tb, Lu and Y doped fluorites observing that the impurity associated color centers which had undergone photo ionization by ultraviolet light lead to reversible color changes; thus the material is photochromic.

Fig. 3. 78K° absorption curves for 0.6 mm thick additively colored sample of CaF₂ doped with 0.5 mole % Ce. (A) Thermally stable state (B) After UV (3100-4000Å) irradiation at 300 K° (After, Staebler and Kiss, 1969).



I.2.3. Review of coloration models

A good understanding of the origin of coloration of fluorite was not achieved until fairly recently, when the technology for growing considerably pure or desirable composition fluorites, along with the delicate instrumentation for analyzing them, was developed. With these developments the study of coloration theory has become much more clearly and scientifically directed.

Allen (1952) gives a concise and comprehensive summary of the models of the coloration of natural fluorites. As early as 1866, Wyruboff was an advocate of organic coloring theory, but by and large most studies were done after the turn of the century. Blount and Sequeira (1919), and Garnett (1920) and Morrison (1935) demonstrated the presence of hydrocarbons and bituminous impurities in fluorites, respectively. Prziham (1938) suggested that bivalent europium and samarium caused coloration, but Yoshimira (1933), Eysank (1936) and Mukherjee (1948) did not agree. The colloidal calcium theory was reported by Poelter (1925), Göbel (1931) and Yoshimura (1933), while Pohl (1936) interpreted the coloration as being caused by F-centers similar to those developed in the alkaline halides. Finally, Prziham (1947) cited radioactive material in the fluorite as a cause of coloration.

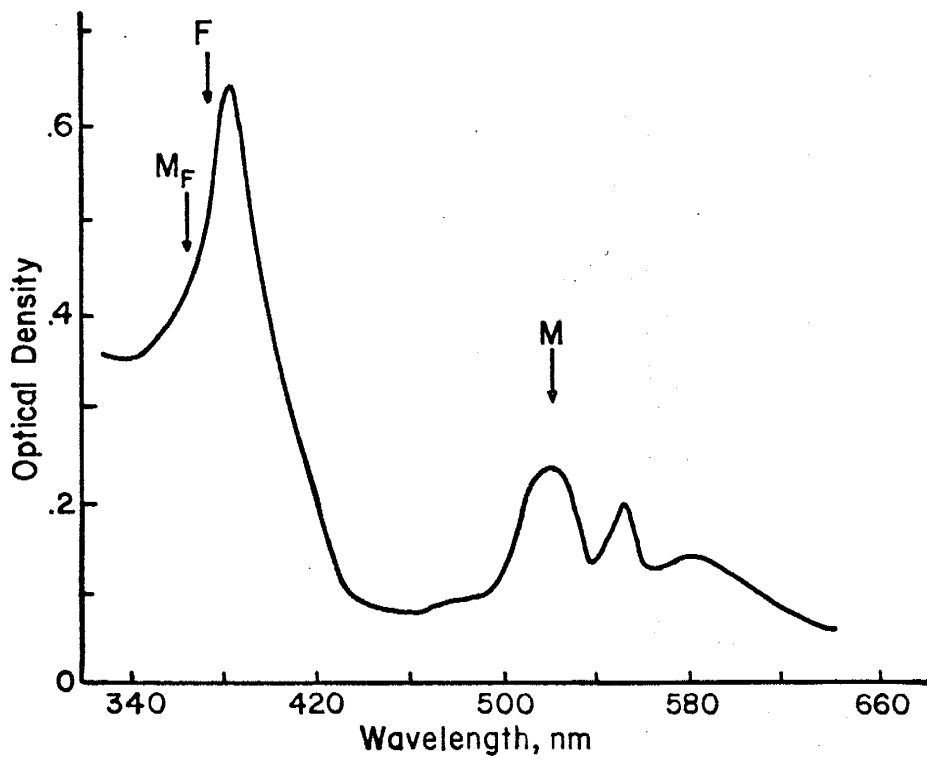
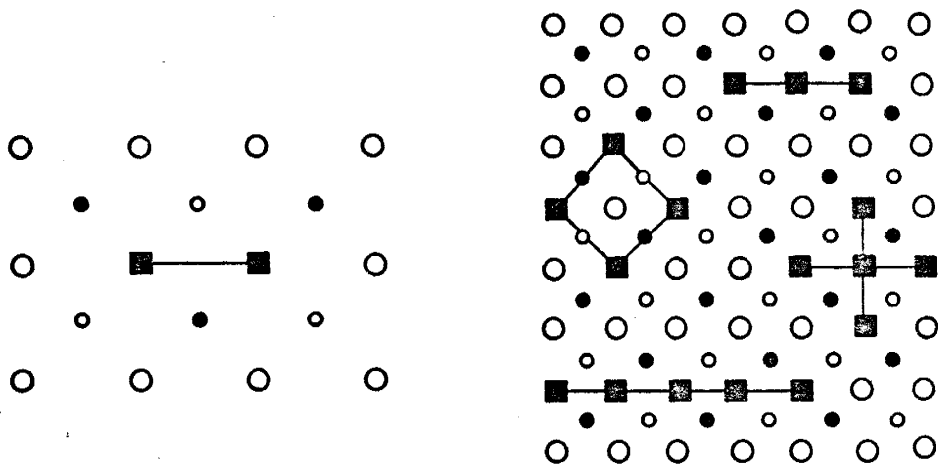
Early investigators using the synthetic fluorites thought the entire spectrum and the consequent coloration were a result of electrons trapped at the lattice defects (Smakula, 1950). Later, portions of the spectrum were attributed to simple color centers. The 5250Å band

(Bontinck, 1958), 3750Å band (Arends, 1964; Kamikawa et al., 1966; Görlich et al., 1968; Beaumont and Hayes, 1969) and 3800Å to 4050Å bands (Allen, 1952) have been attributed to electrons trapped in a fluorine ion vacancy (F-center). However, the F-center (3750Å band) cannot be produced by x-radiation at room temperature or, if produced it reverts to another type of center (Kamikawa et al., 1966). Thus Kamikawa et al. (1966) propose that either a large number of anion vacancies (lattice sites which are evacuated) or low temperatures (where trapped electrons are stable) would be needed to produce the F-center (3750Å band). A clearer explanation of the creation of the F-center at low temperatures by x-rays is given by Görlich et al. (1968), who show that the 3750Å band cannot be impurity related because the crystal that produced it was pure. They note that Frenkel defects, i.e. anion vacancies and interstitial fluoride ions, occur in equal numbers, are always present in the fluorite structure, and new ones are generated by coloration processes. At temperatures lower than room temperature, the interstitial ions are not sufficiently mobile to join with the anion vacancies, so they are free to be able to trap electrons.

Aggregation of F-centers has been suggested by Arends (1964) as a mechanism of coloration. He proposed that the 6700Å band is created by a combination of the two F-centers (so called M-center). However, Beaumont and Hayes (1969) identified the 5200Å band as an M-center which is composed of two nearest neighbor F-centers and aligned along $\langle 100 \rangle$ (Fig. 4.a). The 5210Å band is due predominantly to absorption of the M-center; the absorption is associated with impurities (Hayes et al., 1970) (Fig. 5). Higher degrees of F aggregate centers have

Fig. 4. Schematic representation of F-aggregate centers. a) M center (5200Å band): After, Beaumont and Hayes, 1969. b) Models, in a (100) plane, of F aggregate centers with D_{2d} point symmetry. ○ fluorine ion, ■ F centers, ● calcium above plane of paper, ○ calcium below plane of paper (After, Beaumont et al., 1972).

Fig. 5. Optical density at 77 K of an additively colored CaF_2 crystal (After, Hayes et al., 1970).



also been suggested (Fig. 4). The R-center is composed of three nearest neighbor F-centers aligned along $\langle 100 \rangle$; other F aggregate centers have four and five center configurations with D_{2d} point symmetry (Beaumont et al., 1972a; Beaumont et al., 1972b). Roach and Senff (1974) reported that the four band spectrum represents one sort of center, and high symmetry of the centers indicates an aggregate of four F-centers in the tetrahedral configuration. The creation of large F-center aggregates with a hexagonal configuration has been directly observed using transmission electron microscopy (Murr, 1974a). F-aggregate equilibrium arrays forming void lattices have been characterized in natural fluorite irradiated in the electron microscope (Murr, 1974b, 1976).

Colloidal calcium in the natural fluorite crystal has also been reported as an agent of coloration. 5750\AA and 6500\AA absorption bands are thought to be caused by colloidal calcium (Allen, 1952) trapped in the lattice defects along (111) planes and through [001] growth zones (Braithwaite et al., 1973).

Hayes and Twidell (1962) found that in the system of $\text{CaF}_2:\text{Tm}$, Thullium traps electrons after x-irradiation at room temperature or 80°K ; in addition, self trapped holes $[\text{F}_2^-]$ are also produced, causing an absorption band at 3500\AA . The ionizing x-radiation generates electrons and holes which can migrate to create F° atoms neighboring the fluorine interstitial ions, leading to the formation of the $[\text{F}_2^-]$ molecular ion. Thus the 3350\AA band was attributed to self trapped holes $[\text{F}_2^-]$ (Sashital and Vedam, 1973).

The relationship between coloration of fluorite and its impurities

has long been recognized. Bill et al. (1967) proposed that red coloration of natural fluorites is the result of an R-center (an R-center is defined as an association of an Yttrium ion with two oxygen ions existing as an impurity and ionized in course of time by natural radiation). Shulmann et al. (1952) observed an enhancement of coloration of fluorite doped with monovalent ions. They attributed the 2000Å° and 2200Å° absorption bands to diffusion of oxygen ions into the bulk of the crystal, forming Frenkel defects (Bontinck, 1958). The 6000Å° absorption band has been related to Na⁺ and K⁺ impurities (Arends, 1964). Scouler and Smakula (1960) suggest, however, that the absorption bands originate from defect complexes of Yttrium, Oxygen and Na impurities, and along lattice defects such as anion and cation vacancies and interstitials. Experiments by Messner and Smakula (1960) showed that the 4000Å° absorption band was enhanced by YF₃ addition into the fluorite and related to neutral interstitial fluorine atoms. They traced the 3350Å° absorption band to electrons bound to calcium interstitials and the 2200Å° band to holes bound to Ca⁺² vacancies.

Yttrium (which has chemical behavior very similar to that of the rare-earth elements) and rare-earth elements substituting in the crystal structure of fluorite have been intensively studied in relation to their effects on coloration. Natural fluorites contain rare-earth elements, and even "pure" synthetic fluorites contain Yttrium. O'Connor and Chen (1963) suggested that because synthetic fluorite contains Yttrium impurities, the observed coloration is a result of the reduction of Y⁺³; they also reported that this reduction is suppressed by the presence of electron traps such as Sm⁺³. X-ray irradiation at room temperature

converts the trivalent Yttrium to divalent Yttrium during the coloration process. Thus they attributed the resulting four band spectrum to the $4d'$ electron transition of the divalent Yttrium ions. All four bands can be thermally bleached, which supports the concept of the presence of electron traps (Ratnam, 1966). However, it has been found that only cubic sited rare earths are converted to the divalent rare earths after exposure to ionizing radiation; this explains why the absorption spectrum of the trivalent rare earth remains the same, while a new absorption band appears in the spectrum of the divalent rare-earth after irradiation. As the additive coloration process proceeds as a result of more baking with Ca vapor, the trivalent rare earth lines change in intensity at various rates, indicating that ions with different charge compensators reduce at different rates (Kiss and Yocom, 1964). Because Yttrium behaves like the rare-earth elements, Theissing et al. (1969) suggested that only crystals which have sufficient trivalent Yttrium impurities at cubic sites are colorable, and only those Y^{+3} which are located at cubic sites are effective as electron traps. They also note that there is more than one color center responsible for all of the bands in the composite spectrum of fluorite; this is supported by the fact that after gamma-radiation the divalent Yttrium which it formed, in addition to the defects which are produced at the remote charge compensators, become the color centers or share in the generation of new color centers. Because trivalent Yttrium is located at cubic sites, F^- interstitials are also in the cubic sites causing the charge compensating. Then trivalent Yttrium and F^- interstitial ion give rise to the so called REF-centers (Sashital and Vedam,

1973) which produce the 2250Å°, 4000Å° and 5800Å° absorption bands.

Staebler and Kiss (1969) suggested that ultraviolet absorption bands are a result of the 4f-5d transition of trivalent Ce in the system of CaF₂:Ce (see Fig. 3). Defect centers produced during the additive coloration process combine with the rare-earth and cause the generation of the observed spectrum (curve A in Fig. 3); subsequent ultraviolet radiation (3100-4000Å°) produces another spectrum, (curve B). The ultraviolet radiation ionizes an electron from a defect center produced by additive coloration, and this electron can then be trapped by a trivalent Ce ion. After exposure to light or thermal radiation, the rare-earth releases the electron, thereby effecting a return to the original spectrum (curve A). This describes the photochromic property of the CaF₂:La-Ce-Gd or Tb systems. Staebler and Schnatterly (1971) studied each of the CaF₂:La, Ce, Gd, Tb or Y systems separately and suggested that additive coloration does not produce the reduction of the trivalent ion to the divalent ion. Instead, the coloration produces an impurity-associated color center (i.e. a divalent rare earth next to an F₂-center), called an REF complex center. When these centers are photoionized by absorption of ultraviolet light, the released electron can be trapped at an isolated RE⁺³. This procedure creates two new absorption bands, one for the divalent rare-earth and the other for the ionized REF center.

EPR (Electron paramagnetic resonance) studies by Anderson and Sabisky (1971) were also carried out on the systems of CaF₂:La, Ce, Gd, Tb and Y. These workers suggested also that the stable photochromic center of fluorite consists of a trivalent rare-earth element next to a fluorine vacancy combined with two electrons to form a neutral complex

which can be ionized and excited by 4000Å light. They designated the stable and ionized centers as $[-|2e|RE^{+3}]$ and $[-|e|RE^{+3}]$ respectively, where within the brackets, - symbolizes a missing ion, m refers to m trapped electrons, and RE^{+3} is the added ion.

Uranium doped CaF_2 crystals studied by McLaughlin et al. (1970) exhibited brown, yellow, green and red colorations. Their results show that green coloration results from U^{+4} with trigonal symmetry, with F^- ion occupying the centers of cubes whose corners are common to the opposite corners of the cube containing the U^{+4} ion. Brown coloration is also caused by the U^{+4} with trigonal symmetry, where two O^{-2} ions are substituted for the two F^- ions at the opposite corners of the cube. They attributed yellow coloration to the presence of U^{+6} in the crystal.

A summary of authors, their experimental results and corresponding models for coloration of fluorite are given in Appendix A.

I.3. Use of the natural coloration of fluorite for geological age determination

Absolute age determinations of geologic processes has long been a problem for geologists. Many methods are available for determining geologic age; however, some of these work only in special cases (for example: presence of fossils are needed to determine the age of sedimentary rocks), and others, although they work (for example: fission track method), are tedious or very expensive. Thus geologists are still looking for a method which will work easily and inexpensively for a majority of cases.

Because colored fluorites, particularly purple fluorites, are

often found associated with deposits of radioactive materials, the phenomenon of fluorite coloration has been investigated as a means of geological age dating. Berman (1957), taking the visible purple coloration as a reference, asserted that neither purple fluorites nor the intensity of the structural damage produced by radioactivity which caused the purple coloration could be used for geological age determination. It would be very difficult to make an adequate estimate of external radioactivity, and even if it were possible, the method could show only the time since the sample had cooled below 175°C.

Titley and Damon (1962) studied a variety of different colored fluorites from different locations in terms of their ultraviolet absorption spectrum. All of the fluorites which they investigated had a strong absorption band at 3050Å, which was stable in terms of shape, intensity and the position up to 250°C; exposure to x-irradiation did not effect this absorption band. The radioactivity measured for each sample ranged from 0.1 to 1 ppm Uranium equivalent, and it was observed that unradioactive fluorite samples did not have the 3050Å absorption band. Analysis using x-ray fluorescence indicated impurities present in some fluorite, although no consistent relationship between quality and quantity of the impurities and the 3050Å absorption band could be detected. They concluded that the 3050Å absorption band could be used effectively as a tool for determining geological age.

CHAPTER II

EXPERIMENTAL METHODS

II.1. The scope of this study

As summarized in previous sections, there has been considerable research made into the coloration processes and properties of colored fluorites and models relating to the coloration of natural and synthetic fluorites. Most of the investigations were limited to a single colored natural fluorite and its properties, or to synthetic fluorites colored artificially in one or two procedures. Such studies, involving only one or two colored samples of natural fluorite, neglecting the influence of impurities and radioactive materials, understandably lead to largely speculative conclusions; and results produced by artificially colored fluorites, when only one or two coloration procedures are utilized, can easily be misconstrued. Thus, although gains have been made in many areas of fluorite research, much remains to be accounted for.

One thing certain from previous investigation is that colored fluorites possess physical properties or chemistries different from that of the colorless crystals. The influence of impurities, including rare-earths, radioactive materials and possibly monovalent and divalent elements, on the coloration of fluorites has long been recognized, and guidelines have been established regarding the mechanisms of coloration. Synthetic fluorites artificially colored with ionizing radiation and/or additive coloration and doped with a predetermined concentration of

impurities, show the importance of radiation and rare-earth elements in the process of coloration. Nevertheless, no attempt has been made to single out the properties common to identically colored natural fluorites, and to relate these properties to similar effects produced in synthetic fluorites by ionizing and particle radiation.

This experimental program was designed to 1) study the location differences of radioactive materials (Th, U) and other impurities (rare-earth elements, Na and Yttrium), 2) study their contribution to the various bands of the absorption spectrum and the common properties of each color, 3) investigate the possibilities of using the 3050A° absorption band for geological age dating of fluorites, and 4) establish possible models for coloration. For this purpose the following procedure was applied:

1) After exposing synthetic fluorites to different types and amounts of radiation (α , γ , x-ray, electron, neutron and proton) the samples were analyzed to establish their absorption spectrums and color changes; thermal bleaching of a sample submitted to one energy level of each radiation was carried out at 100°C, 200°C, 300°C and 400°C. This was done to establish information about the color changes and behavior of defects, and whether these were impurity related or physically related to the coloring.

2) Various naturally colored and color-banded fluorites were selected.

a) Three different colored samples were crushed and washed of their fluid inclusion impurities. Then along with their unwashed parts and other colored fluorites, they were analyzed in terms of the rare-earth

elements and radioactive materials present in order to obtain information about the location differences of these elements and the relation between colorations and compositional differences.

b) Absorption spectra were taken of all of the fluorites, and homogenization temperatures of the samples having observable fluid inclusions were measured to gain some idea of the coloration processes and possible effects of crystallization temperatures on the color changes.

c) Finally, both synthetic and natural fluorites were examined under the transmission electron microscope (TEM) to determine their similarities and differences in terms of coloration and defect structures.

II.2. Sample preparations and instrumentation

The synthetic fluorite used in this study was purchased as a single, whole chunk crystal from Harshaw chemical company, Cleveland, Ohio. Pieces of it were used in irradiation experiments, subsequent absorption spectrum measurements and thermal bleaching experiments, impurity analyses and TEM studies.

The natural fluorites were, as much as possible, of different colors, and from different locations. They were used for fluid inclusion homogenization temperature measurements, impurity analyses and absorption spectrum measurements.

The absorption spectrum measurements were made with a Heath Ultraviolet/Visible, single beam spectrophotometer in the range of 2500Å° to 7000Å°. All natural and synthetic fluorites were prepared

following the same procedure. A chunk of a single natural fluorite crystal was first washed and cleaned. Then it was examined under a light microscope to ascertain that no mineral inclusions were present. Both natural and synthetic fluorites were cut or cleaved to a piece 11 x 11 and about 3mm thick. Synthetic fluorites 11 x 11 x 0.5mm were also prepared. Each sample was then polished in three stages.

To clean the fluid inclusions from the samples, first the samples were hand picked to obtain approximately 100 grams of fluorite fragments with no associated minerals. They were then crushed in a mortar to about 8 mesh, washed in a 6:1:1 H₂O:HNO₂:HCl solution at about 80°C in a teflon beaker, and run in an ultrasonic cleaner for ten minutes to clean the secondary inclusions generally located along the cleavages. After rinsing them with distilled deionized water, the samples were crushed to 200 mesh in a mortar with a 0.1 N HCl acid solution then filtered and rinsed again with distilled deionized water. The dried samples were used for analyses. The impurity analyses of the solid specimens employed a neutron activation technique for La, Ce, Sm, Nd, Eu, Tb, Yb, Lu, Th and Na, for both natural and synthetic fluorites. Y analyses were obtained using Emission Spectrometry and U analyses were made by the delayed neutron technique.

Two samples were prepared for the transmission electron microscopy (TEM) study; they were a synthetic fluorite and a natural purple fluorite. Large, single crystals of fluorite were cleaved and crushed to smaller sizes, and the finest flakes were selected to be used for the study. These flakes, generally cleaved along (111), were examined in a Hitachi Perkin-Elmer H.U. 200F electron microscope (operated at 175 kV accelerating

potential), and fitted with a goniometer-tilt stage.

Homogenization temperatures of the fluid inclusions were measured with a heating stage attached to an optical microscope. Measurements were made for different colored and banded natural fluorites which had been cut into small pieces; only the homogenization temperatures of primary fluid inclusions were measured.

All irradiations were carried out at room temperature. Applied irradiations and energies are tabulated in Table 2 (Chapter III).

Bleaching experiments were established using a furnace with a heating rate of about 2°C/minute at atmospheric pressure. This treatment was applied to the irradiated and best colored samples of each radiation set. One sample from each set was heated from 100°C up to 400°C, depending on the bleaching obtained. After each heating, samples were cooled very slowly and absorption spectra were taken at room temperature.

CHAPTER III

EXPERIMENTAL RESULTS

III.1. Experiments on synthetic fluoritesIII.1.1. Chemical Analyses

Synthetic fluorite from the Harshaw chemical company was analyzed for the rare-earth elements, sodium and Yttrium. As noted in Chapter I, many other investigators indicated that Harshaw fluorites contain impurities, especially Yttrium. The fluorite for this study also contained impurities; the results of the analysis are:

La	0.59	ppm	Tb	-	ppm
Ce	-	"	Yb	-	"
Nd	-	"	Lu	0.01	"
Sm	0.01	"	Na	72.0	"
Eu	-	"	Y	<1.0	"

The significance of these impurities will be evident in the coloration behavior of the samples after exposure to different kinds and amounts of radiation. Because the amount of impurities in a given sample remains constant, a change in the amount of energy or flux applied to the sample should indicate the extent of lattice defects involved at each absorption band in generating the coloration. In a similar study, Harshaw chemical company fluorite analyzed by Sashital and Vedam (1973) was found to contain 20 ppm Na and 4.5 ppm Yttrium. If the impurities found in the fluorite of this study are significant enough to be affected by irradiation, the resulting absorption spectrum of the gamma

irradiated sample, although exposed to the same energy level, should not be the same as the spectrum of Sashital and Vedam's sample, as the concentrations of impurities involved are not the same.

III.1.2. Results of irradiation and absorption spectrum measurements

The Harshaw chemical company fluorite which was the subject of this study was taken from a whole single crystal. Because all irradiation experiments were carried out using the same synthetic fluorite, containing a known and fixed amount of impurities, the effect of different radiations on the impurities and the subsequent coloration obtained should indicate the effective impurity concentrations and effective kinds and amounts of irradiation. The colorations obtained after the fluorite was submitted to different kinds and amounts of energy are given in Table 2.

X-irradiation

Two 11 x 11 x 0.5 mm synthetic fluoroites and one colorless 11 x 11 x 0.5 mm natural fluorite (F-N-14) were exposed to x-radiation. The synthetic fluorites F-S-1 and F-S-2 at 200 kV, 600 mA and at 100 kV, 450 mA, respectively, showed no color changes after two hours of x-ray exposure. The colorless natural fluorite (F-N-14) also showed no coloration after two hours of exposure to the x-ray at 100 kV, 450 mA. Synthetic fluorites F-S-3 and F-S-4 which were exposed to 50 kV, 30 mA for two hours and 45 kV, 35 mA for thirty-two hours, respectively did not show any coloration. The absorption spectra of the x-irradiated synthetic fluorites showed no absorption bands in the ultraviolet

Table 2. Coloration of synthetic fluorites obtained after different radiation and/or energy and flux.

	Energy	Munsell* color designation	Color name
X-ray			
F-S-1	200 kV, 600 mA (2 hrs)		
F-S-2	100 kV, 450 mA (2 hrs)		
F-N-14	100 kV, 450 mA (2 hrs)		
F-S-3	50 kV, 30 mA (2 hrs)		
F-S-4	45 kV, 35 mA (34 hrs)		
F-N-2	45 kV, 35 mA (15 min)		
Gamma			
F-S-1	2.5 x 10 ⁵ rads 1.1701.13 MeV	10 YR 7/8	Mod. yellow orange
F-S-2	8.8 x 10 ⁶ rads "	10 R 6/8	Mod. red orange
F-S-3	2.5 x 10 ⁷ rads "	10 YR 6/10	Dk. yellow orange
F-S-4	5.2 x 10 ⁶ rads "	10 R 6/10	Lt. orange pink
Alpha			
F-S-1	10 ¹⁸ He ⁺⁺ /cm ² at 250 kV	5 P 3/2	dusky purple
F-S-2	10 ¹⁷ He ⁺⁺ /cm ² "	5 P 5/4	weak purple
F-S-3	10 ¹⁶ He ⁺⁺ /cm ² "	5 P 6/4	pale purple
Proton			
F-S-1	10 ¹⁸ H ⁺ /cm ² at 250 kV	5 P 4/8	Mod. purple
F-S-2	10 ¹⁷ H ⁺ /cm ² "	5 P 2/2	very dusky purple
F-S-3	10 ¹⁶ H ⁺ /cm ² "	5 P 7/4	pale purple
F-S-4	10 ¹⁵ H ⁺ /cm ² "	colorless	
Neutron			
F-S-1	3.700 x 10 ¹³ n/cm ² 3.0 MeV	5 B 7/1	Lt. blue grey
F-S-2	7.02 x 10 ¹³ n/cm ² "	5 BG 7/2	pale blue green
F-S-3	1.57 x 10 ¹⁴ n/cm ² "	5 YR 8/2	weak orange pink
Electron			
F-S-1	10 ¹⁶ e/cm ² at 1.0 MeV	colorless	colorless
F-S-2	" at 1.2 "	5 P 8/1	high purple grey
F-S-3	" at 1.4 "	5 B 8/1	Lt. blue grey

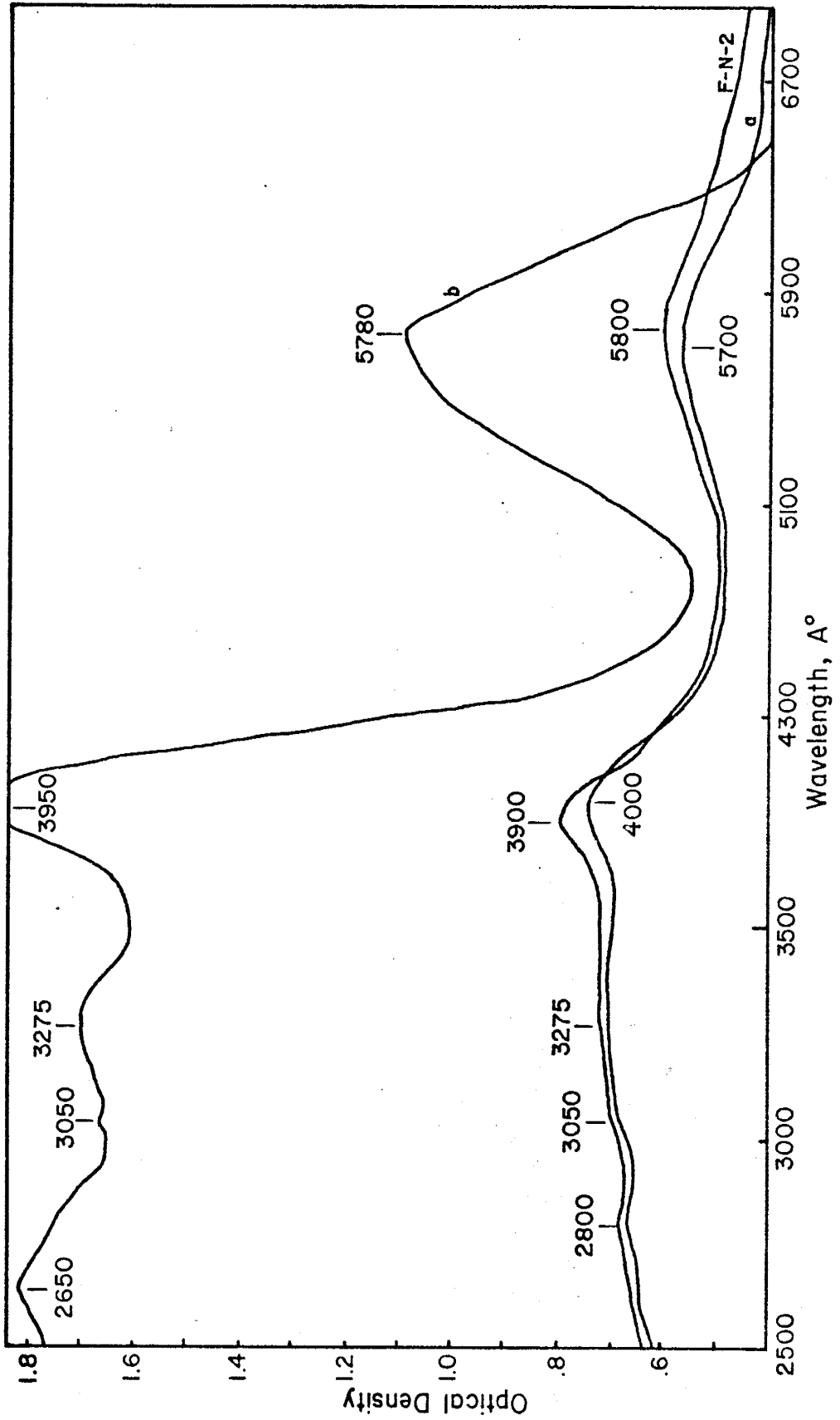
*Munsell numerical designations for each sample were obtained by comparison with Munsell color standards in the Munsell Book of Colors (1929).

Color names corresponding to each Munsell numerical designation were established by Judd and Kelly (1939).

region either. However, green and blue colored natural fluorites showed drastic color changes after only 15 minutes of irradiation at 45 kV, 35 mA. The absorption spectra of x-irradiated blue fluorite (F-N-2) are shown in Figure 6 before and after heating to 200°C, (Homogenization temperature measurements indicated that this fluorite formed at about 192°C) and later after irradiating with x-rays. As can be seen from Figure 6, heating of blue fluorite resulted in the shift of the 3900Å absorption band to 4000Å and the 5800Å absorption band to 5700Å. Then, heating with x-rays brought the bands back to very nearly their original positions, with an increased intensity. This experiment indicates that if the fluorite is pure or relatively pure, it has resistance to x-irradiation in terms of coloration.

These results of irradiation of artificial fluorite are consistent with the results of Gorlich et al. (1968), Bessent et al. (1969) and Roach and Senff (1974), who could not obtain any coloration with x-rays at room temperature without adding a chemical agent to the crystal. The purity of the crystal used was justified by its resistance to x-rays in terms of coloration by Roach and Senff (1974). However Ratnam (1966), Rao and Bose (1970), who used Harshaw chemical company fluorites, were able to produce coloration resulting from a four band absorption spectrum after x-irradiation at room temperature. Staebler and Schnalterly (1971) believed that only impure synthetic fluorite can give a four band absorption spectrum and show coloration when irradiated with x-rays at room temperature. Thus it appears that 0.59 La, about 1.0 ppm Yttrium and 72.0 ppm Na are not significant enough amounts of impurities to be used for color generation when irradiated with x-rays, i.e. without an

Fig. 6. Absorption spectra of blue colored natural fluorite (F-N-2), before, and after heating and x-ray radiation treatment. F-N-2 sample spectrum without any treatment, a) spectrum after heating the sample to 200°C. b) same sample, the spectrum, after irradiating with x-rays for 15 minutes at 45 kV, 35 mA.



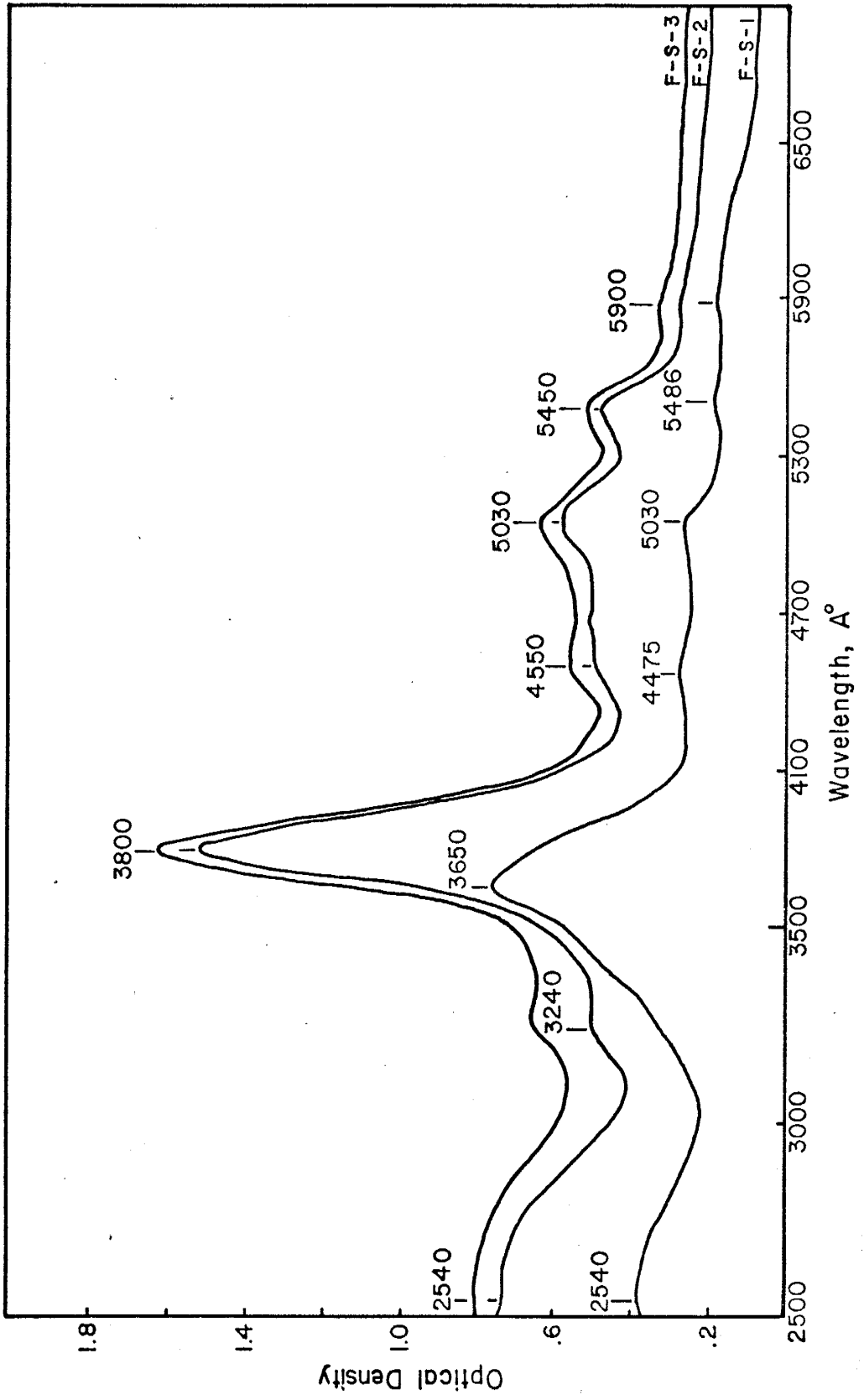
extensive exposure time, x-rays cannot be effective on this relatively pure fluorite as a coloring process.

Gamma-irradiation

Hard-gamma-irradiation of synthetic fluorites, the resulting colorations and absorption spectra are given in Table 2 and Fig. 7, respectively. F-S-1, irradiated with 2.5×10^5 R, resulted in major absorption bands at 2540\AA , 3650\AA and 5030\AA , and weaker bands at 4475\AA , 5486\AA and 5900\AA . When the irradiation dose was increased to 8.8×10^6 R (F-S-2), a new absorption band appeared at 3240\AA and the 3650\AA absorption band shifted to the wavelength of 3800\AA . The 4475\AA absorption band also shifted to 4450\AA . With F-S-3, which was irradiated with 2.5×10^7 R, no shifting of absorption bands was observed, although intensities of the absorption bands increased relative to F-S-2. Because of this shifting of absorption bands, F-S-1, F-S-2 and F-S-3 had different colorations. For each of the samples, the entire thickness was colored.

The absorption bands obtained from this study are not the same as those obtained by Sashital and Vedam (1973), although in each case the same radiation doses and the same thicknesses were established. Neither are the number of absorption bands or the maximums of the absorption band the same, although Harshaw chemical company fluorites were used in both investigations. However, as it was indicated in section III.1.1. the synthetic fluorites studied by Sashital and Vedam contained different amounts of impurities than did the synthetic fluorite used in this experiment; thus the resulting absorption spectra are expected to be different as a result of the different impurities present.

Fig. 7. Gamma irradiated synthetic fluorites and their absorption spectra. F-S-1 after 2.5×10^5 R irradiation, F-S-2 after 8.8×10^6 R irradiation and F-S-3 after 2.5×10^7 R irradiation.



The pattern of growth of the absorption bands, with radiation dosage is different for each band (Fig. 8). The 3800A°, 5030A° and 5450A° absorption bands show fairly similar patterns, beginning with about a 0.50 slope, progressing to a steeper slope. The 5900 and 4550A° absorption bands start with a very low slope (0.02-0.05) which increases up to 1.0. The 3240A° absorption band, however begins with 0.58 slope and progresses with no slope. The relative growth of these absorption bands with respect to each other also shows growth pattern differences; for example, the growth of the absorption bands with respect to the 3800A° absorption band follows a pattern similar to that of the growth with radiation dose. This indicates that many of these absorption bands are not originated from the same center. In fact, at least three different centers appear to be involved in generating the observed absorption spectrum.

Alpha-irradiation

Irradiation with alpha particles produced the absorption spectrum shown in Fig. 9. An 11 x 11 x 3 mm sample of synthetic fluorite F-S-3 was irradiated with 10^{16} He⁺²/cm² flux at 250 kV and generated a broad absorption band at 5450A°. When the irradiation flux was increased, equally sized samples of F-S-2 (irradiation flux; 10^{17} He⁺²/cm²) and F-S-1 (irradiation flux 10^{18} He⁺²/cm²) showed no shifting of the absorption band, but an increase in intensity. Color changes were observed only on the surface, to the thickness at which Helium can penetrate and remain located in the fluorite. The observed colorations are given in Table 2. The growth pattern of this absorption band is similar to that of the 5450A° absorption band generated by gamma-irradiation,

Fig. 8. Growth of color center concentration (n_c , see page 67) of the various absorption bands with radiation dosage.

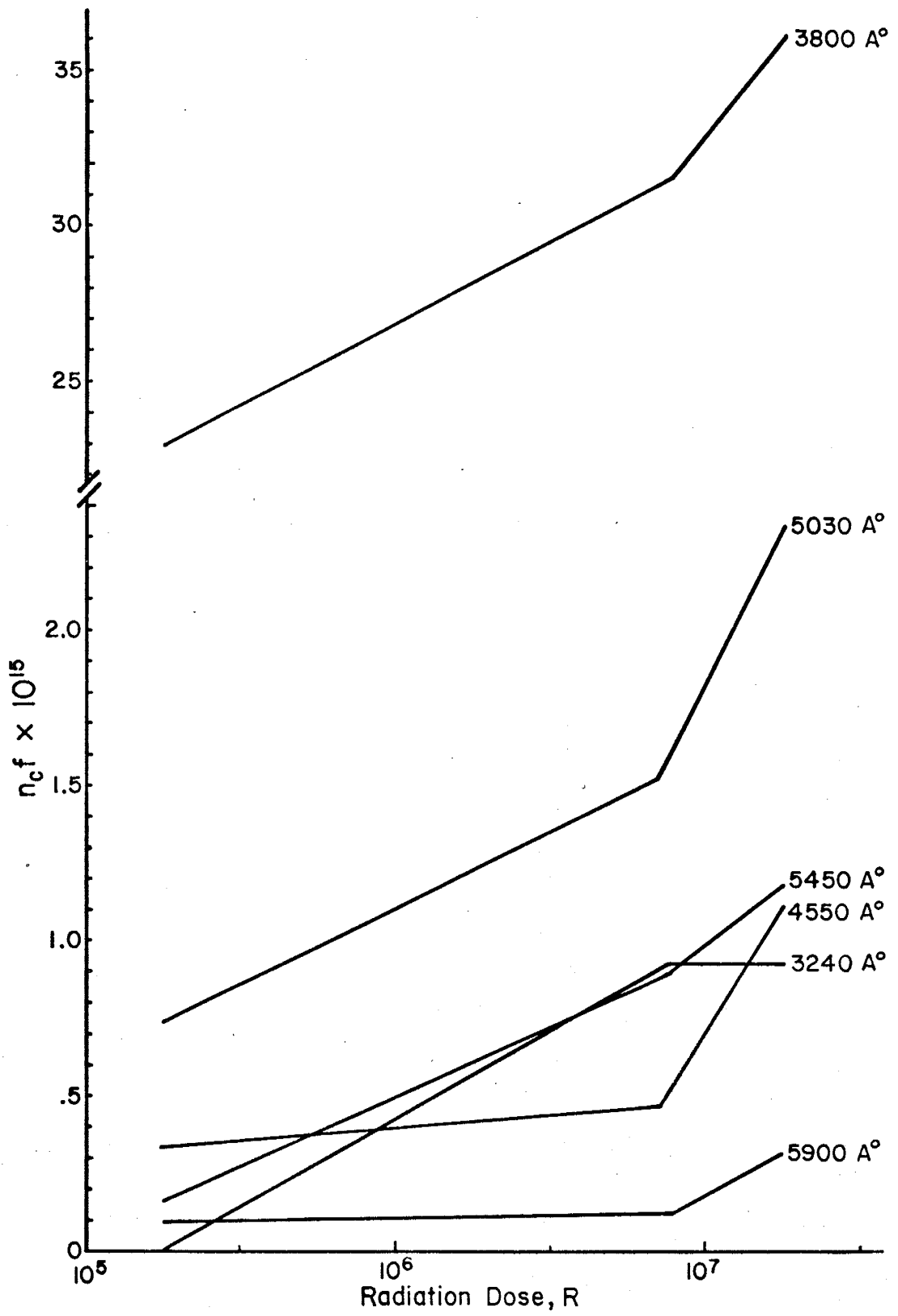
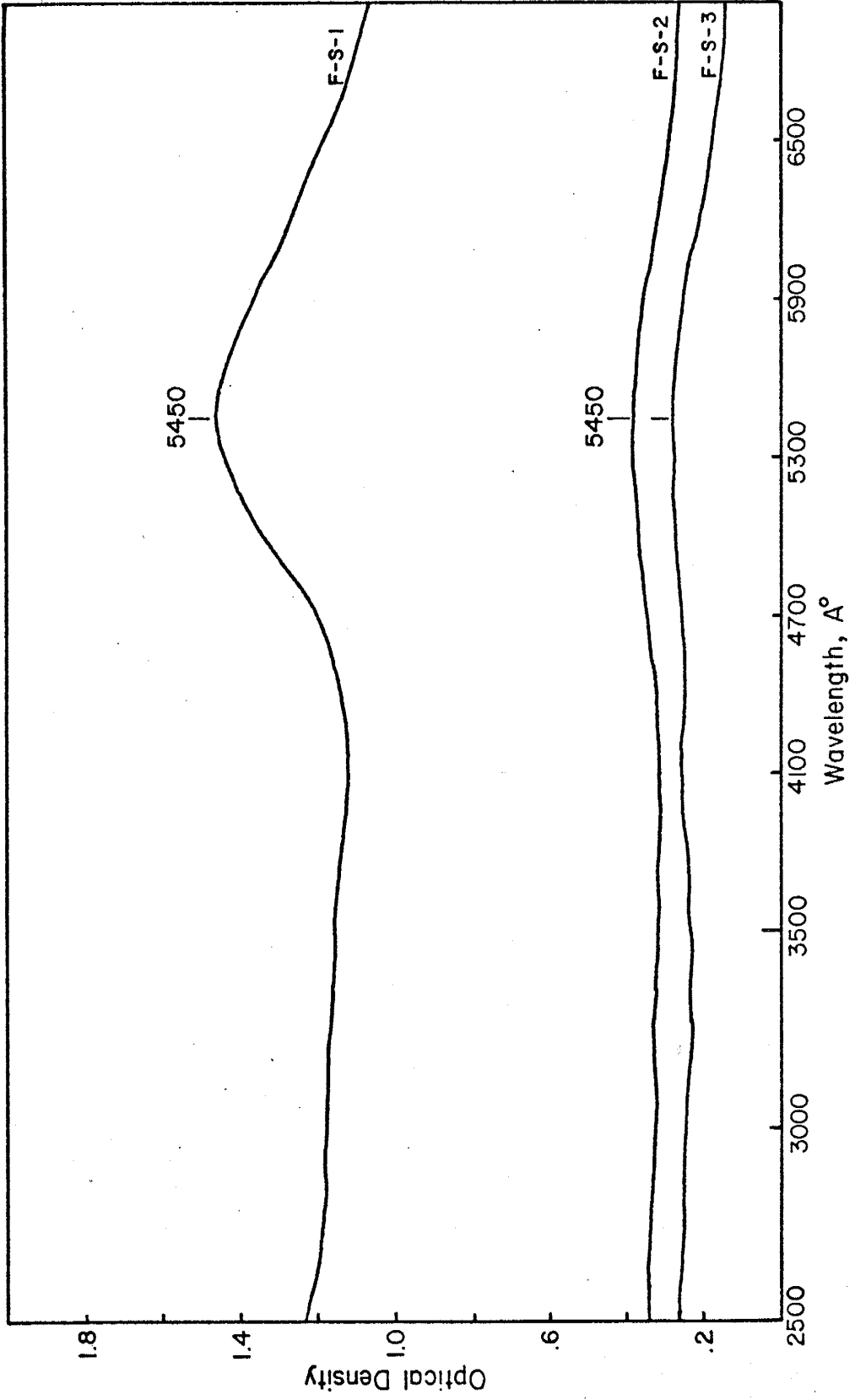


Fig. 9. Absorption spectra of Alpha irradiated synthetic fluorites. F-S-1 was radiated with a flux of 10^{18} $\text{He}^{++}/\text{cm}^2$, F-S-2 with a flux of 10^{17} $\text{He}^{++}/\text{cm}^2$, and F-S-3 with a flux of 10^{16} $\text{He}^{++}/\text{cm}^2$, at 250 kV.



although its beginning slope is smaller.

Proton-irradiation

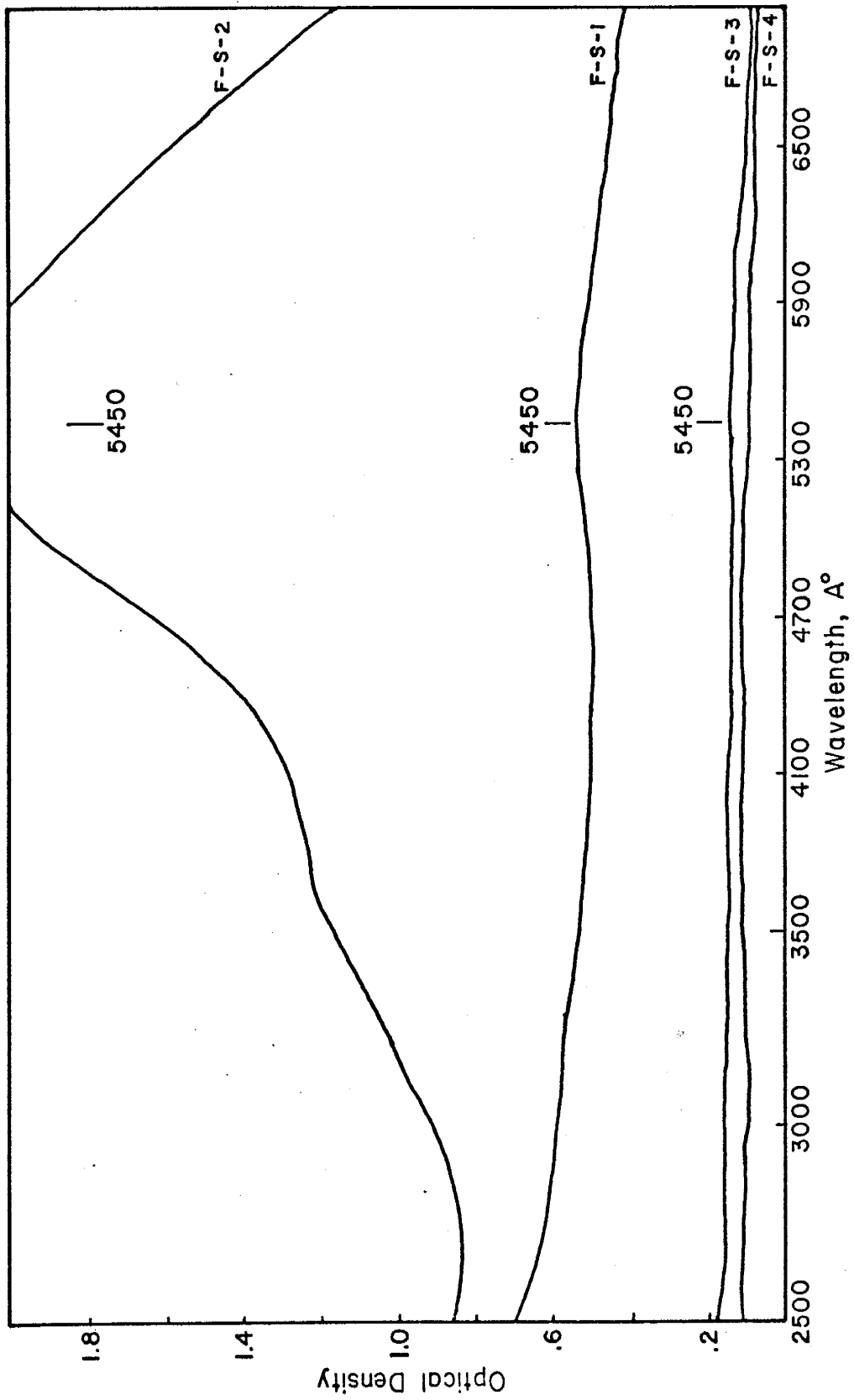
Proton irradiation produced an absorption spectrum very similar to that produced by alpha irradiation. The results of this irradiation experiment are given in Fig. 10. The synthetic fluorites used were all 11 x 11 x 3 mm. The fluorite sample F-S-4 which was irradiated with 10^{15} H^+/cm^2 flux at 250 kV, produced no color changes and no absorption bands. F-S-3 (irradiation flux; 10^{16} H^+/cm^2 at 250 kV) and F-S-2 (irradiation flux 10^{17} H^+/cm^2 at 250 kV) both showed color changes; F-S-3 produced an absorption band at 5450\AA , while F-S-2 showed increased color intensity and increased intensity at 5450\AA , in addition to a weak absorption band at about 3500\AA . F-S-1, which was irradiated with 10^{18} H^+/cm^2 at 250 kV, showed a lower intensity of color than F-S-2 and lower intensity of the 5450\AA absorption band; the absorption band at 3500\AA was also diminished. However the sample was sputtered because the dosage applied to it was so high. As with the alpha-irradiated fluorite, the coloration or proton irradiated samples (given in Table 2) could be seen only on the surface of the sample, just to the thickness to which the proton radiation could penetrate.

The growth of the 5450\AA absorption band was the same as that of the 5450\AA absorption band produced by alpha radiation.

Neutron irradiation

Neutron irradiation of F-S-1, with 3.706×10^{13} n/cm² at about 3.0 MeV, generated a color change over the entire thickness of the crystal, and produced absorption bands at 3860\AA and 5900\AA . With increasing flux, at a fixed amount of energy, the irradiated sample F-S-2 showed

Fig. 10. Absorption spectra of proton irradiated synthetic fluorites. Irradiation fluxes are 10^{18} H^+ / cm^2 for F-S-1, 10^{17} H^+ / cm^2 for F-S-2, 10^{16} H^+ / cm^2 for F-S-3 and 10^{15} H^+ / cm^2 for F-S-4 at 250 kV.



intensified color, and the 3860Å° absorption band shifted to 3830Å°; the 5900Å° absorption band showed no changes. Irradiation of F-S-3 with 3.158×10^{14} n/cm² flux at 3.0 MeV, produced a change in color as well as a shift of the 3860Å° absorption band to 3650Å°, while the 5900Å° absorption band remained unchanged. The resulting absorption spectrums and color changes are given in Figure 11 and Table 2, respectively.

Growth of the absorption bands at 3830Å° and 5900Å° is different than the growth of the gamma irradiated samples' absorption bands at the same wavelengths. An increase in the irradiation flux (F-S-3 at 31.58×10^{14} n/cm²) caused a lowering of the color center concentrations of both absorption bands.

Electron irradiation

Electron irradiation of three synthetic fluorite samples F-S-1 (10^{16} e/cm² at 1.0 MeV), F-S-2 (10^{16} e/cm² at 1.2 MeV) and F-S-3 (10^{16} e/cm² at 1.4 MeV) did not produce good coloration. A trace of coloration was detectable in F-S-2 and F-S-3 only when compared to unirradiated samples of the same thickness. As a result, no clear-cut absorption bands were established; this is not unexpected, because it is well known that low energy electrons are not capable of generating coloration and color centers in fluorites at room temperature. High energy electrons or higher temperatures are needed for color production (Rao and Bose, 1970). According to these workers, at temperatures above 100°C electrons generate a two band absorption spectrum. Their results, along with absorption spectrum measurements from this study, are given in Fig. 12. They produced absorption maxima at 3780Å° and 5600Å° by increasing

Fig. 11. Absorption spectra of neutron irradiated synthetic fluorites. Irradiation fluxes were applied to F-S-1 with 3.706×10^{13} n/cm², to F-S-2 with 7.028×10^{13} n/cm², and to F-S-3 with 1.58×10^{14} n/cm², at 3.0 MeV.

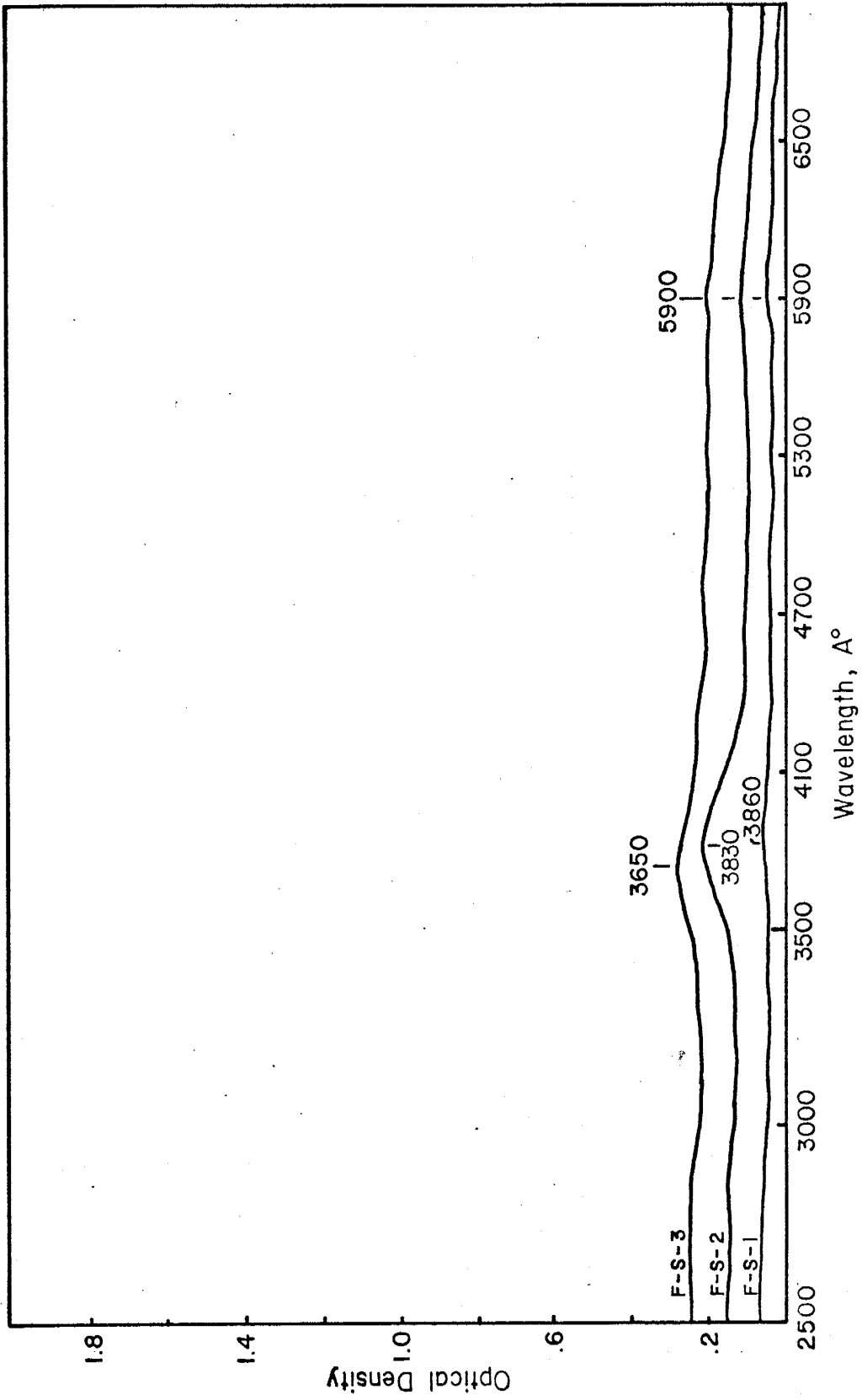
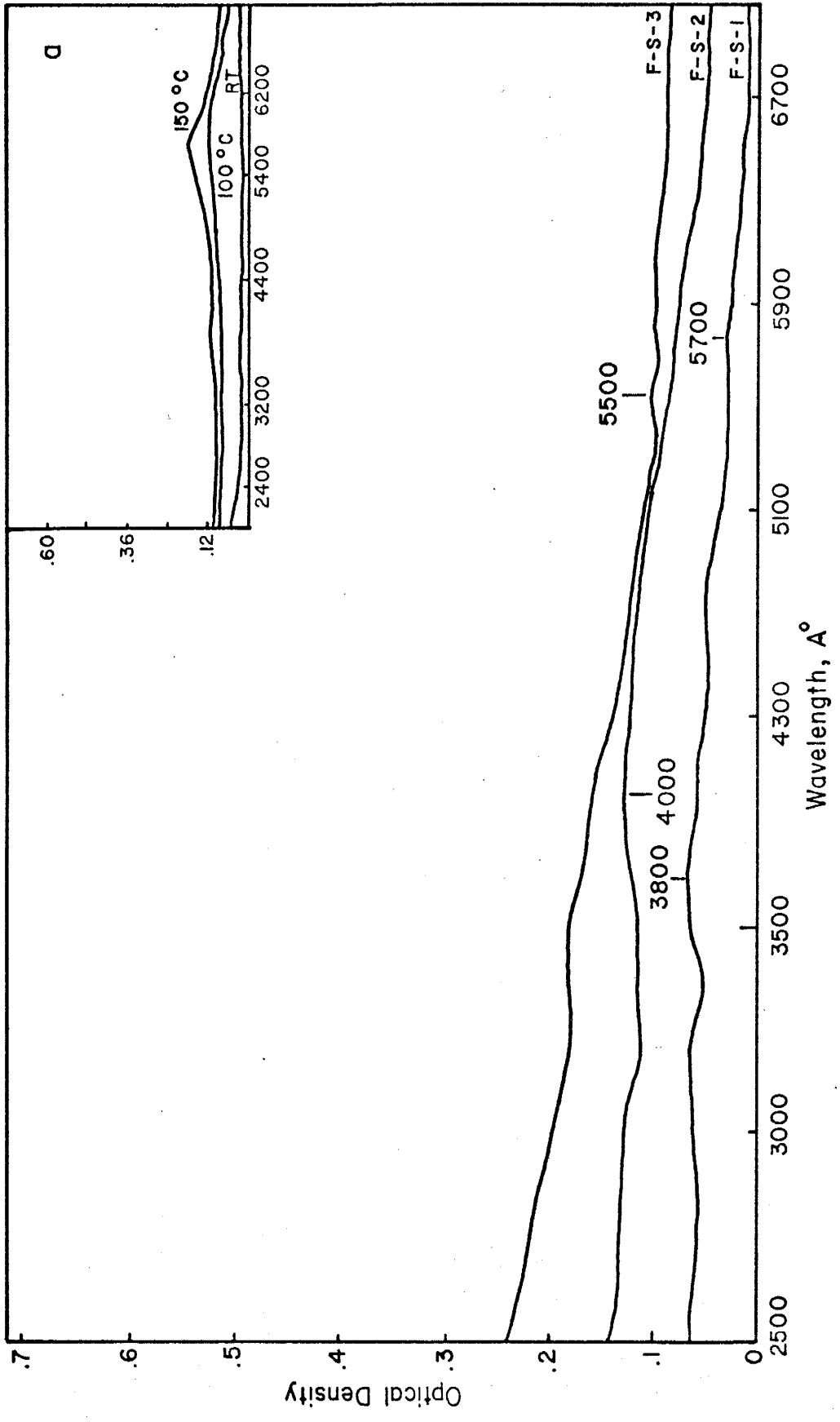


Fig. 12. Absorption spectra of the electron irradiated synthetic fluorites. F-S-1, with 10^{16} e/cm² at 1.0 MeV, F-S-2, with 10^{16} e/cm² at 1.2 MeV, and F-S-3, with 10^{16} e/cm² at 1.4 MeV.
a) Results of absorption spectrum measurements taken by Rao and Bose (1970), at room temperature, 100°C and 150°C.



the temperature while keeping the energy constant.

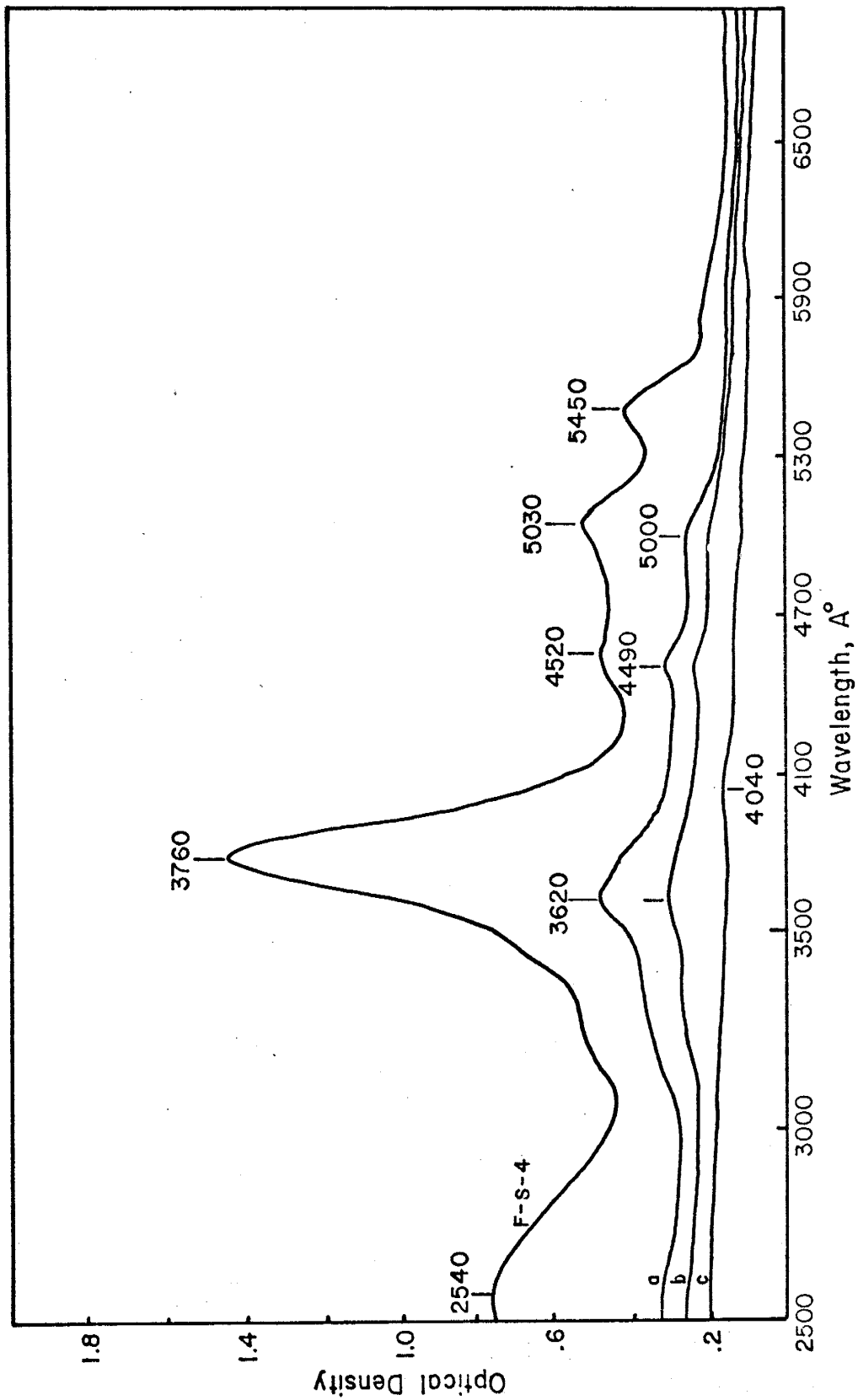
III.1.3. Results of thermal bleaching experiments

Gamma-irradiated fluorite

Gamma-irradiated synthetic fluorite (F-S-4), which was given a 5.2×10^6 R dose, generated absorption bands at 2540A°, 3760A°, 4520A°, 5030A° and 5450A°. The observed coloration was light orange pink, which in Munsell notation is 10 R 6/10. When the sample was heated to 100°C, the color changed to moderate yellow (5 Y 7/6) and the 2540A° and 5450A° absorption bands were completely diminished. The 3760A° absorption band shifted to 3620A°, the 4520A° absorption band shifted to 4490A°, and the 5030A° absorption band shifted to the 5000A° wavelength. Further heating to 200°C caused a change in color to weak yellowish orange (10 YR 7/6) and a diminishing of the 5000A° absorption band, while the 3620A° and 4490A° absorption bands were lowered in intensity. Heating to 400°C left residual color, recognizable only when the sample was compared to non-irradiated synthetic fluorite of the same thickness, and one absorption band at about the 4040A° wavelength.

The thermal bleaching patterns of these absorption bands show that the 3760A°, 5450A° and 5900A° absorption bands bleach faster than the other absorption bands up to 100°C. Between 100°C and 200°C, bleaching of the 3760A° absorption bands is slower, but speeds up again at higher temperatures. The 4520A° absorption band bleaches at a constant rate between 100°C and 400°C. The results of the bleaching of the gamma-irradiated synthetic fluorite are given in Fig. 13.

Fig. 13. Absorption spectra and bleaching experiments results of synthetic fluorite F-S-4, after exposure to 5.2×10^6 R gamma ray. a) After heating to 100°C . b) After heating to 200°C . c) After heating to 400°C . Spectra were taken at room temperature after slow cooling.



Proton irradiated fluorite

The synthetic fluorite F-S-2, which was irradiated with protons at 250 kV and 10^{17} H^+/cm^2 flux, showed an absorption band at 5450\AA and had a very dusky purple color (5 P 2/2). Heating up to 100°C and 200°C did not change the color or the absorption spectrum. Heating to 400°C changed the color to moderate purple (5 P 5/6), decreasing the intensity of the 5450\AA absorption band and shifting it to 5270\AA . The results are given in Fig. 14.

Alpha irradiated fluorite

F-S-1, irradiated with alpha particles at 250 kV and a flux of 10^{18} $\text{He}^{+2}/\text{cm}^2$, became dusky purple in color (5 P 3/2) and showed a broad absorption band at 5450\AA . Heating the sample to 100°C and 200°C did not change the color and absorption spectrum. However, heating to 400°C changed the color to weak purple (5 P 3/4); the intensity of the 5450\AA absorption band was lowered and it was shifted to the 5300\AA wavelength. The absorption spectrum is given in Fig. 15.

Neutron irradiated fluorite

The synthetic fluorite F-S-2 which was irradiated with neutrons at 3.0 MeV and 7.02×10^{13} n/cm^2 was colored pale blue green (5 BG 7/2) and gave absorption bands at 3800\AA and 5900\AA . Heating the sample to 100°C diminished the 5900\AA absorption band and lowered the intensity of the 3800\AA band. The color was changed to weak yellow (5 Y 8/4). Heating to 300°C left a residual of the 3650\AA absorption band, and color detectable only by a comparison to nonirradiated synthetic fluorite of the same thickness. At 400°C the color and the residue of 3800\AA absorption band were completely diminished. Absorption spectrum results

Fig. 14. Absorption spectra of proton irradiated fluorite, F-S-2 (10^{17} H⁺/cm² at 250 kV), before and after heating experiments; a) After heating to 100°C and 200°C. b) After heating to 400°C.

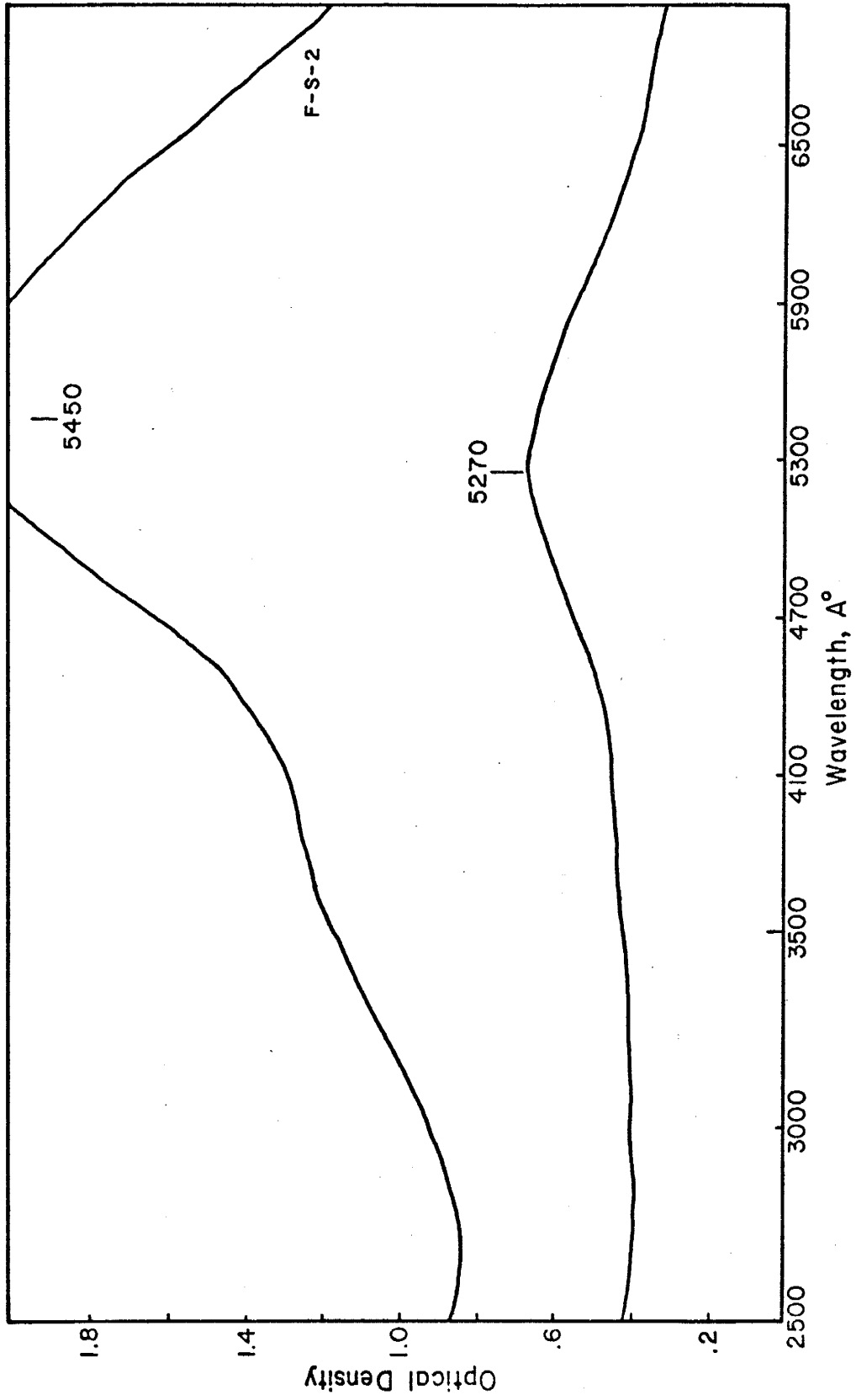
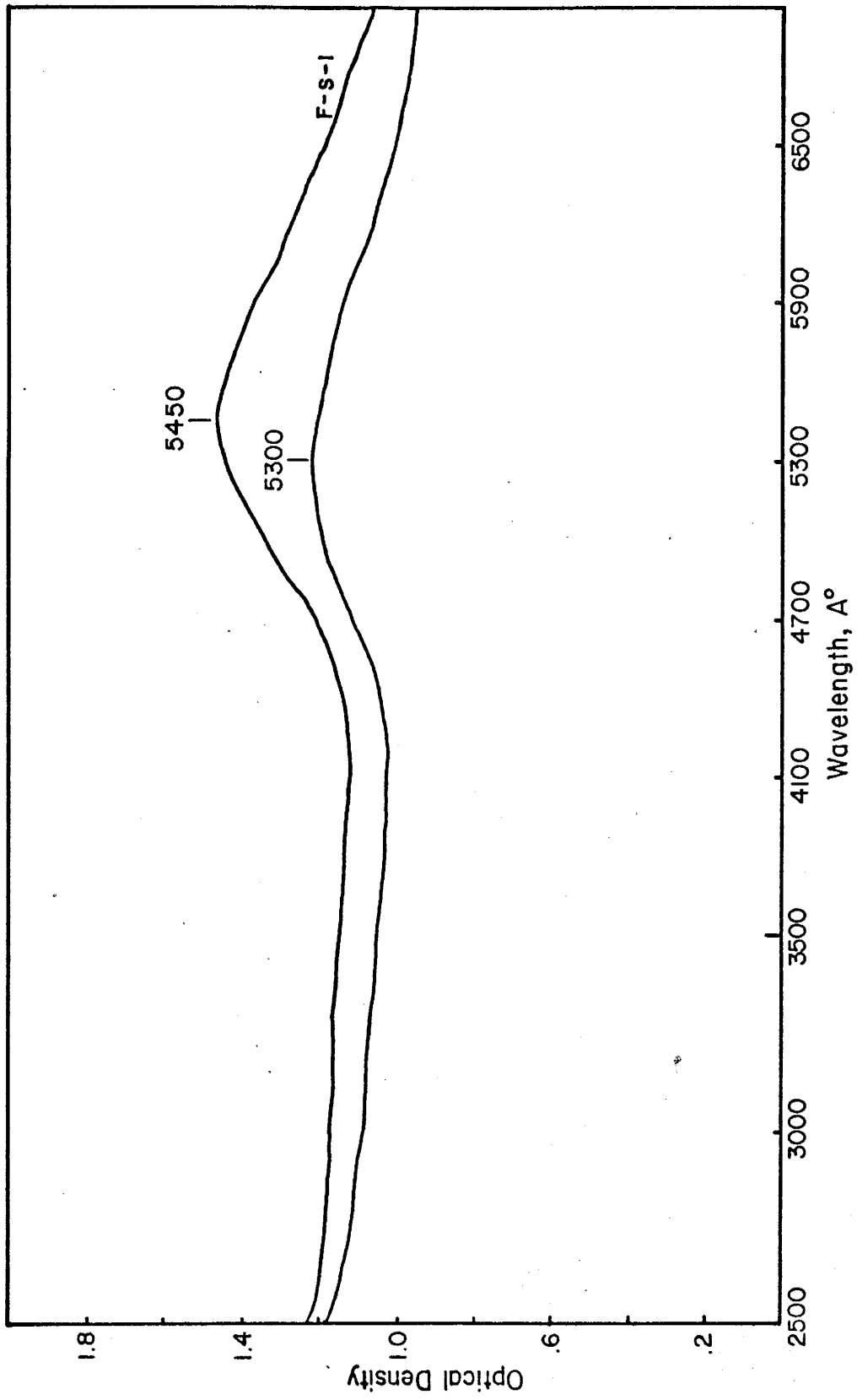


Fig. 15. Absorption spectra of alpha irradiated (10^{18} $\text{He}^{++}/\text{cm}^2$ at 250 kV) and thermally bleached F-S-1 fluorite, after heating to 100°C and 200°C . a) shows the spectrum after heating to 400°C .



of this heating experiment are given in Fig. 16.

Electron irradiated fluorite

Low energy electron (10^{16} e/cm² at 1.4 MeV) irradiated synthetic fluorite, F-S-3, showed very weak coloration and very weak absorption bands at 4000Å° and 5500Å°. When heated to 100°C, these weak absorption bands were diminished, and heating to higher temperatures (up to 400°C) produced no further changes. Results are given in Fig. 17.

III.2. Studies of natural fluorites

III.2.1. Geological occurrences of natural fluorites subjected to this study.

The fluorites investigated in this study come mainly from New Mexico. Some were from a Kentucky-Illinois area, and others come from Mexico and Thailand. They exhibit a diversity of colors.

The New Mexico fluorites were obtained from locations in Gonzales, Hansanburg (Bingham), the Magdalena Mountains and Gila District. The general geological features of the fluorite deposits are given in Table 3 (Allmendinger, 1975). Gonzales fluorites were green in color and show very good cleavages. Hansanburg (Bingham) fluorites exhibit color of blue, purple and green. Purple fluorites are also banded with color combinations, such as colorless-purple and purple-colorless blue. Magdalena fluorites are pale yellow green in color and include fractures in different directions. Gila fluorites are green-purple-colorless banded in the direction of growth.

Fig. 16. Absorption spectra of synthetic fluorite F-S-2 irradiated with neutrons (7.02×10^{13} n/cm² 3.0 MeV) before and after heating experiments. a) After 100°C heating. b) After 300°C heating. c) After 400°C heating.

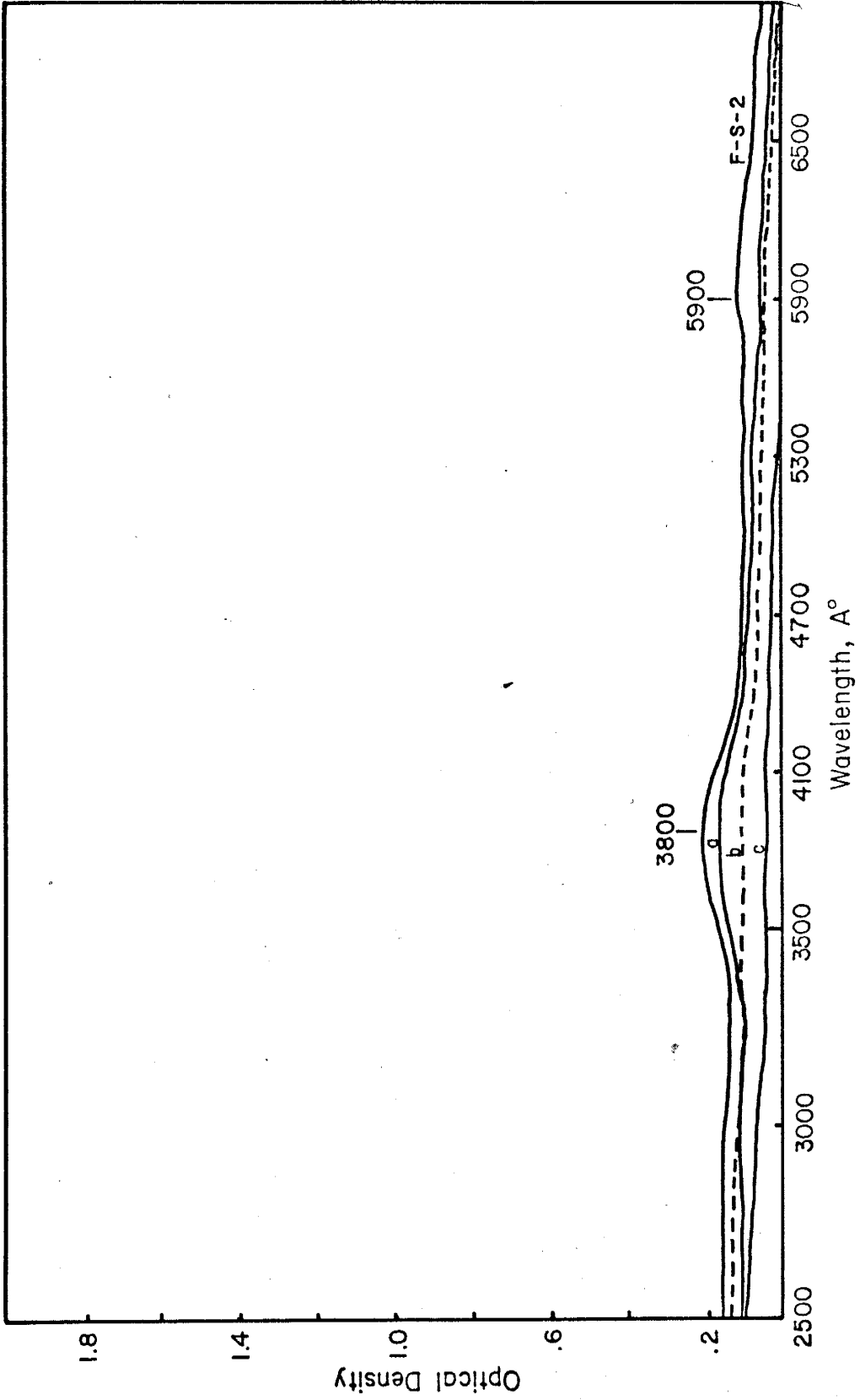
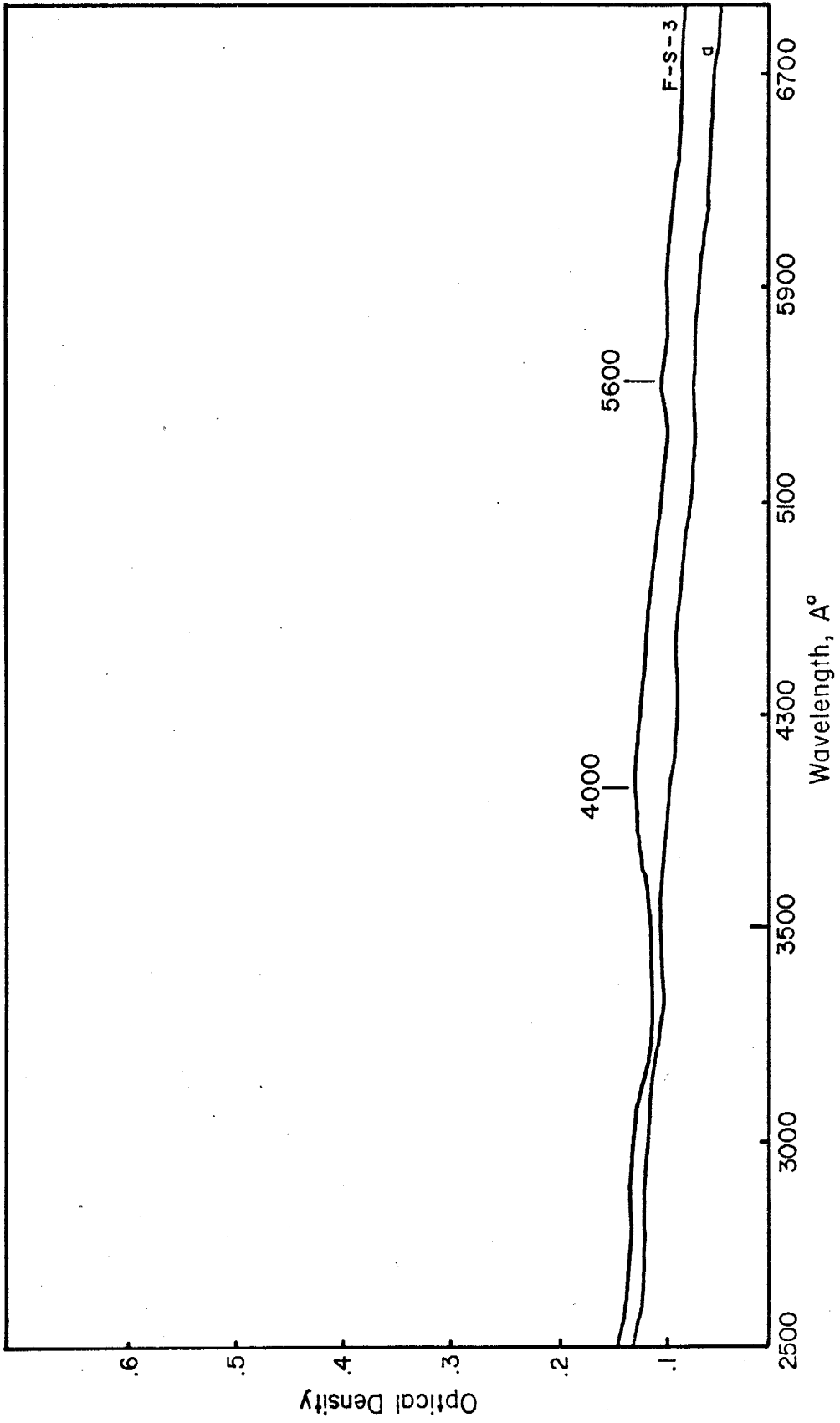


Fig. 17. Absorption spectra of the electron irradiated sample, F-S-3, exposed to 10^{16} e/cm² at 1.4 MeV; a, the spectrum after heating to 100°C, 200°C, and 400°C.



The Kentucky-Illinois fluorites were taken from the Rosiclaire Cave-in-Rock District. The general geological features of this deposit are also listed in Table 3 (Heyl. et al., 1965). Fluorites from Kentucky-Illinois are mainly pale yellow in color. Some are yellow-purple banded.

The exact localities of the fluorites from Mexico are not known, but in general, Mexican fluorites have been investigated by van Alstine (1961) and information about the general geological features are given in Table 3. The fluorites are pale purple, dark purple and colorless. Some of the purple fluorites are banded with colorless fluorite.

No details are available about the general geological features of the Thailand fluorites. They are generally dark and pale purple, green and colorless.

The approximate locality and Munsell color designation (Munsell, 1929) of each sample is listed in Table 4.

III.2.2. Chemical analyses

The results of the analyses of eight rare-earth elements, Sodium, Yttrium, Thorium and Uranium in ten fluorites and three fluid inclusion free samples are given in Table 5. Notice that there is little difference between the impurity concentrations of the whole samples of F-N-1, F-N-2 and F-N-7, and their fluid inclusion-free counterparts F-N-1W, F-N-2W and F-N-7W. It is most likely that the differences that are observed come from the error involved in the method used. However it is known that fluid inclusions may make up approximately 1% of the fluorite volume and the very concentrated impurities in them can effect the

Table 3. Geological features of Fluorites used in this study.

<u>Deposit Name</u>	<u>Mineral Occurrence</u>	<u>Host Rock</u>	<u>Intrusive Associations</u>	<u>Mineralogy</u>	<u>Homogenization Temperature</u>
Hansonburg (NM)	Open space filling, limestone replacement	Pennsylvanian limestone and arkose	Dikes and sills in vicinity	sphalarite, barite, galena quartz, fluorite calcite	192-198°C
Gonzales (NM)	Vein filling minor replacement	Precambrian granite	none exposed nearby	sphalarite, barite, galena quartz, fluorite calcite	189°C
Magdalena Mtns. (NM)	Open space filling, limestone replacement	Mississippian limestone	many stocks and dikes in vicinity	barite, fluorite galena quartz	185°C
Gila (NM)	Vein filling	Tertiary volcanics	none exposed nearby	fluorite quartz	195°C
Kentucky-Illinois	Vein deposits or bedded replacement deposits	Breccia	dike and sills	calcite-fluorite, barite and galena	207-243°C
Mexico	Veins, pipes, conical bodies, tubular and irregular replacement bodies	Limestone, shale or volcanic rocks	Rhyolite	fluorite, calcite and quartz (small amount of barite, celestite gypsum, native sulfur, pyrite and galena)	187-190°C

Table 4. Approximate locations and Munsell color designations of natural fluorites.

Sample Number	Approximate Location	Munsell hue, Munsell number/ Munsell chroma	Designated color name
F-N-1	Bingham, N.M.	5 G 9/2	very pale green
F-N-2	Bingham, N.M.	5 B 7/6	light blue
F-N-3	Bingham, N.M.	10 P 6/8 - colorless	light reddish purple - colorless
F-N-4	Bingham, N.M.	5 B 7/4 - colorless	pale blue - colorless
F-N-5	Magdalena, N.M.	5 GY 8/2	pale yellow green
F-N-6	Gila Dist., N.M.	10 P 5/8 - 5 G 7/6 - colorless	moderate reddish purple - light green - colorless
F-N-7	Gonzales, N.M.	10 GY 7/4	pale yellowish green
F-N-8	Rock Dist., IL-KY	10 PB 7/4	very pale bluish purple
F-N-9	Illinois-Kentucky	5 Y 9/6	light yellow
F-N-10	Illinois-Kentucky	5 Y 8/6 - 5 P 6/4	moderate yellow - pale purple
F-N-11	Illinois-Kentucky	5 P 6/6	light purple
F-N-12	Illinois-Kentucky	5 Y 8/4	weak yellow
F-N-13	Mexico	5 P 7/2	pale purple
F-N-14	Mexico	colorless	colorless
F-N-15	Mexico	10 P 7/6	light reddish purple
F-N-16	Thailand	5 YR 7/2 - 5 GY 7/2	weak orange pink - colorless - weak yellow - green
F-N-17	Thailand	5 Y 8/3	weak yellow
F-N-18	Thailand	5 RP 8/2	pale purplish pink
F-N-19	Thailand	8 GY 8/2	pale yellow green
F-N-20	Thailand	5 YR 7/2	weak orange pink
F-N-21	Thailand	5 Y 8/2	yellowish grey
F-N-22	Thailand	colorless	colorless
F-N-23	Thailand	10 PB 2/4	dusky bluish purple
F-N-24	Mexico	5 P 3/6	dark purple

Table 5. Analyses of rare-earth elements, Y, Na, Th, and U which present in Natural fluorites. All results are in ppm. Sign of - indicates not detected and not A indicates not analyzed.

	La	Ce	Nd	Sm	Eu	Tb	Yb	Lu	Y	Na	Th	U
F-N-1	3.14	4.82	0.46	1.87	0.23	1.21	0.57	0.03	74.0	83.0	0.02	0.07
F-N-1W	3.49	4.95	not A	1.10	0.31	1.40	0.53	0.03	66.0	59.0	-	0.07
F-N-2	1.27	2.52	4.71	1.59	0.53	4.42	1.40	0.06	106.0	125.0	-	0.05
F-N-2W	0.98	1.96	1.62	2.12	0.66	3.83	1.13	0.02	90.0	97.0	-	-
F-N-3,4	0.66	1.29	1.37	0.43	0.18	0.64	0.14	0.44	26.0	114.0	-	0.08
F-N-5	7.95	7.95	not A	3.34	0.81	2.75	2.74	0.19	130.0	63.0	-	0.07
F-N-6	25.74	35.38	0.77	4.50	1.58	1.50	0.40	0.04	17.0	41.0	0.09	0.29
F-N-7	7.08	12.07	0.54	2.24	0.28	1.22	2.17	0.38	85.0	73.0	-	0.08
F-N-7W	5.32	11.50	not A	2.27	0.19	1.14	1.84	0.47	83.0	63.0	-	0.05
F-N-9	0.27	0.77	4.61	1.07	0.38	1.32	0.25	0.02	29.0	341.0	0.07	-
F-N-14	1.01	1.03	-	0.36	0.06	0.03	0.27	-	9.2	141.0	0.02	-
F-N-15	1.33	0.96	0.08	0.60	0.13	0.44	0.28	0.05	14.0	144.0	-	0.10
F-N-24	0.82	0.50	-	0.13	-	0.11	0.02	-	2.7	118.0	1.19	0.13

results. Nevertheless, most of the analyzed impurities are located at the structure of the fluorite itself.

As indicated by the results of the analyses for rare earth elements, the whole fluorite samples under study are richer in the light rare-earth elements as compared to heavy rare-earth elements. However, generally not all of the samples follow the Oddo-Harkins rule, indicating that the rare-earth elements were selected by the fluorite, rather than occurring naturally (Fig. 18). Another more important point made from the analyses is that the light rare-earth element concentrations differ from color to color; i.e., rare-earth element concentrations increase with colors in order of purple, yellow, white, blue and green. The total concentrations of rare-earth elements increase with color in the same order. Yttrium is concentrated in green and blue fluorites, with lower concentrations in yellow, white and purple fluorites, similar to that of rare-earth elements (see Table 4 and 5).

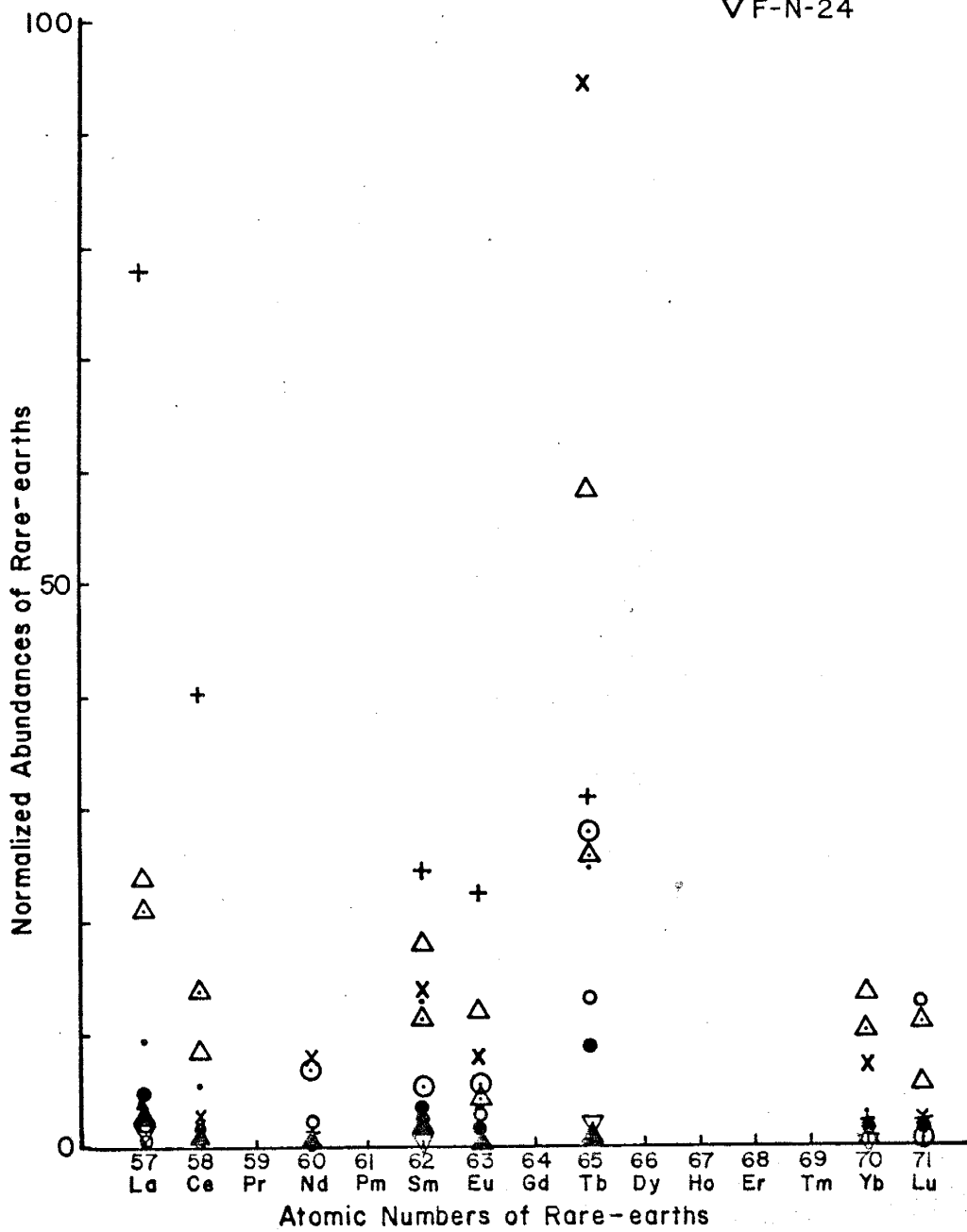
Impurities of Sodium occur in increasing concentrations in order of green, white, blue, purple, and yellow. Radioactive Thorium is highly concentrated in F-N-24, which is purple. Uranium shows a different trend, increasing in concentration with color in the order of white, yellow, blue, green and purple. From these observations it is seen that rare-earth elements, Yttrium, monovalent ions and radioactive materials all contribute to the coloration of fluorite differently, and their composite contributions define the observed specific coloration.

III.2.3. Absorption spectrum measurements

As mentioned earlier in Chapter II, an attempt was made to measure

Fig. 18. Plotting of rare-earth normalized abundances versus atomic numbers of rare earths. All the samples generally do not follow Oddo-Harkins rule.

- F-N-1
- x F-N-2
- o F-N-3
- △ F-N-5
- + F-N-6
- △ F-N-7
- ⊙ F-N-9
- ▲ F-N-14
- F-N-15
- ▽ F-N-24



the absorption spectra of the samples between 2000A° and 10000A°. However, because of instrumentation used, only the interval between the 2500A° and 7000A° wavelengths could be measured.

The absorption spectrum was taken of two colorless fluorites, namely F-N-14 and F-N-22. Both samples showed only a weak ultraviolet region absorption band at 3050A° (Fig. 19).

Nine various intensities of purple coloration were observed in fluorites measured in terms of their absorption spectrums. As shown in Figure 20 and 21, F-N-13, -15, -20 and -23 exhibit ultraviolet absorption bands at 3050A°. F-N-13 also shows weak 4100A°, 5100A° and 6000A° absorption bands while F-N-20 and F-N-23 show a weak 5800A° absorption band and a very intense 5650A° absorption band, respectively. F-N-8 exhibits 3250 and 5400A° absorption bands, F-N-3 shows 4000 and 5800A° absorption bands, while F-N-18 exhibits only a 6100A° absorption band. F-N-11 is characterized only by a 550A° absorption band. A very intense 5600A° absorption band was produced by the F-N-24. F-N-18 and -20 indicate some possibility of an ultraviolet region absorption band the wavelength of 2500A°.

The absorption spectrum of two blue fluorites show very well defined visible region absorption bands. F-N-2 and F-N-4 exhibit 2800A°, 3275A°, 3900A° and 5800A° absorption bands, and 4000A° and 5870A° absorption bands respectively (Fig. 22). The blue fluorites show very weak ultraviolet region absorption bands at 3050A°.

Six green fluorites all show a very well defined ultraviolet absorption band at 3050A°. The fluorite F-N-6 has the most intense ultraviolet absorption band at 3050A°, in addition to very well defined

Fig. 19. Absorption spectra of natural colorless fluorites, F-N-14 from Mexico, and F-N-22 from Thailand.

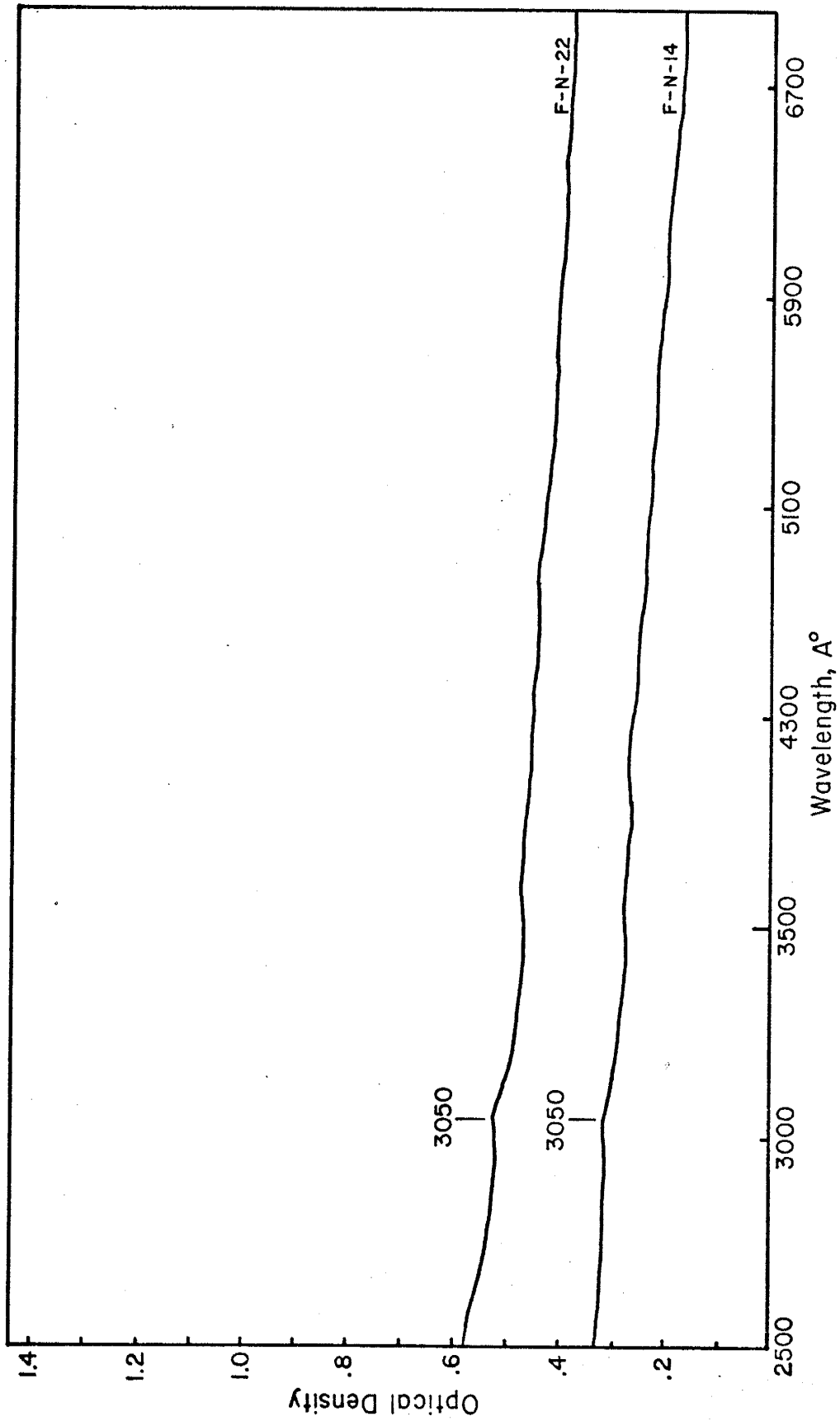


Fig. 20. Absorption spectra of purple colored natural fluorites.

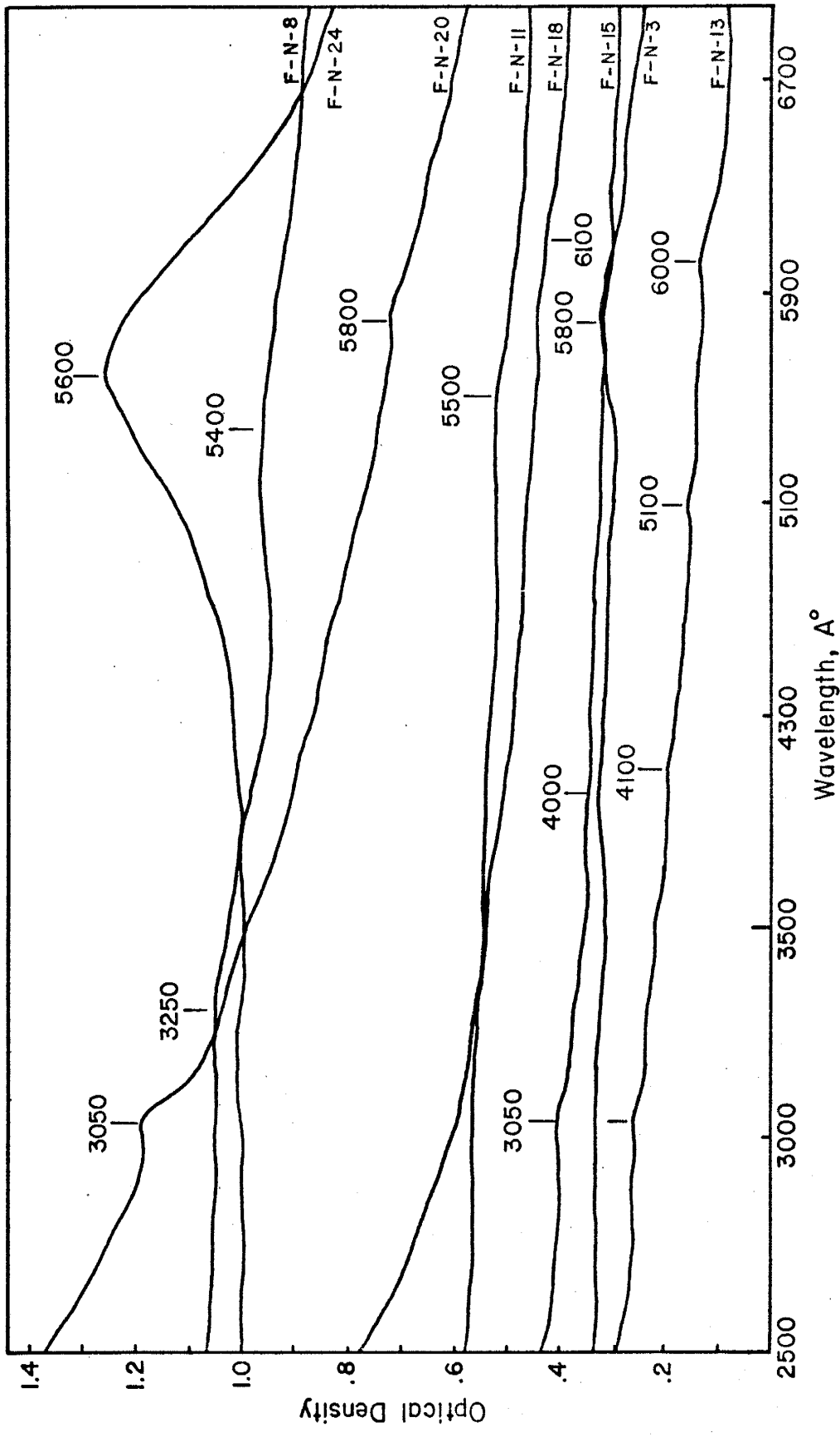


Fig. 21. Absorption spectrum of purple and colorless banded fluorite.

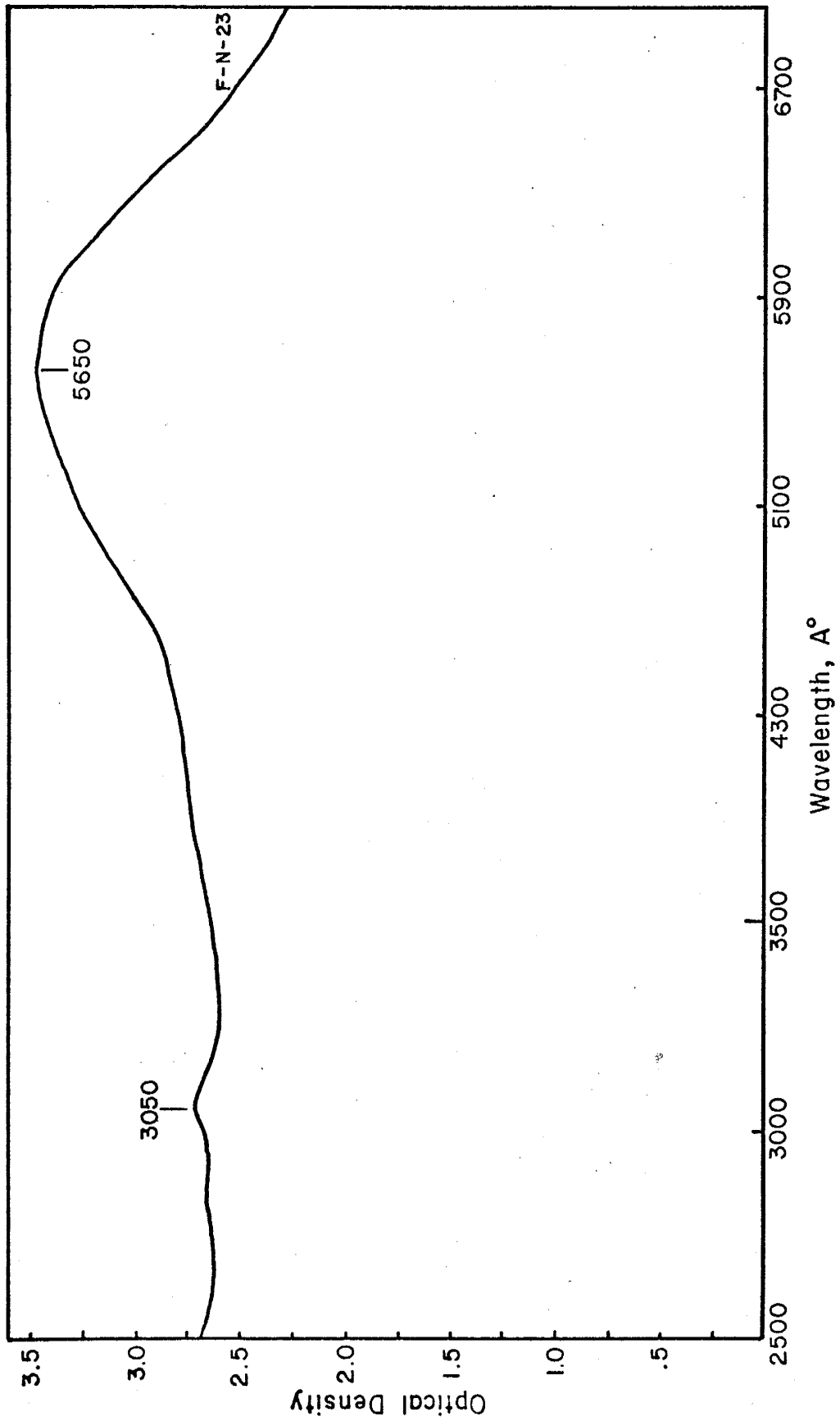
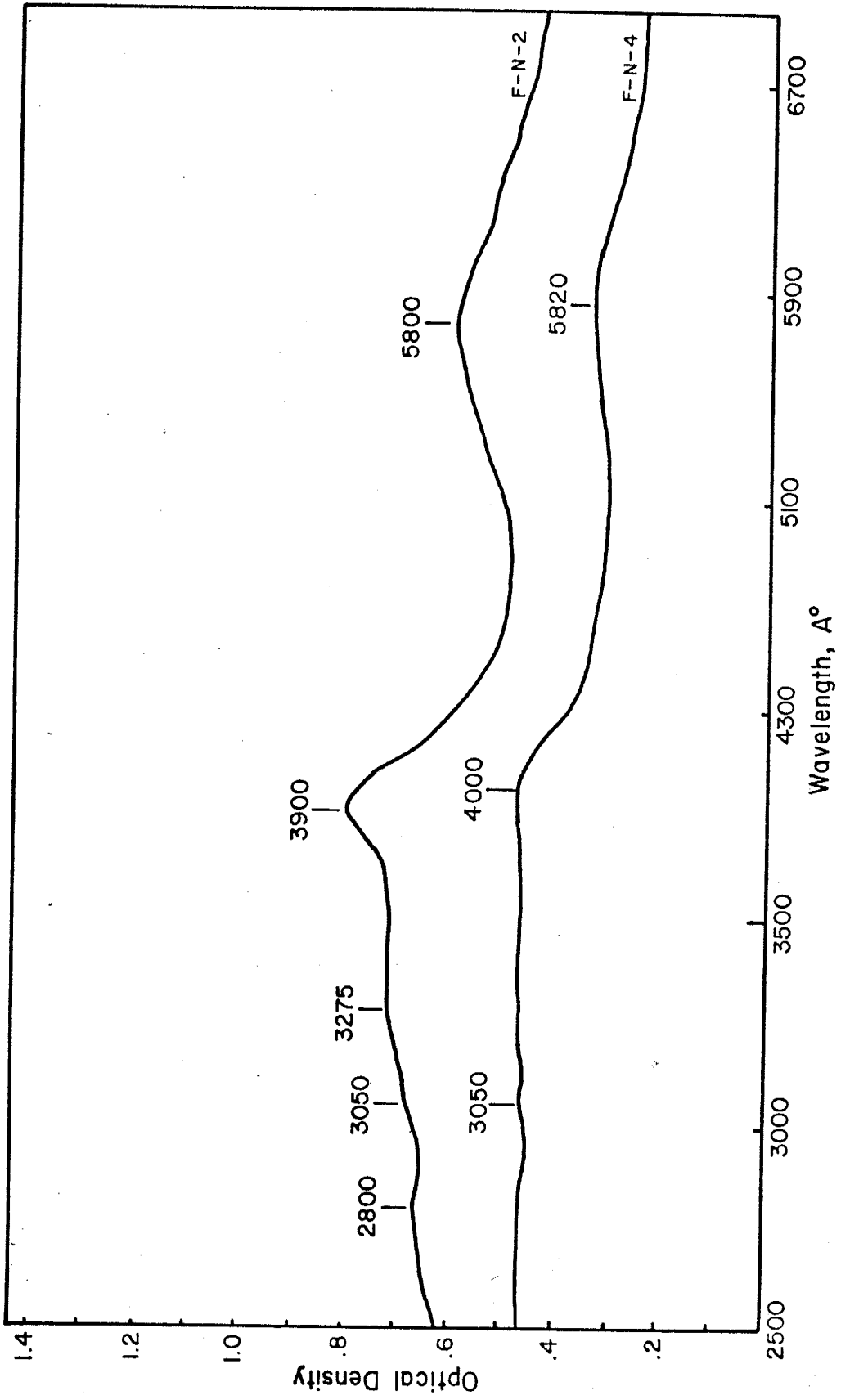


Fig. 22. Absorption spectra of blue and blue-colorless banded natural fluorites.



4000Å° and 5400Å° absorption bands. F-N-5 and F-N-16 have 4100Å° and 5900Å° absorption bands, and 6000Å° absorption bands respectively, while F-N-7 shows 4450Å° and 5800Å° absorption bands. The 4700Å° and 5800Å° absorption bands of F-N-1 have almost the same intensity as that of the 3050Å° absorption band of the ultraviolet region. F-N-19 has quite an intense 3050Å° absorption band in the ultraviolet region, but weak 4250Å° and 5820Å° absorption bands in the visible region (Fig. 23 and 24).

F-N-12, one of the four yellow colored fluorites, has a very weak ultraviolet absorption band at 3050Å°; very weak 4400Å° and 5800Å° absorption bands are also observable. F-N-10, which is banded with purple coloration, has only one broad absorption band at 4300Å°, and possibly one ultraviolet region absorption band in addition to the very broad 5300Å° absorption band; an ultraviolet region absorption band below 2500Å° can be expected. F-N-21 and F-N-17 show no clear absorption bands, with very high background absorption and possibly an absorption band below 2500Å° (Fig. 25 and 26).

Both F-N-3 and F-N-4 are samples of the same single Bingham fluorite; the purple-colorless banded part of the crystal is the F-N-3, and the blue-colorless banded part is F-N-14. The samples have different visible region spectra and also exhibit different ultraviolet absorption spectra; F-N-3 does not show the 3050Å° absorption band, while F-N-4 does. Purple colored F-N-11 and yellow colored F-N-12 come as a chunk from the same Kentucky-Illinois deposit; F-N-12 has an 3050Å° absorption band, while F-N-11 does not show this absorption band in the ultraviolet region. However, F-N-13 and F-N-14, which are pale purple and colorless,

Fig. 23. Absorption spectra of green fluorites.

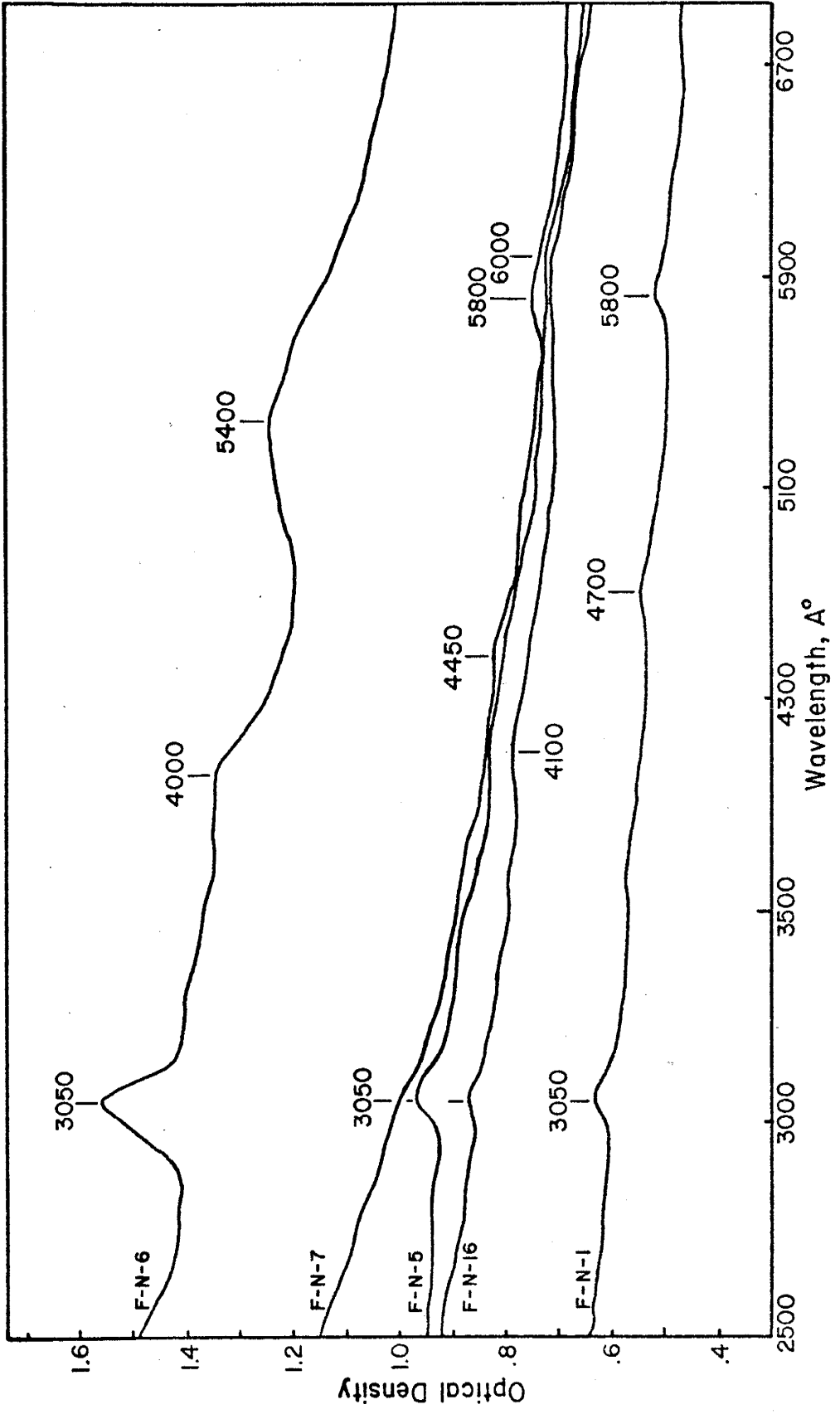


Fig. 24. Absorption spectrum of green fluorite.

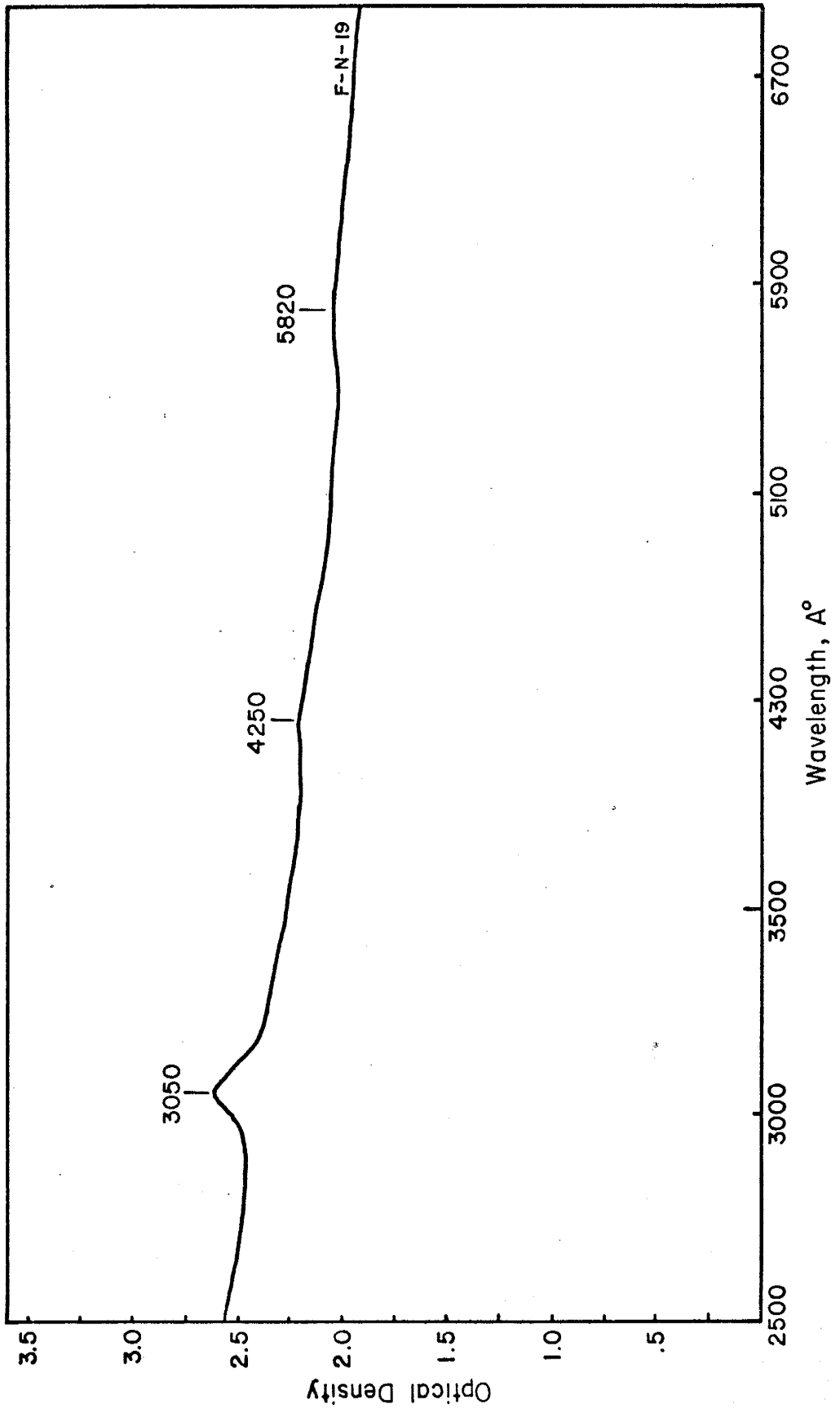


Fig. 25. Absorption spectra of yellow colored natural fluorites.

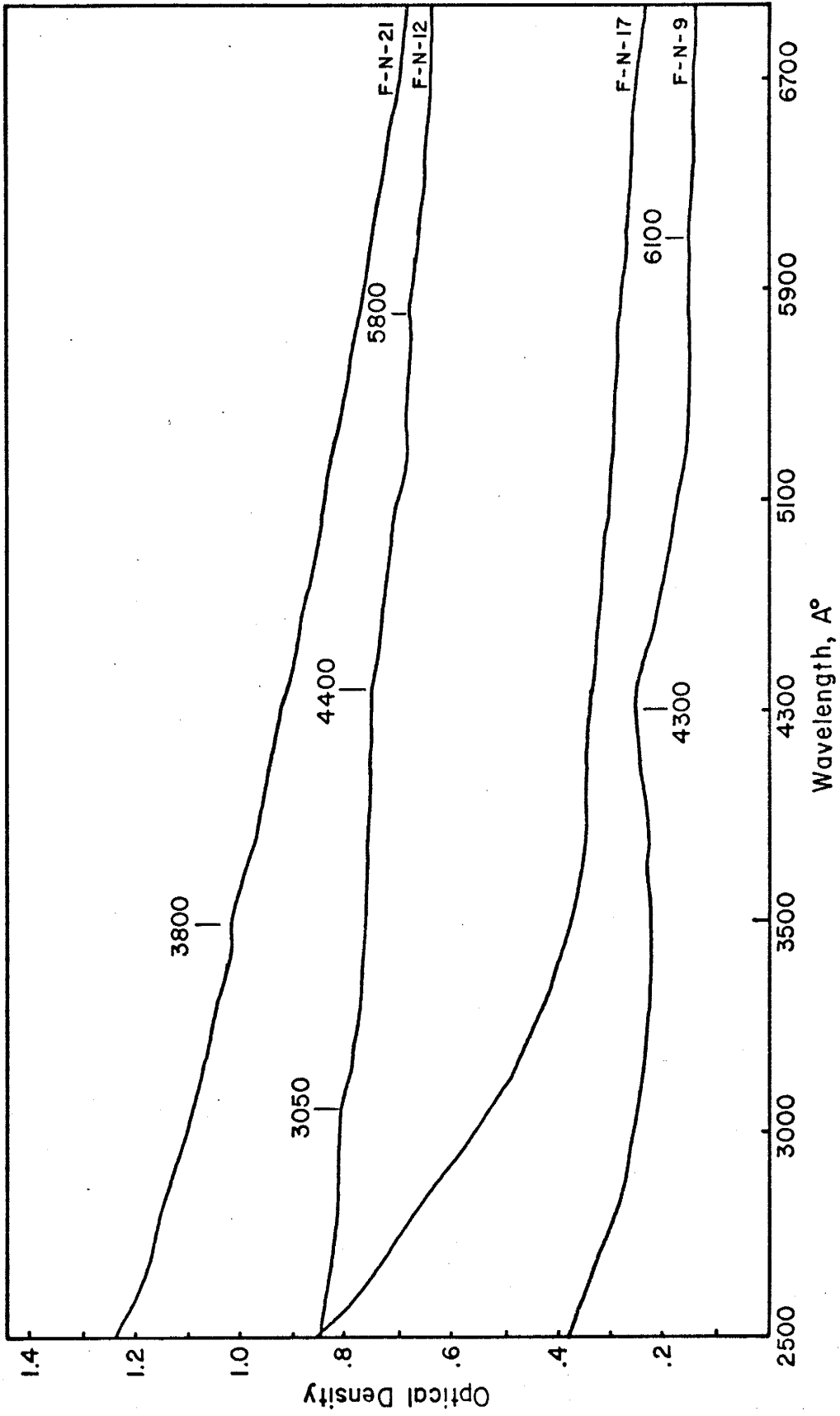
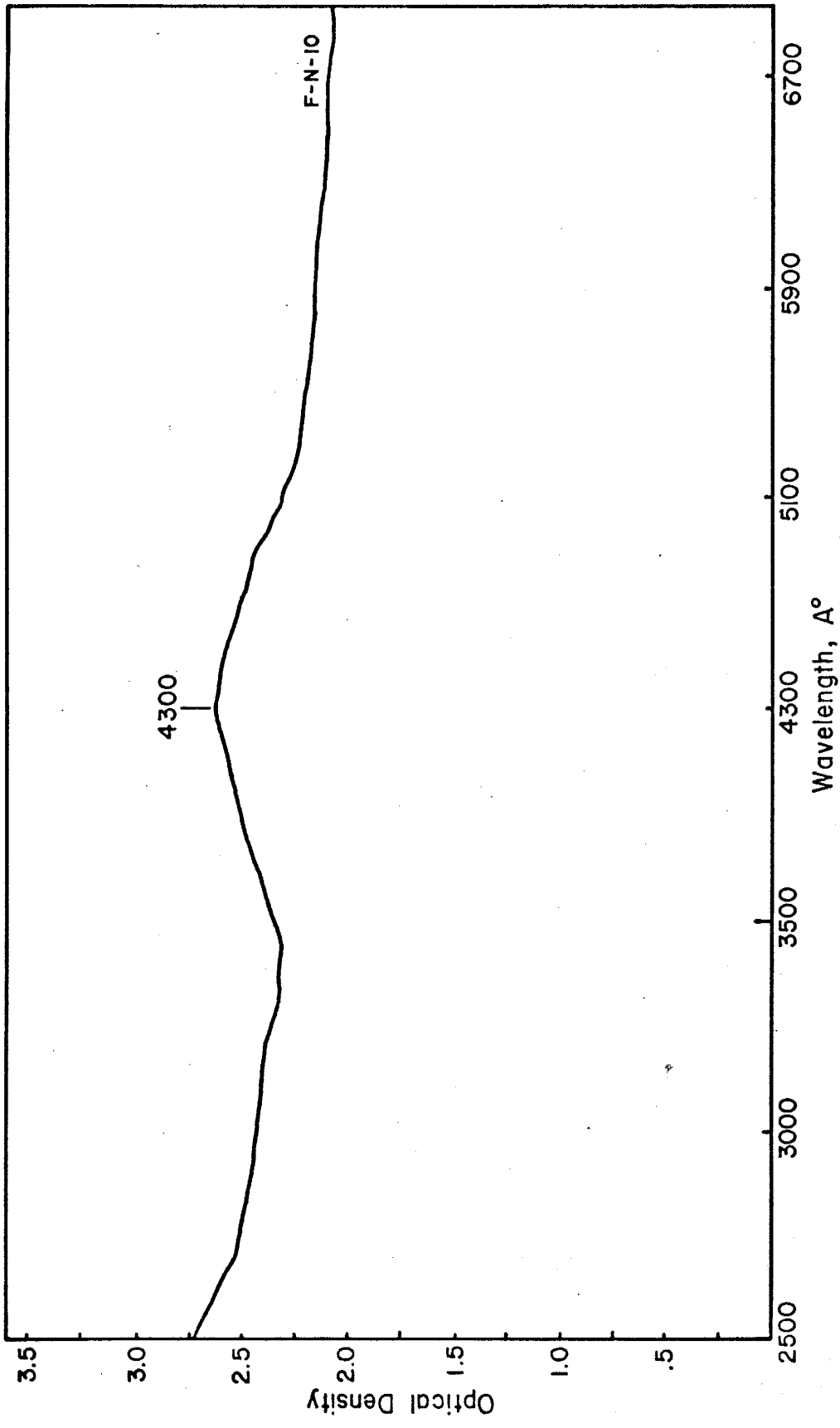


Fig. 26. Absorption spectrum of yellow and purple banded natural fluorites.



respectively, and come from the same deposit in Mexico, both have the same intensity of the 3050A° ultraviolet region absorption band. This optical property indicates that the generation of coloration and absorption bands are defined by chemical properties which were changed during the growth of the samples.

As indicated in section III.2.2. of the chemical analyses, impurities are a controlling factor of coloration, and because the coloration is defined by the presence of absorption bands, impurities involved in each sample could define these absorption bands. Thus, in order to obtain any relation between impurities and absorption bands, the concentrations of the color center absorption bands, and the concentrations of impurities, need to be analyzed and compared.

The concentrations of color centers were calculated using the Smakula-Dexter equation (Dexter, 1956)

$$n_c f = 0.87 \times 10^{17} \frac{n}{(n^2 + 2)^2} \alpha_{\max} W_{eV}$$

where n_c is the number of the color centers per cm^3 , f is the oscillator strength for the specific absorption, n is the refractive index for the wavelength at the peak of absorption, α_{\max} is the optical absorption coefficient at the absorption maximum and W_{eV} is the half width in eV of absorption band. The product $n_c f$ is a measure of concentration of color centers. Throughout the text, the value of $n_c f$ is regarded as color center concentration. Also, since the value of n for wavelength at the peak of absorption does not change greatly in the range in which this study is involved, n was assumed to be constant, at 1.434 for each wavelength (Ramachadran, 1947).

The color center concentrations of the samples ($n_c f$) were calculated, taking into account each absorption band of each sample. The plotting of the color center concentration of the ultraviolet absorption band at 3050\AA versus the concentration of each of the rare-earth elements shows that the concentrations of the light rare-earth elements, La, Ce and Sm in the fluorites increase as the color center concentrations of the 3050\AA absorption band increase (Fig. 27 and 28). This suggests that the 3050\AA absorption band and rare-earth elements are related, and that the absence of the rare-earth elements causes the absence of the 3050\AA absorption band. However, the plot of the color center concentration of absorption bands in the visible region between $5600\text{--}5900\text{\AA}$ versus La, Ce and Sm concentrations shows a different trend. As the concentrations of these rare-earth element increase, the color center concentrations of the absorption bands between $5600\text{--}5900\text{\AA}$ decrease (Fig. 29 and Fig. 30). This indicates some involvement of rare-earth elements in the occurrence of visible region absorption bands. Similar plotting of the color center concentrations of $3900\text{--}4700\text{\AA}$ absorption bands showed no definite trend. Graphs of Yttrium concentrations versus the color center concentrations of the 3050\AA , $3900\text{--}4700\text{\AA}$ and $5600\text{--}5900\text{\AA}$ absorption bands also showed no pattern or trend. Points were distributed very randomly.

Plotting of Sodium concentration versus the color center concentration of the 3050\AA absorption band (0 designation, Fig. 32a) showed the 3050\AA absorption band to be suppressed by sodium concentration, i.e., the sodium concentration increases as the color center concentration of the 3050\AA absorption band decreases. However, the graph of sodium

Fig. 27. Plot showing the relation between color center concentration (n_c) of 3050Å absorption band as a function of La, Ce concentrations in natural fluorites.

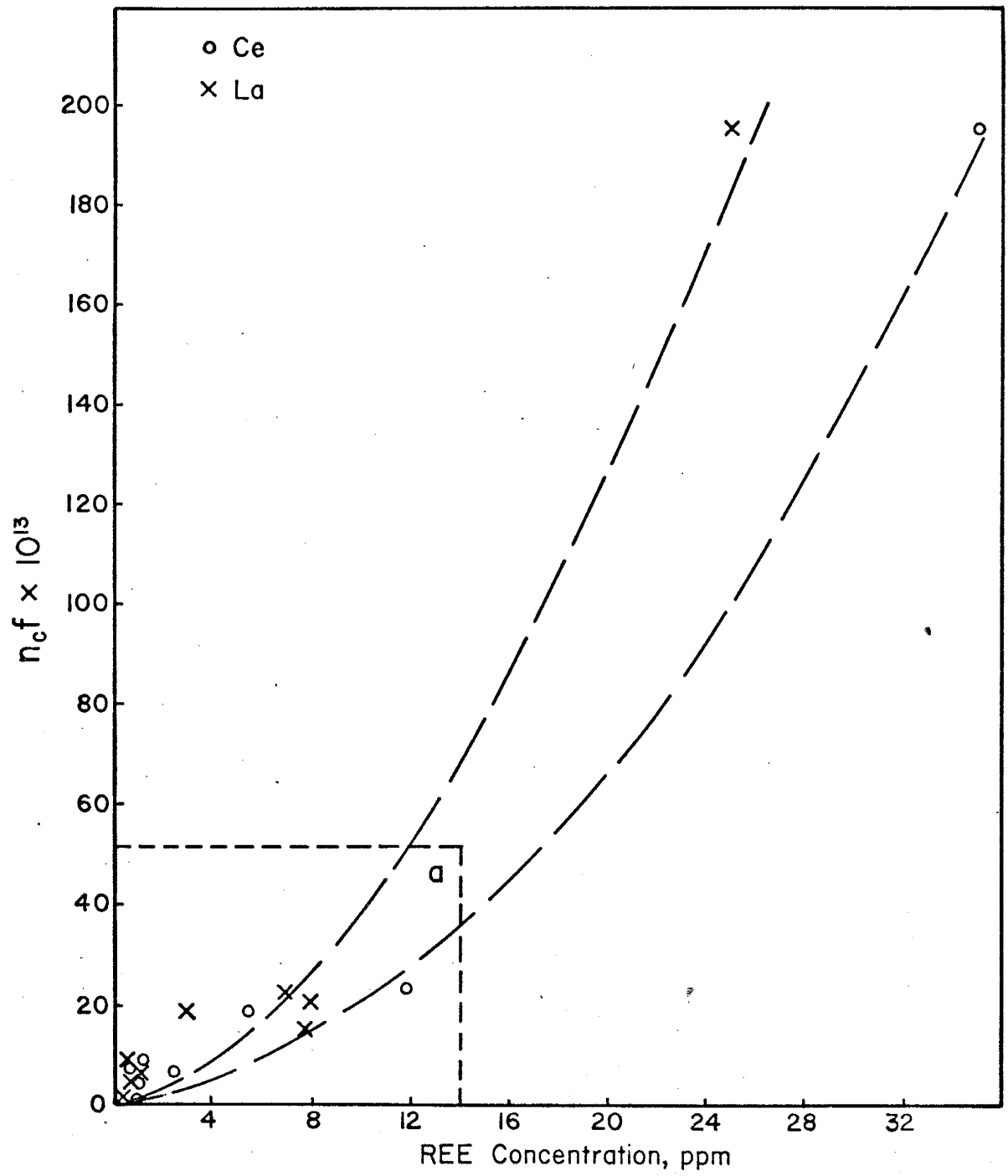


Fig. 27a. Enlargement of lower left corner of Fig. 27.

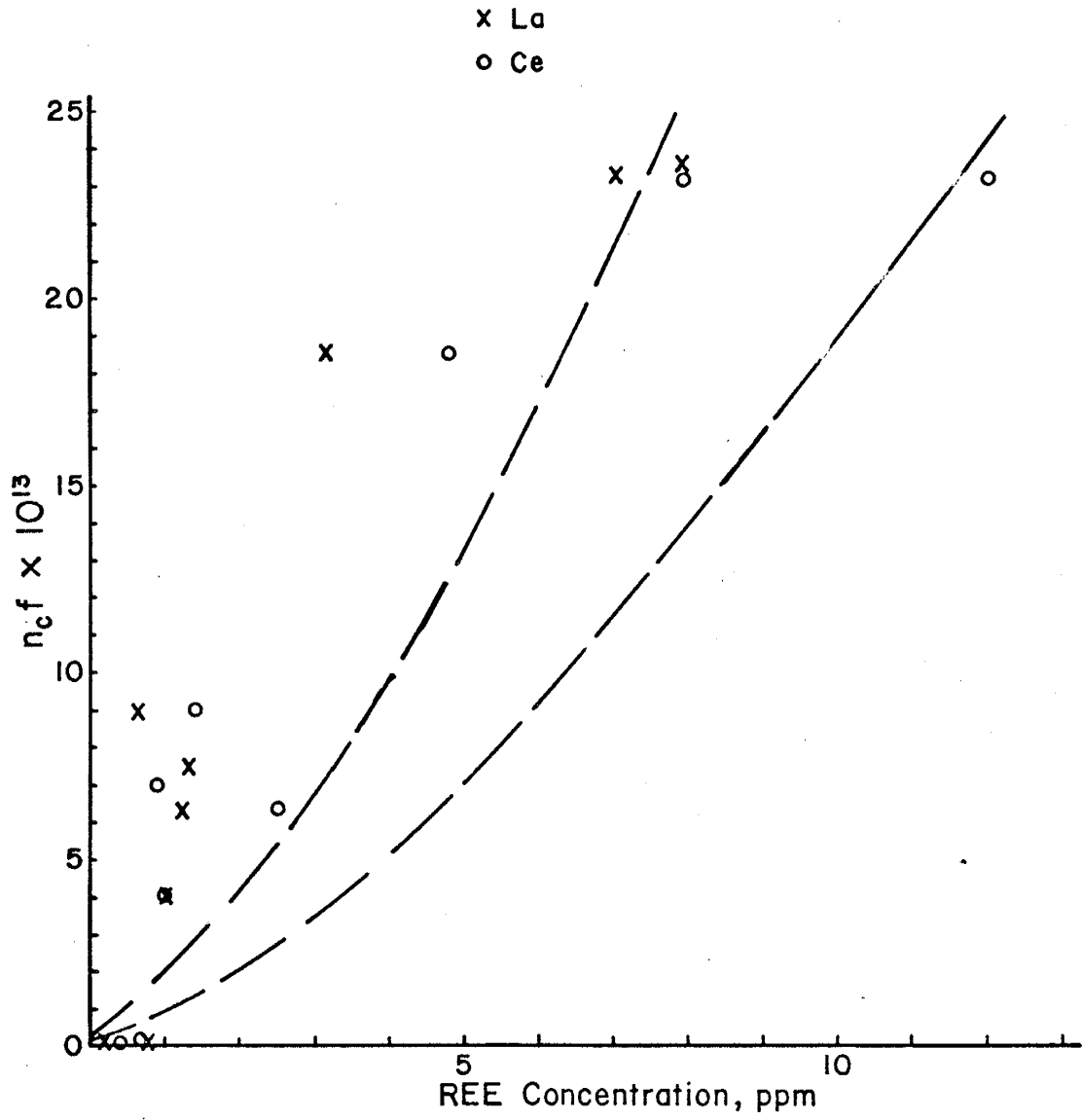


Fig. 28. Plot showing the relation between color center concentration (n_c) of 3050A° absorption band as a function of Sm concentrations.

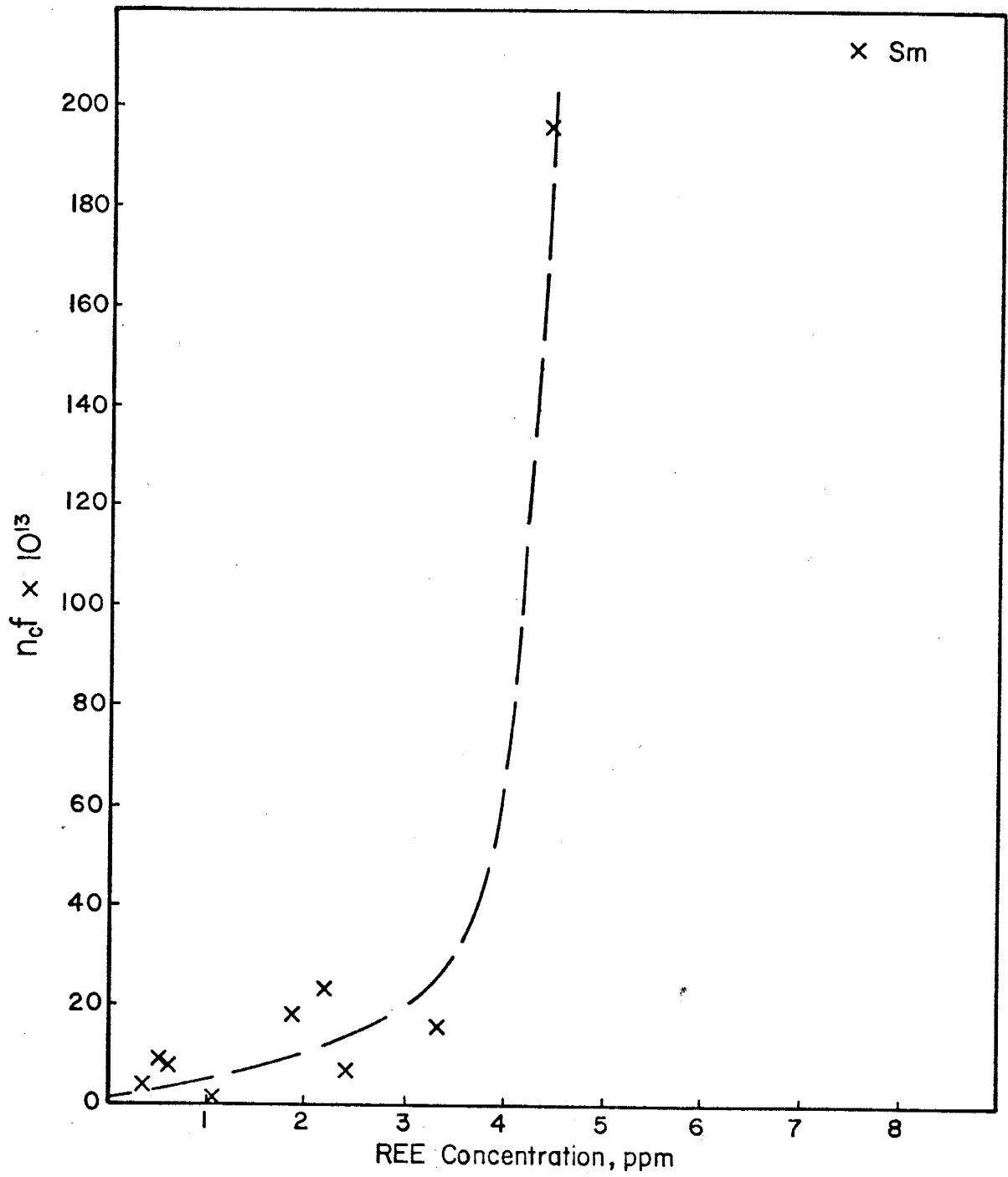


Fig. 29. Plot showing the relation between the color center concentration (n_f) of the 5600-5900Å absorption band as a function of La, Ce concentrations.

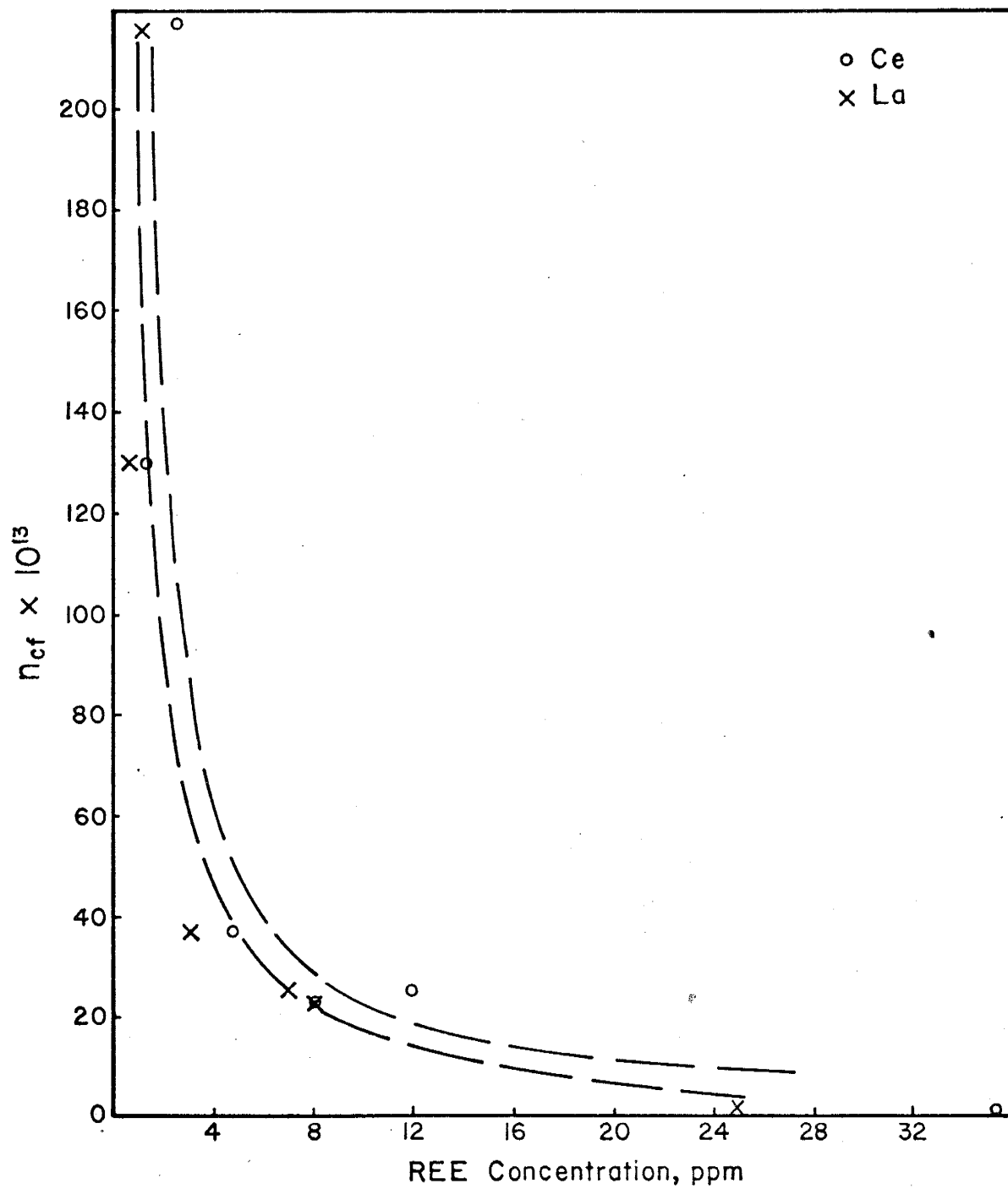
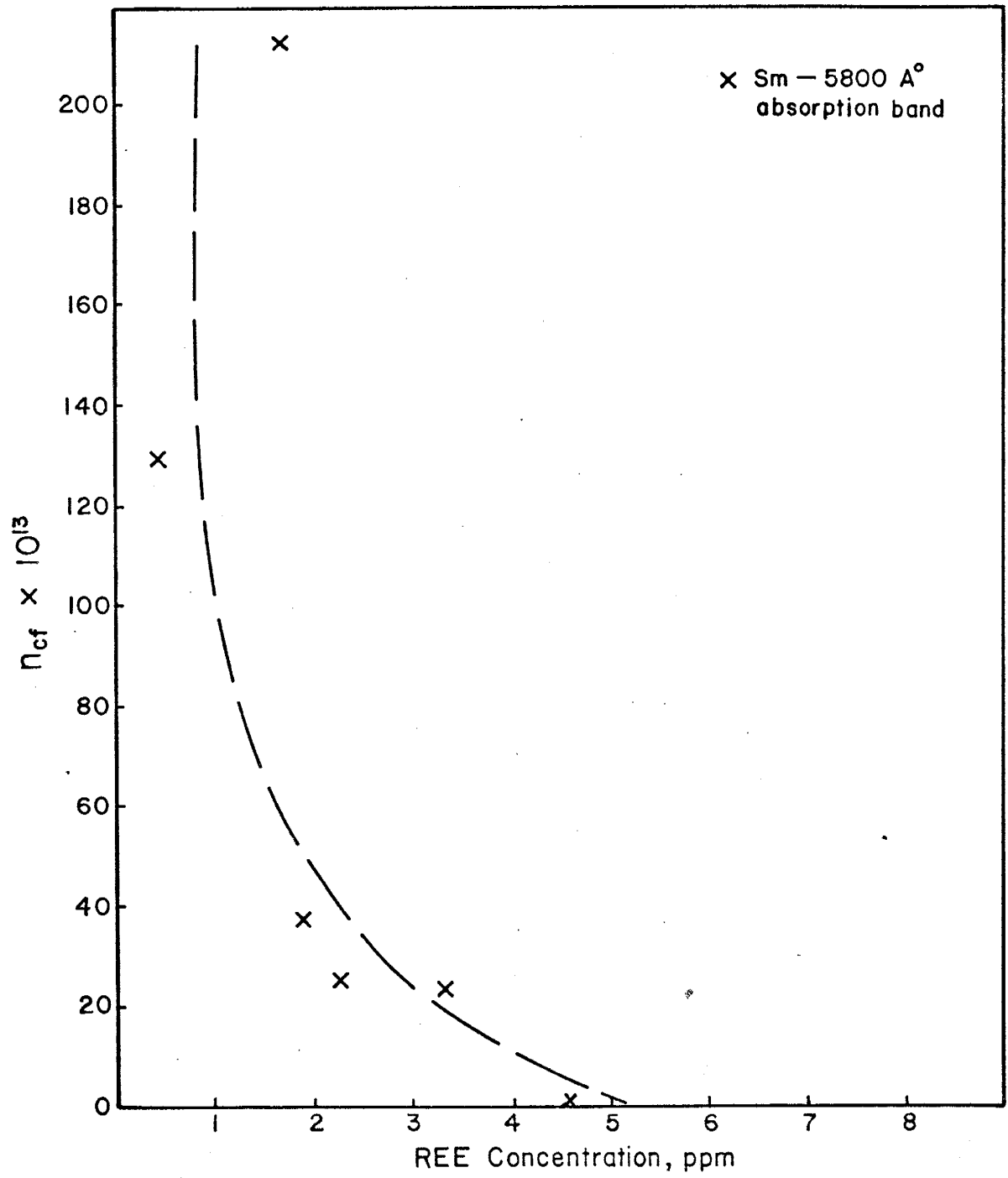


Fig. 30. Plot showing the relation between the color center concentration (n_c) of the 5600-5900Å absorption bands as a function of Sm concentration.



versus the color center concentration of the 5600-5900A° absorption band shows that sodium enhances the color center concentration of this band (x designation, Fig. 32a). Thus it appears that the visible region absorption band and ultraviolet region absorption bands are controlled by monovalent ions and trivalent ions, (Fig. 31), respectively.

The radioactive materials Uranium and thorium are generally present in fluorites. Concentrated amounts of K and Pb are contained in the fluid inclusions of the fluorite. Analyses showed that F-N-14 had 0.48×10^{-3} ppm K^{40} and 0.25×10^{-1} ppm Pb^{204} , but no Uranium and Thorium, while F-N-6 had 0.89×10^{-1} ppm Thorium, 0.29 ppm Uranium, 0.11×10^{-2} ppm K^{40} and 0.28×10^{-1} ppm Pb^{204} . Thus, Uranium rather than Pb and K, is the main contributor to the radioactivity of the samples. When rare-earth elements and radioactive materials are correlated in terms of their effect on the 3050A° absorption band, it appears that the 3050A° absorption band is present as long as the rare-earth elements are present. If there is little or no radioactive material but an abundance of sodium present the 5600-5900A° absorption bands do not appear. Thus the concentration of sodium and radioactivity are related in the generation of the 5600-5900A° absorption bands.

Although no relationship is evident between the 3900-4700A° absorption bands and any one of the isolated rare earth elements impurities, when the sodium concentration is plotted against the color center concentration of the 3900-4700A° absorption bands, as in Fig. 32b, an increasing trend is observable. This trend indicates that if rare-earth elements, Yttrium and radioactive material are present, the color center concentration of the 3900-4700A° absorption band increases as the sodium

Fig. 31. Plot of total rare earth element concentration ($n_c f$) versus 3050Å° and 5800Å° absorption bands.

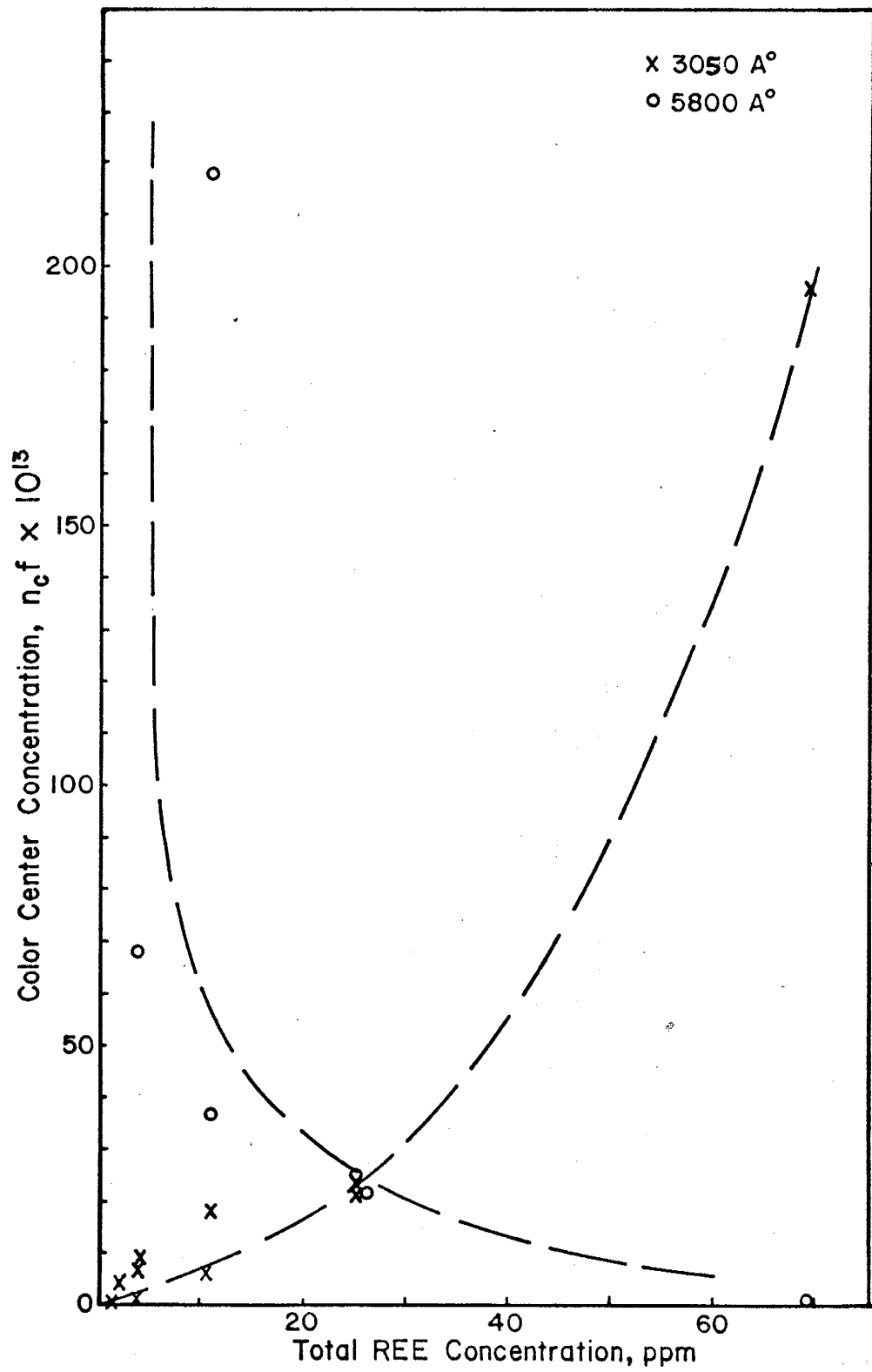


Fig. 32a. Plot of sodium concentrations versus the color-center concentrations (n_c) of the 3050Å° and 5600-5900Å° absorption bands.

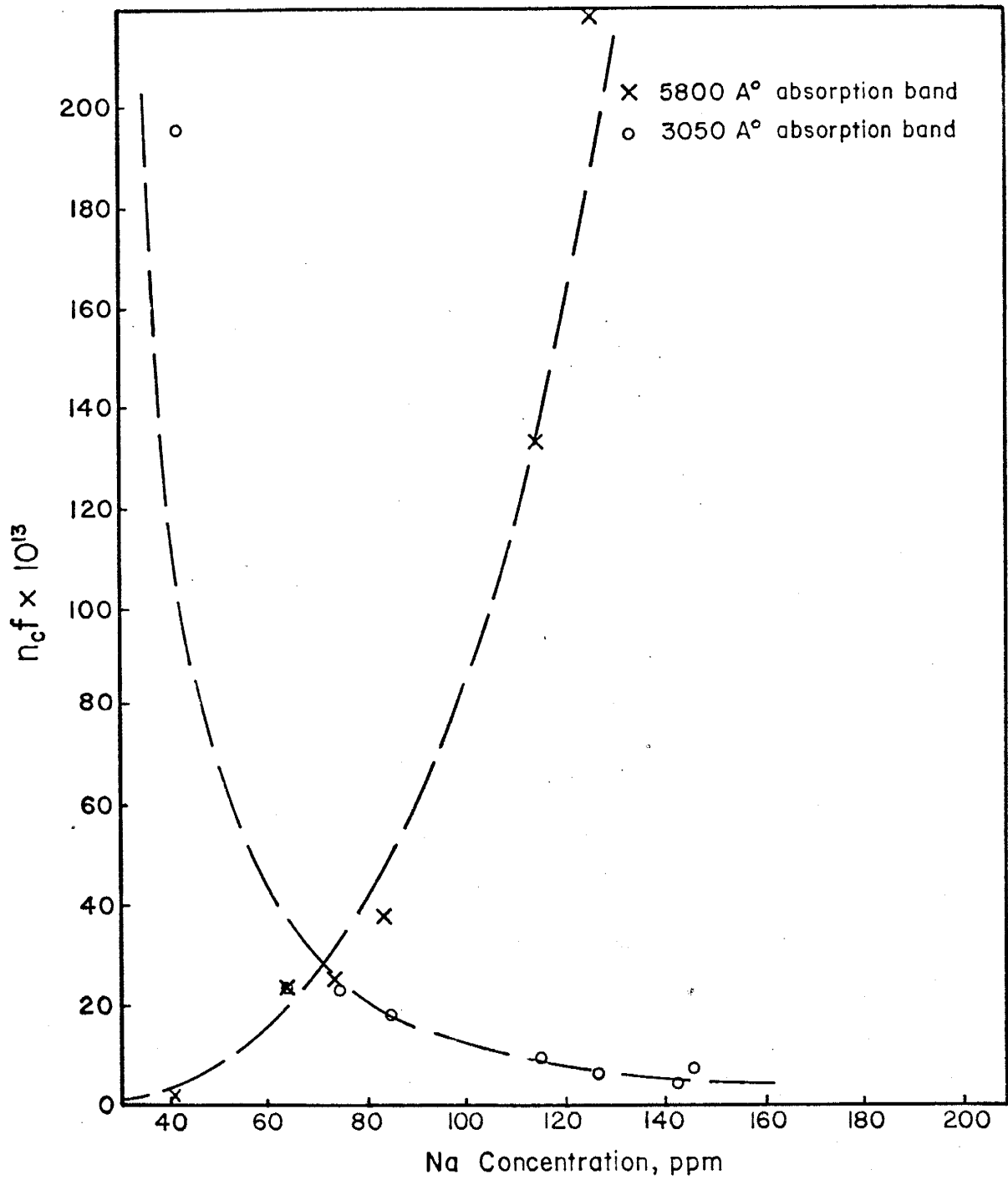
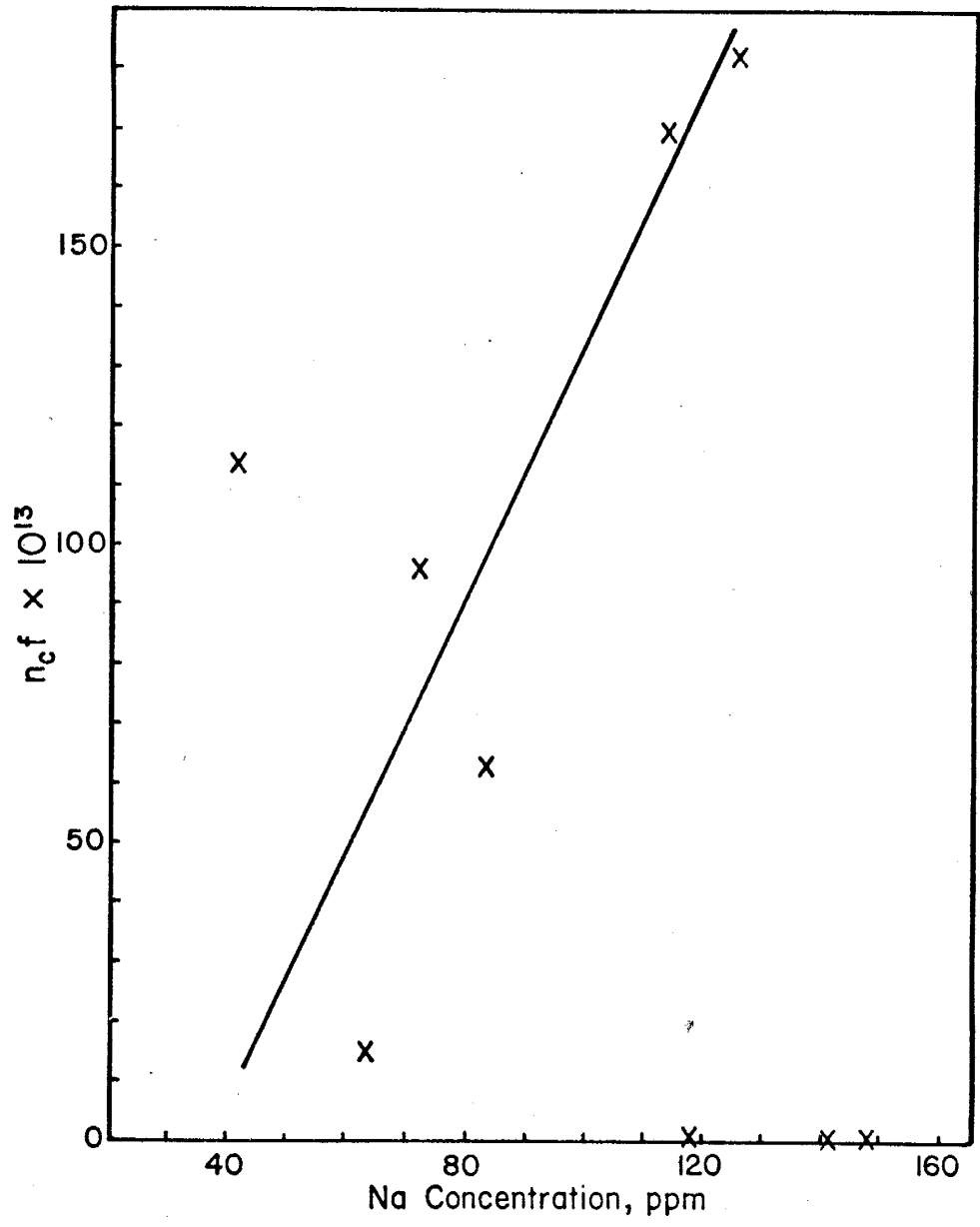


Fig. 32b. Plot of the 3900-4700A° absorption band versus Na concentration. The data points which are out of the increasing trend of sodium are low in REE + Yttrium and/or very high in concentration of radioactive material.



concentration increases. However, even the sodium concentration is low, if the radioactive material concentration is very high the center concentration of the 3900-4700A° absorption band increases. This result shows that the 3900-4700A° absorption bands are the most structurally complex color center of the absorption spectrum.

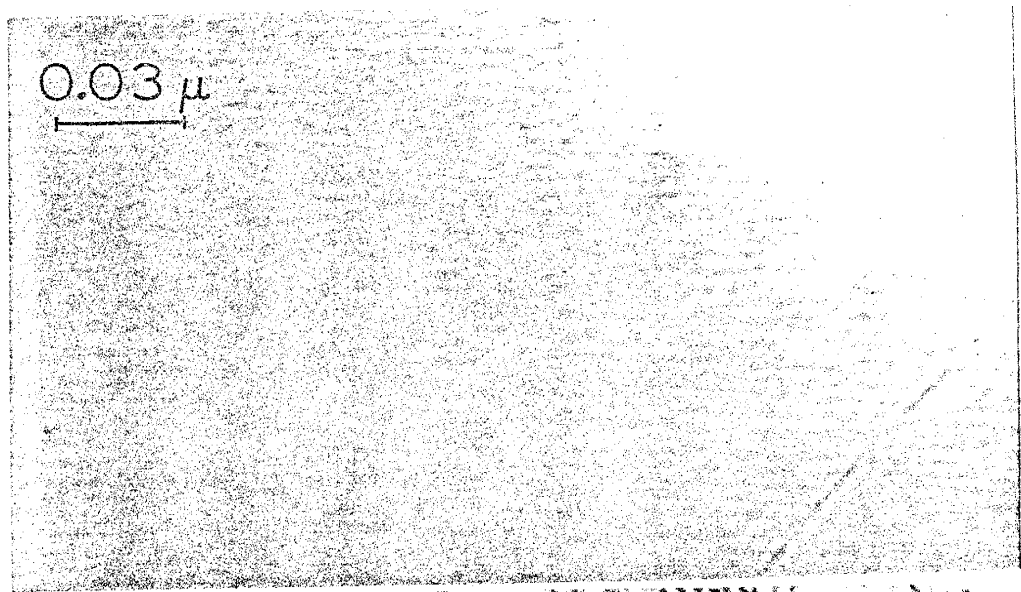
III.3. Transmission Electron Microscopy (TEM) studies of natural and synthetic fluorites

Because the main systematic cleavages in fluorite occur along the [111] plane, the fluorite flakes observed in the transmission electron microscope were oriented with (111) perpendicular to the electron beam almost without exception. When initially subjected to the electron beam, synthetic fluorite showed no observable defect structures; however, because of the electron irradiation, imperfections quickly started to develop. These developments of mosaic-like point defects or defect clusters continued until the photograph shown in Fig. 33a was taken, after 10 seconds of exposure to radiation (10 seconds is the minimum amount of exposure at which a micrograph could be taken with the electron microscope). It can be seen from the figure that the mosaic-like point defects exhibit an ordered array. As exposure to the electron beam continues beyond 10 seconds, the mosaic structure intensifies and grows by a gathering together of smaller structures. Fig. 33b shows the same area of the synthetic fluorite after saturation by the electron radiation (it takes about 5 minutes). Fig. 33b and Fig. 33c, which is a magnified part of Fig. 33b, show the development of an ordered hexagonal defect array which aggregated from other small

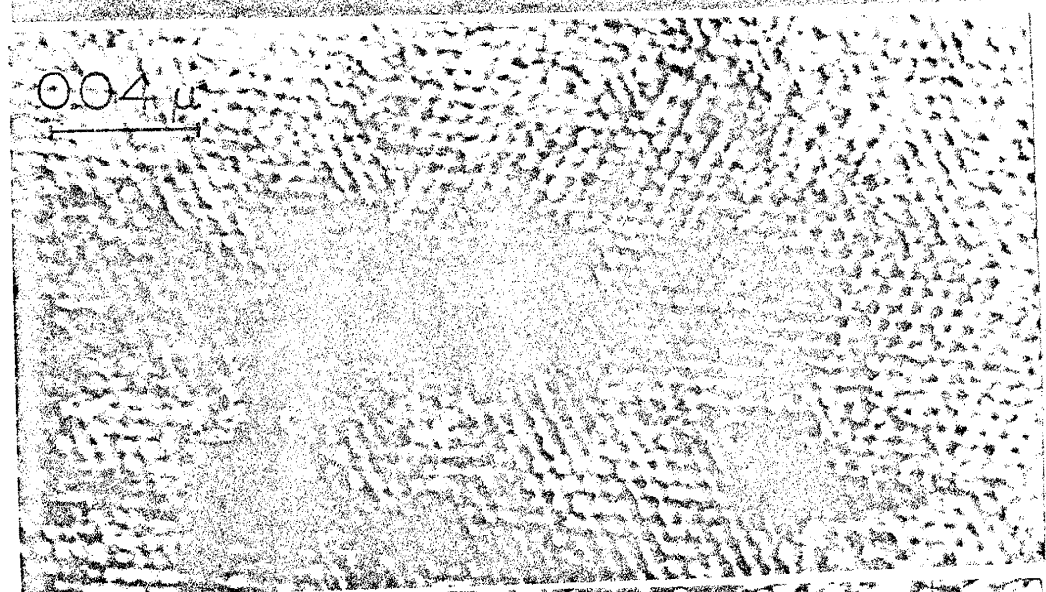
Fig. 33. Ordered defect aggregates of synthetic fluorite, and their development in (111) plane. a) Initial bright field electron transmission image of ordered defect aggregates, b) the same area of Fig. 33a, after electron irradiation saturation, c) Magnified portion of Fig. 33b), showing the hexagonal arrangement of individual defect aggregates.

defects, or defect aggregates. As the hexagonally ordered defect structure developed, the electron diffraction pattern of the same area developed superlattice reflections in the diffraction pattern on the (111) plane, along with the normal (111) reflection of calcium fluorite. The hexagonally ordered defect structure and the superlattice diffraction pattern developments are illustrated in Fig. 34. When the electron saturation was reached, single defect aggregates were approximately 60\AA in size and had hexagonal-like symmetry; no movement of these aggregates was observed after the electron-irradiation saturation. When the flake examined in the electron microscope was removed, it showed blue coloration, with different intensities depending on the exposure time; longer exposed areas showed purple coloration.

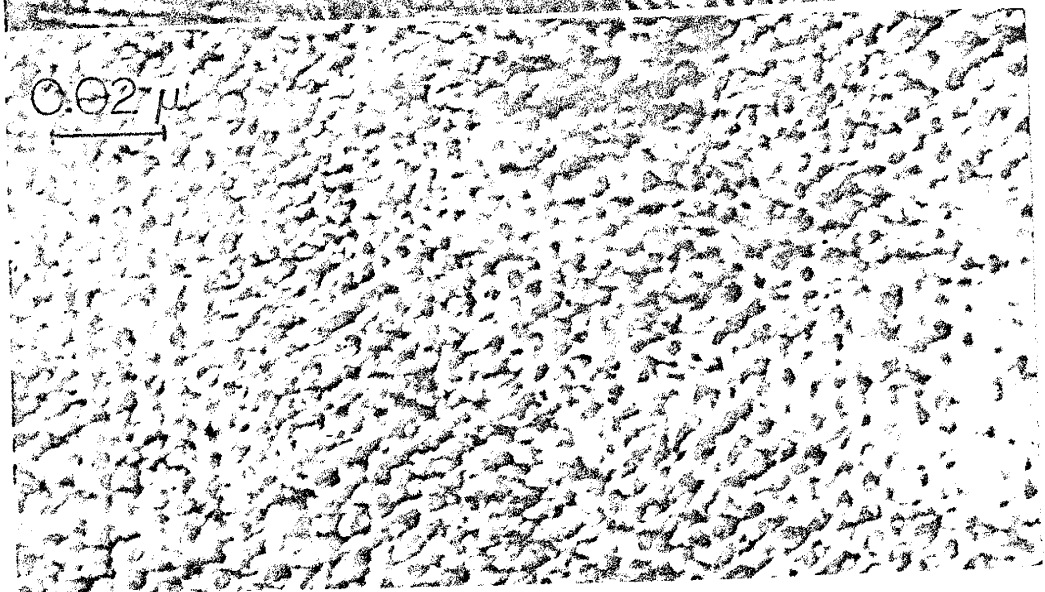
In contrast to the synthetic fluorite, purple colored natural fluorite (F-N-24) exhibited imperfections prior to the electron radiation. These imperfections are illustrated in Fig. 35 and are seen to be scattered over the flake under observation. The imperfections have been observed in other natural fluorites (Murr, 1974a), and consist of large dislocation loops exhibiting a double-arc or strain field contrast. Upon exposure to the electron beam, the loops started to move from the center of the specimen to the sides, where the electron beam was less intense. The loops also exhibited rapid expanding or contracting, or disappeared completely to generate the defect aggregates (mosaic-like structures), during the study of the sample. These loops aligned along the [110] direction, as illustrated in Fig. 35a. The area surrounding the loops, like the synthetic fluorites, started to generate mosaic-like defect aggregates after electron exposure.



a



b



c

- Fig. 34. a) Ordered arrangement of defect aggregates in the (111) plane of synthetic fluorite and an associated selected area electron diffraction pattern, after 3 min. exposure.
- b) Defect aggregates in the (111) plane of synthetic fluorite and associated diffraction pattern, with superlattice diffraction pattern development after electron-irradiation saturation has been reached.

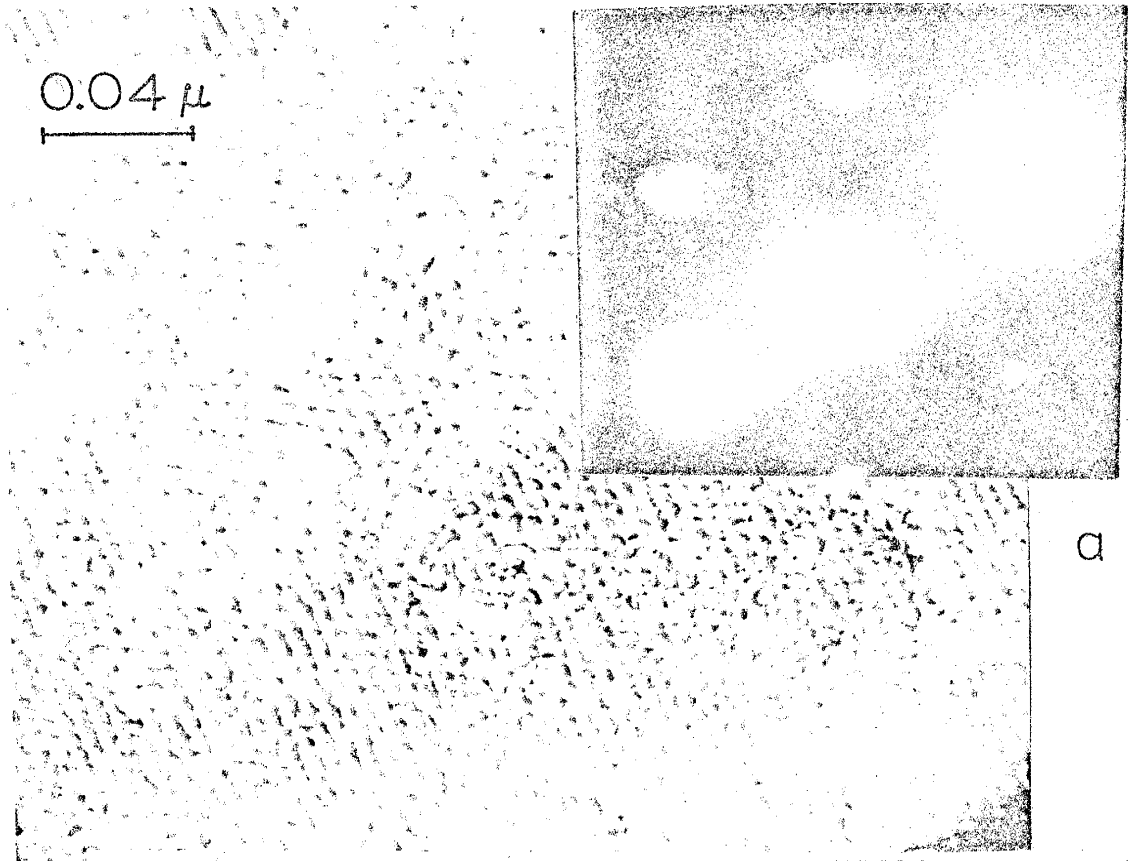
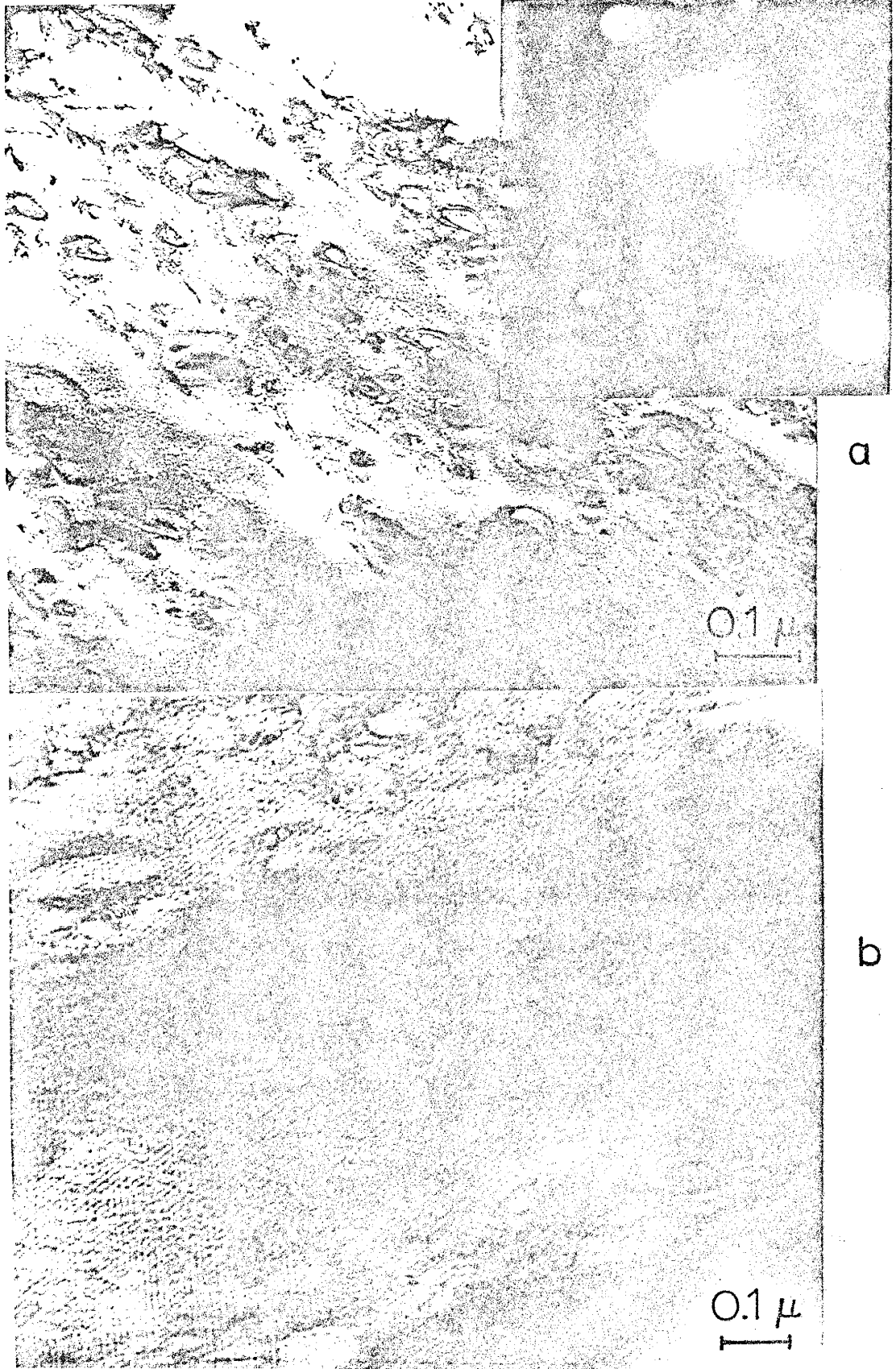


Fig. 35. (111) plane of purple colored natural fluorite a) Dislocation loops with defect aggregate mosaic structures in the background with associated selected area diffraction pattern, loops lying along 110 direction. b) The same dislocation loops with hexagonal arrangement of defect aggregates after an addition of 5 min of exposure.

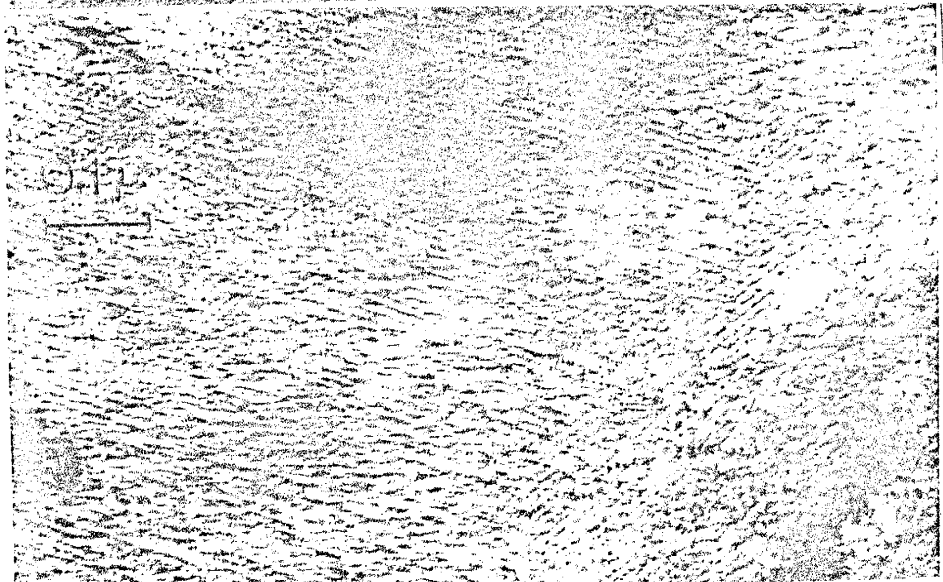


Development of these defect aggregates followed the same pattern as that of the synthetic fluorite, ending as a hexagonally-ordered defect structure. In Fig. 36, development of color-center aggregates in the naturally colored purple fluorite is illustrated, associated with a selected area diffraction pattern. As shown in the diffraction pattern, after a long exposure the selected area diffraction micrograph generated a superlattice diffraction pattern in addition to the normal calcium fluoride diffraction pattern. Because the electron microscope specimens were extremely thin (about 2500\AA) before study in the electron microscope, even very intense colorations were not detectable; however, after examination under the electron microscope, the sample exhibited the same intensive blue and purple coloration as the synthetic fluorites studied previously. It has been recognized that both pure (or approximately pure) fluorites and natural fluorites containing impurities generated the same kind of defect structures after electron irradiation; thus the generation of color by electron irradiation in the transmission electron microscope is not composition related.

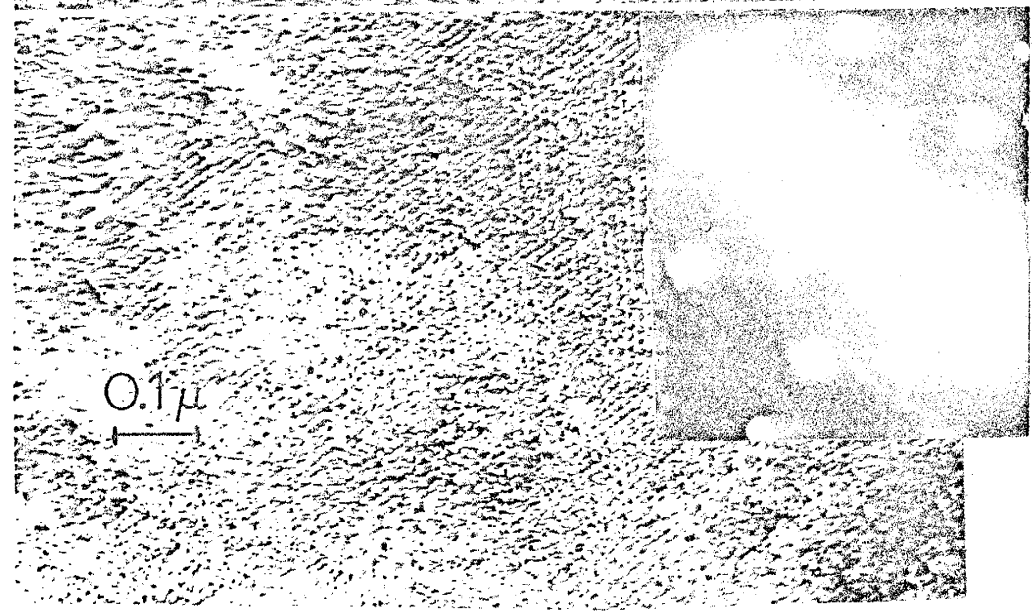
Fig. 36. a) Initial bright field electron transmission image of hexagonal defect aggregates of purple colored natural fluorites. b) Approximately the same area as Fig. 36a after 5 additional minutes of exposure. c) Fig. b, after 5 min. more exposure; defect aggregates which reached saturation are associated with a selected area diffraction pattern.



a



b



c

CHAPTER IV

DISCUSSION AND CONCLUSIONS

IV.1. Discussion of the experimental resultsIV.1.1. Natural fluorites

The results of the chemical analyses and absorption spectrum measurements of natural fluorites are given in sections III.2.2. and III.2.3. As indicated, Yttrium and sodium are concentrated relative to the rare-earth elements, and the light rare-earth elements are concentrated relative to the heavy rare-earth elements in the investigated natural fluorites. In the natural fluorites of this study, the main absorption bands generally originate at the 3050\AA in the ultraviolet region and exhibit no shifting from fluorite to fluorite, and at 4000\AA and 5800\AA where they tend to shift toward lower or higher wavelengths from fluorite to fluorite. The 3050\AA absorption band is enhanced by increased rare-earth element concentration, but it is suppressed by an increase in sodium concentration. In the case of the 5800\AA absorption band (which includes the $5600\text{-}5900\text{\AA}$ absorption bands) the opposite relation is observed; that is, it is enhanced by increased sodium concentration, but suppressed by an increase in rare-earth element concentration. Also it has been observed that the presence of radioactive material is necessary for this band to appear. These findings indicate that the 3050\AA and 5800\AA absorption bands suppress one another, and that the rare-earth elements, sodium and radioactive material are related to the generation of these absorption bands or color

centers (see Fig. 27 to 32a).

McLaughlan (1967) noted that in fluorite crystals grown in reduced conditions, the rare-earth elements occupy sites having tetragonal symmetry, and are charge-compensated by fluorine ion interstitials in the interstitial site nearest to the rare-earth ion. The rare-earths in crystals grown under oxidizing conditions, on the other hand, occupy sites having trigonal symmetry. If the charge compensating ion in the fluorite is remote, the symmetry of the rare-earth element is cubic (Phillips and Duncan, 1971). In a study by Phillips and Duncan (1971) the rare-earth Ce^{+3} was found to occupy sites of tetragonal symmetry and cubic symmetry, and produced absorption bands at the 3050-3100A° wavelengths. These bands were suppressed when the crystal was additively colored by calcium vapor, because the excess calcium generates fluorine vacancies instead of fluorine interstitials, and rare earth can not trap electron. In this study, presence of sodium in the natural fluorites caused suppression of the 3050A° absorption band. When a monovalent ion substitutes for a divalent ion. It is charge compensated by a trivalent rare-earth element; if no trivalent ions are present, the generation of divalent ion with an accompanying hole must occur in order to preserve the electrical neutrality of the sample.

McLaughlan (1967) showed that when fluorite was doubly doped with sodium and rare-earth elements (Ce^{+3} and Nd^{+3}) its epr (electron paramagnetic resonance) spectrum showed two lines, one with tetragonal symmetry, the other with rhombic symmetry. When the sodium concentration was increased he observed that the rhombic spectra was enhanced, while the intensity of the tetragonal spectrum was suppressed, and another

tetragonal symmetry spectrum appeared. In this study, the 3050A° absorption band was suppressed by an increase in sodium concentration. Thus, the absorption band was probably caused by a center with tetragonal symmetry, because such a center is known to cause this absorption band. Also the 5600-5900A° absorption bands could have been caused by the new tetragonal symmetry center generated with the increase in the sodium concentration. The enhancement of the rhombic spectrum noted by Mclaughlan (1971), which resulted from the increase of sodium, is consistent with and parallel to the results of this study, in which an increase in both sodium concentration and total concentration of rare-earth elements and Yttrium, produced an increase in the color center concentration of the 3900-4700A° absorption band. The results of Mclaughlan (1967) plus the findings of this study together support the concept that rare earth elements can be substituted for divalent calcium ions, which can associate with interstitial fluorine ions in tetragonal symmetry (epr spectra) to form the center which causes the 3050A° absorption band. When monovalent ion such as sodium (which also can substitute for Ca^{+2} in the fluorite) is added to the system, trivalent ions (rare-earths and Yttrium) can charge compensate for the monovalent ion when the two are nearest neighbors. This monovalent-trivalent combination comprises the center which produces the rhombic symmetry of the epr spectrum, which causes the 3900-4700A° absorption band. But some of the rare-earth elements can also compensate with the next nearest neighbor monovalent ion to produce the other tetragonal symmetry of the epr spectrum which was generated after sodium addition or the 5600-5900A° absorption band of the optical spectrum. It should be noted

however that the 3900-4700Å absorption band is not solely impurity related, because F-center aggregates (which are related to lattice defects such as fluorine vacancies and electrons) can also produce an absorption band at the same wavelength (Hayes et al., 1970). According to Staebler and Schnaltery (1971), the maxima of the bands shift to a lower wavelength as the radius of the substituted trivalent ion decreases. The contribution of the aggregates of F-centers, coupled with the radius effect of the substituted trivalent ions, produces the shifted wavelength of the 3900-4700Å absorption maximum. Thus, both the 3900-4700Å and the 5600-5900Å absorption bands are not only the results of chemical impurities or simple lattice defects, but also the result of different arrangements of these impurities, lattice defects and their associations. Trivalent ions (REE, Yttrium), monovalent ions, interstitials, vacancies, holes and F-center aggregates contribute differently to each absorption band. The addition of these new members to the color center is defined or controlled by the amount, kind and symmetry of these centers.

IV.1.2. Artificially colored synthetic fluorites

Chemical analyses of synthetic fluorites show that even the purest available synthetic fluorite is not completely free of chemical impurities. The presence of these impurities explains why many discrepancies have arisen between researchers as to the causes of the coloration of fluorite; each investigator used differently originated synthetic fluorite, so each had different impurities to deal with. As a result, even duplicate conditions by different investigators gave

different coloration behaviors and different conclusions regarding the origin of color in fluorite. Sashital and Vedam (1973) indicated that Harshaw fluorites contain 4.5 ppm Yttrium, 20 ppm Na and 0.0 ppm La. In this study, the Harshaw fluorites contained less than 1.0 ppm Yttrium, 72.0 ppm sodium and 0.58 ppm La. It is clear then, that even different single fluorites from the same company may contain different amounts of impurities, and would not, as was observed, be expected to exhibit the same coloration behavior, although experimental conditions are duplicated.

When synthetic fluorite is bombarded with protons (H^+), these particles can substitute for Ca^{+2} or interstitial sites, because H^+ is very small. During the proton bombardment, anion and cation vacancies and interstitials can also be generated. It is known that clustering or pairing of defects is also possible, because this clustering lowers the energy of the system by an added configuration entropy term ($-TS$). In order to maintain the neutrality of the substance when the H^+ is substituted for Ca^{+2} , H^+ needs to be compensated by Ca^{+2} with a hole somewhere in the crystal. Because the H^+ is very small compared to Ca^{+2} , many vacancies and interstitials have the freedom to move around the side of H^+ ; the substituted H^+ can associate very strongly with clusters or interstitials and vacancies because of its small size (which causes the lattice distortion) and empty outer shell. Most likely compensation will be achieved with another H^+ ion in an interstitial position. The resulting color center has an absorption band at 5450\AA . This center is stable up to 300°C ; at 400°C or above, however, the interstitials and holes become mobile, resulting in a decrease in

the intensity of the 5450Å° absorption band. The clustering of mobilized lattice defects and residual 5450Å° centers can absorb light at lower wavelengths, which causes the shifting of the 5450Å° absorption band to a lower wavelength.

Alpha irradiation (He^{+2}) produced color and an absorption band at 5450Å° similar to that produced by proton irradiation, but with different intensities of the coloration and absorption band. During the coloration both H^+ and He^{+2} generate cation and anion vacancies and interstitials and holes, and both particles probably generate centers which caused the absorption of light at the same wavelength (5450Å°). Also, the bleaching behavior of both the alpha and proton irradiation generated 5450Å° absorption bands was similarly stable until 400°C, and both produced a shifting of the 5450Å° absorption band to a lower wavelength.

Introducing He^{+2} and H^+ to the fluorite indicates that the visible region absorption bands are for the most part governed by monovalent and divalent cations. This result is consistent with the results of fluorite doped with sodium impurities, which enhanced the 5600-5900Å° absorption band in the natural fluorites.

The results of irradiation with low energy electrons are consistent with the previous work of Rao and Bose (1970) and Ratnam and Banargee (1973), which showed that low energy electrons at room temperature did not produce coloration or any absorption spectrum. To produce color centers and a resulting coloration, either the temperature should be above 100°C (Rao and Bose, 1970) or high energy (above 3.0 MeV) electrons are needed. Production of blue and purple coloration

by high energy electrons has been observed under the transmission electron microscope (see section III.3.). Irradiation with electrons (the combined results of this study, Rao and Bose, 1970 and Ratnam and Banarjee, 1973) and transmission electron microscope studies indicate that the first color centers (mosaic-like defect structures) generated by this radiation produce an absorption band at 3800\AA ; results of this study show that these are the F-center aggregates. With longer exposure to higher energy electron radiation or at higher temperatures (above 100°C), these F-center aggregates generate more complex aggregates, causing another absorption band at about 5800\AA . With a further increase in temperature or exposure, the aggregation increases and the shifting of the 5500\AA absorption band to the lower or higher wavelengths occurs. The position of the 3800\AA absorption band also shifts to a lower wavelength. The $5500\text{-}5800\text{\AA}$ absorption bands grow rapidly and consume the 3800\AA band, and the blue coloration of the fluorite becomes purple. Experiments of Rao and Bose (1970) indicate that the 3800\AA and 5800\AA absorption bands always appear together. This is consistent with results of electron microscope studies of electron irradiated samples. High energy electrons could affect the impurities (Na, Y, La) although this is not very likely because the penetration of electrons is very small.

Irradiation with Gamma-rays produced absorption bands different than those obtained by Sashital and Vedam (1973). The 3800\AA absorption band produced by gamma irradiation is the most intense absorption band of the spectrum. The 3800\AA band could possibly have originated from at least three different kinds of centers. The F-center aggregates

of the electron irradiated samples and the presence of monovalent ions and trivalent ions (sodium, Yttrium, and rare-earth elements) contribute to the 3800Å absorption band, as do aggregates of M-centers which are made up of two F-centers (Hayes et al., 1970). Thus color centers of different origins can absorb light together and cause an absorption band at the same wavelength. The faster bleaching of this 3800Å absorption band is also consistent with the concept that F-center aggregates contribute to it, because F-centers diffuse very rapidly at elevated temperatures up to 400°C. Some residual of this band remains above 400°C, and is probably related to Yttrium and Na impurities.

A comparison of the 5450Å absorption bands produced by gamma irradiated synthetic fluorite, and proton and alpha irradiated synthetic fluorites illustrates another interesting feature; i.e., the same absorption band can be generated by different color centers. The 5450Å band of the gamma irradiated sample is most likely caused by Na impurities and gamma-ray induced defects and is not stable above 100°C, while H^+ and He^{+2} related centers are stable up to 400°C. The ultraviolet region absorption band of the gamma ray irradiated samples at 3240Å is possibly caused by electron traps of Yttrium and rare-earth elements which are not stable over 200°C.

Irradiation with x-rays produced no coloration and absorption bands. This indicates that unless there is enough impurity present in the crystal to create vacancies, electrons and interstitials, the x-rays cannot produce coloration. Hard gamma-ray irradiation can produce coloration because it is more energetic and effective with even trace amounts of impurities, and can create significant amounts of vacancies,

interstitials and electrons.

IV.2. Discussion of the use of the coloration and the 3050A° absorption band of fluorite for geological age dating

As noted in Chapter I, section I.3., the coloration of fluorites and other minerals and the use of this coloration for geological age dating has been the subject of several studies (Berman, 1957; Titley and Damon, 1962). In such studies, coloration, color centers and/or absorption bands were assumed to be simple color centers; i.e. F-centers, or simple aggregates of F-centers. These simple F-centers were considered to be caused by radioactive decay of natural impurities such as Uranium. If these assumptions were true, geological age dating of fluorites using the color centers related to various absorption bands would be a very easy method.

The ultraviolet absorption band of fluorite at the 3050A° wavelength was considered by Titley and Damon (1962) to be one of the most characteristic of color centers, for use as a tool for geological age dating. They assumed that the 3050A° absorption band was a simple F-center caused by natural radioactivity, and used rock salt instead of fluorite to determine the efficiency of color center production by artificial radiation. Their suggestions were taken into account in this study, and the purest available synthetic fluorites were exposed to all types of radiation at different energy levels. Because none of the forms of irradiation produced the 3050A° absorption band, it was not possible to determine the efficiency of color center production for this band. However, chemical analyses of natural and synthetic fluorites

showed that even synthetic fluorites contain impurities. The 3050A° absorption band was also shown in this study (see Fig. 27, 28, and section III.2.3.) to be a direct function of the rare-earth element concentration, and thus is not applicable to geologic age dating. Other absorption bands were also found to be caused not just by simple color centers, but also by factors dependent upon or controlled by the impurities present. Particularly in natural fluorites, the color centers are a result of a high degree of impurity and lattice defect complexes. Thus they cannot be used in any way to determine the age of a rock.

IV.3. Possible causes of the coloration of fluorites

In previous investigations of natural fluorites, several models have been proposed to single out the origin of coloration. Actually none of these proposed causes for the coloration of fluorite can be ruled out, because each of them is an essential part of the coloration. Most of the investigations and proposed models on the coloration of fluorites were established using synthetic fluorite, and artificial coloration of these fluorites was obtained using additive and irradiation techniques. Although the results and models based on studies of natural and synthetic fluorites do agree on some points, both types of fluorites should be considered separately, because in many instances the causes for the coloration are not controlled by the same factors. If the reasoning for coloration was the same for each system (natural and synthetic fluorites) the colorations established by both should give the same absorption spectra. In this study, the 3050A° absorption band never appeared when irradiating the synthetic fluorite, just as the

3800Å absorption band was never observed in the spectra of the natural fluorites. It is apparent that the coloration of natural fluorites is governed by the presence of impurities and impurity related centers, while in the synthetic fluorites, coloration is dominated by lattice defects produced by artificial coloration processes (ionizing radiation, additive coloration) which generate defects such as interstitials, vacancies, F-centers or F-center aggregates. But impurities and lattice defects are essential for both systems. Thus the models for coloration of fluorite will be considered separately for both types of fluorite.

Coloration models of the natural fluorites

1. Rare-earth elements substitute for the cation site in calcium fluoride, usually with cubic or tetragonal symmetry (Hayes, 1974). These trivalent rare-earth elements can be compensated with interstitial F^- ions, and can trap electrons easily (Theissing et al., 1969). The relation established in this study, namely that an increase in the concentration of rare-earth elements produces an increase in the color center concentration of the 3050Å absorption band, suggests that substitutional rare-earth elements which trap electrons are responsible for the 3050Å absorption bands of natural fluorites. However, very concentrated Yttrium appeared either not to contribute to this absorption band, or to contribute only very irregularly. And although the presence of radioactive material enhanced the concentration of this absorption band, it was also found not to be an essential element, because as long as rare-earth elements are present in a sufficient amount the 3050Å absorption band is present. Thus the cubic situated substitutional trivalent rare-earth elements which are compensated by

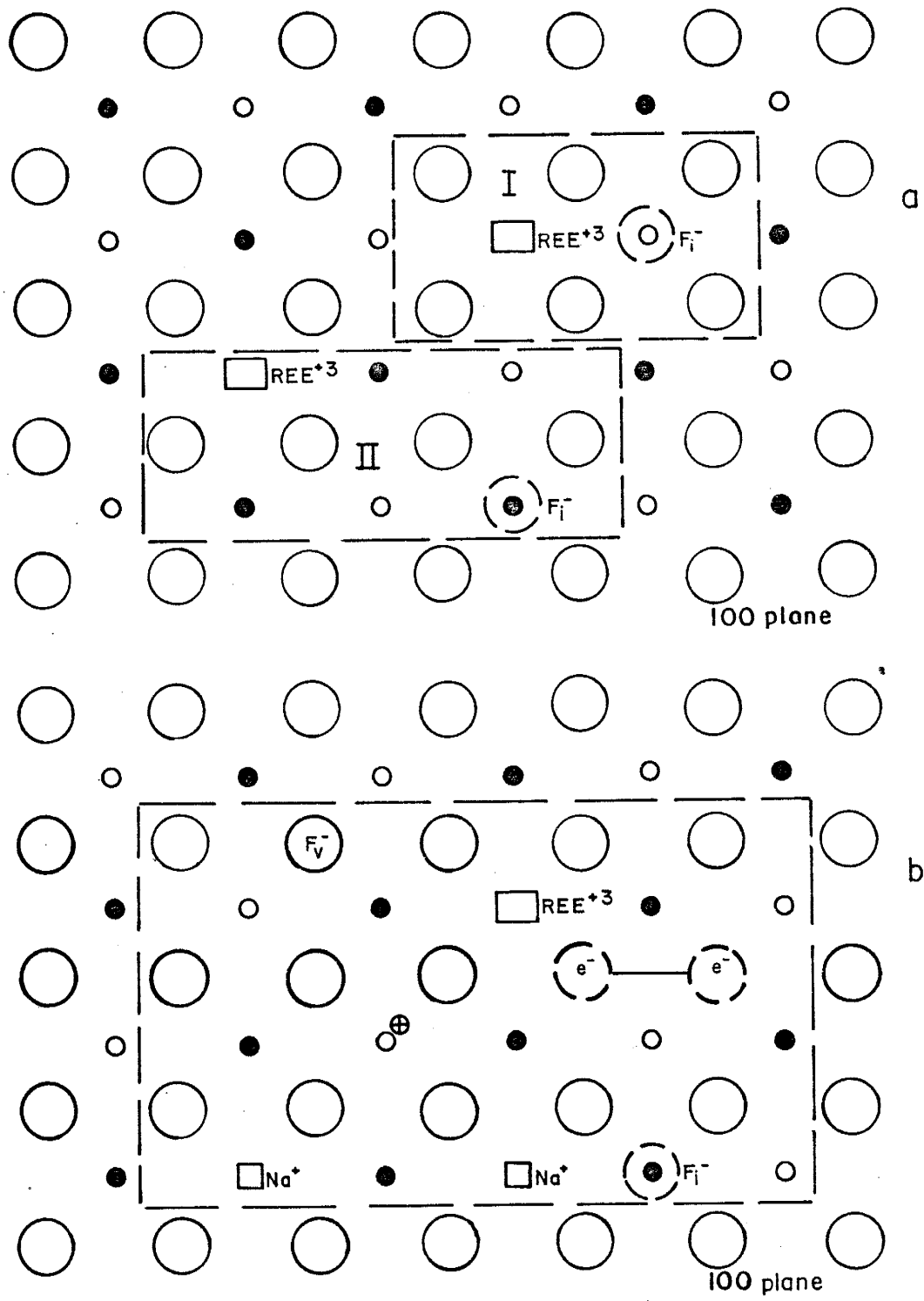
fluorine ion interstitials to create strong electron traps form the basis of a potential model for the production of the 3050Å absorption band (Fig. 37.a.).

2. The color of synthetic fluorite doped with NaF increased in intensity after irradiating it with high energy electrons (Scouler and Smakula, 1960). Increasing the Na concentration in the system CaF_2 : Ce^{+3} - Na^{+} generated a new tetragonal symmetry spectra of the epr spectrum (McLaughlan, 1967). The absorption spectra of rare-earth doped and rare-earth- Na^{+} doped calcium fluoride were compared after additive coloration; the Na-rare-earth doped fluorite experienced a shift of the visible region absorption band to a lower wavelength, and an increase in the concentration of this absorption band with a decrease in background absorption (Phillips and Duncan, 1971). Thus it is clear that the visible region absorption bands are enhanced by the presence of sodium. It is likely that the sample in Phillips and Duncan's experiment, doped only with La, also contained some sodium, as was the case with the synthetic fluorite of this study (results of their chemical analyses were not given). Thus in their experiment, the addition of sodium to the sample simply further increased its Na concentration.

Sodium can also substitute into the calcium site in the fluorite (McLaughlan, 1967); it is charge compensated by a next nearest neighbor rare-earth element. In this study, the color center concentration of the 5600-5900Å absorption band in the natural fluorites increased with increasing Na concentration. Sodium is also possibly associated with other lattice defects, such as vacancies, interstitials and holes,

Fig. 37. a) Color center model for the 3050Å absorption band of natural fluorites. Region I has, tetragonal symmetry in which the compensating ion is local. Region II has cubic symmetry, and the compensating ion is remote. b) Color center model for the visible region absorption band at 5600-5900Å.

○ is fluorine ion, ○ Ca^{+2} , below the plane of paper,
 ● Ca^{+2} , above the plane of the paper, ○ Fi interstitial fluorine ion.



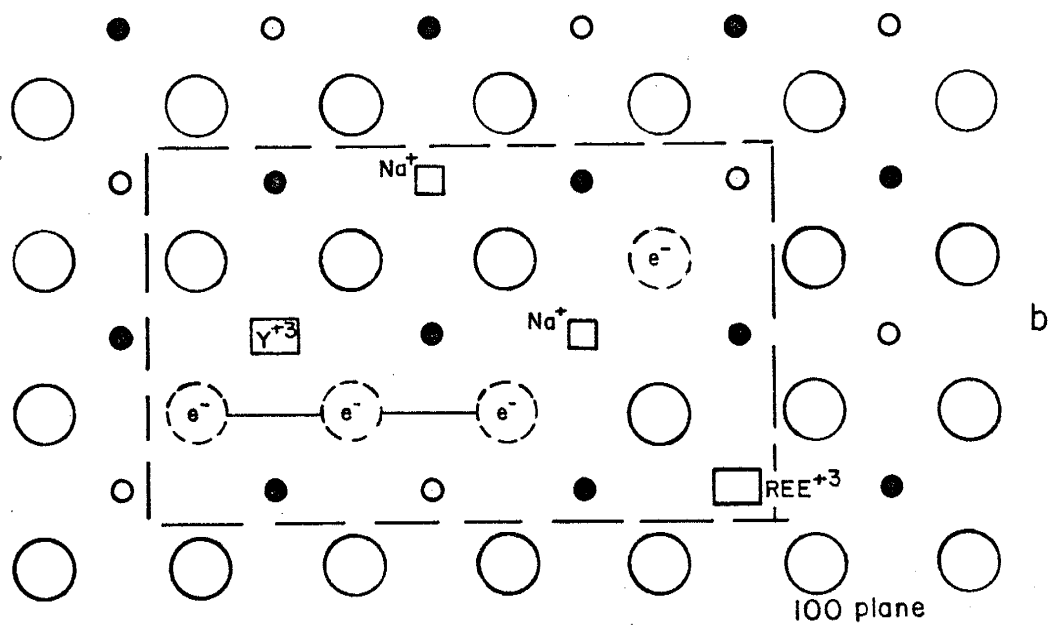
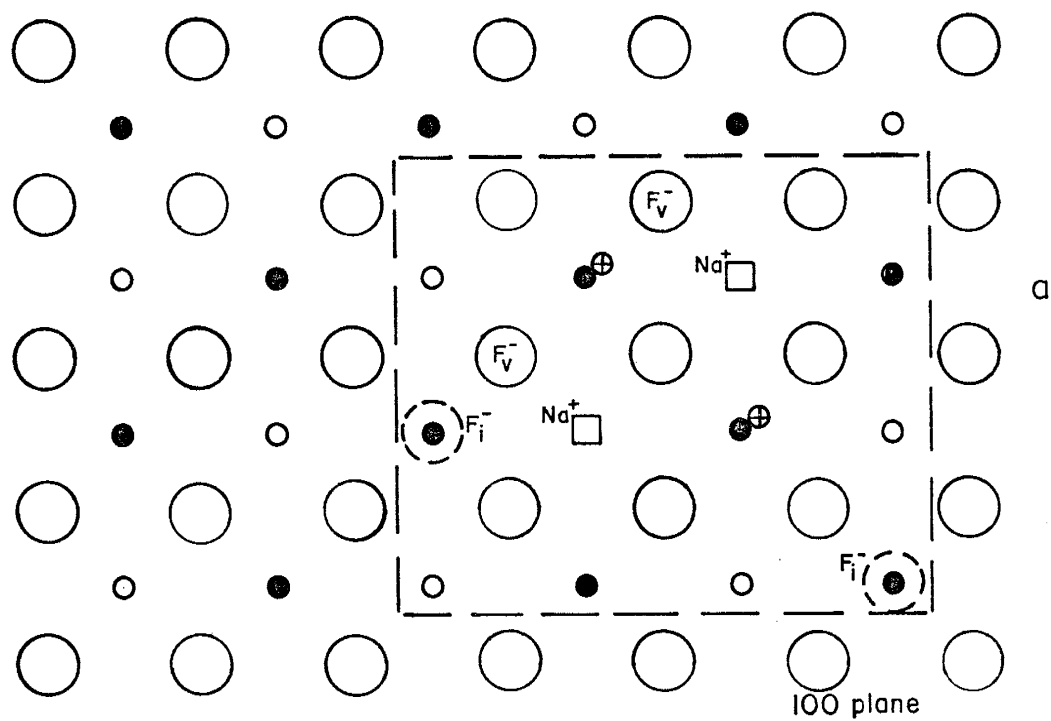
because without a sufficient amount of radioactive material present, the 5600-5900Å absorption band does not appear. The contribution of the Yttrium does not appear to be very essential, although many investigators have suggested it (e.g.: Gorlich et al., 1968). Thus the cause of the 5600-5900Å absorption band could be rare-earth elements which are charge compensated with the next rarest neighbor sodium. This rare-earth-sodium related defect center can trap a hole. Otherwise, Na could be compensated by radiation generated lattice defects such as Ca^{+2} ion plus a hole somewhere in the crystal, which would cause the shifting of the band to lower wavelengths, as is observed in purple colored fluorites (Fig. 37.b).

3. Cavenett et al. (1969) attributed the 3750Å absorption band to F-centers in the fluorite. However, when fluorite was doped with rare-earth element impurities the maximum of the 3750Å absorption band shifted to a higher wavelength (4000Å). Sodium doped samples with or without Yttrium and rare-earth elements showed the same shifting of the maximum of this absorption band (Scouler and Smakula, 1960; Phillips and Duncan, 1971; Staebler and Schnatterly, 1971). Fluorite doubly doped with rare-earth and sodium also showed the enhancement of the rhombic symmetry of the epr spectrum (McLaughlan, 1967). In this study it was shown that the color center concentration of the 3900-4700Å absorption band increases as the sodium concentration increases; radioactive material, Yttrium and total rare-earth elements also contribute to this increase. According to this model, the absorption band results from the substitution of sodium, Yttrium and rare-earth elements in the cation site of the fluorite, with monovalent and

trivalent ions compensating when they are nearest neighbors (Fig. 38b). The absorption maxima are controlled by the presence of F-centers or F-center aggregates and monovalent and trivalent ions. The absorption bands with a maximum above 4000\AA are attributed mainly to the color centers described by this model, although F-centers and M-center aggregates can also contribute to the presence of these band. If F-center aggregates were dominant, the absorption band maximum will shift to a lower wavelength. In natural fluorites, F-center aggregates are minimal and their contribution to the band is not very large. This explains why there is no absorption band present in natural fluorites between 3600\AA and 3900\AA , and why the exposure to gamma rays caused the 3800\AA band of synthetic fluorite to shift to the 4040\AA wavelength and decrease in intensity after heating to 400°C . Presentation of this model is shown in Fig. 38.b.

4. The $5400\text{-}5500\text{\AA}$ absorption bands are probably caused by the monovalent ion (in this case sodium), substituted in the calcium site and compensated with calcium plus a hole. In particular, the 5400\AA absorption band of the purple colored fluorite is generated by this kind of center, as indicated by results of proton irradiation of synthetic fluorite. The presence of radioactive material is important for coloration of fluorite because radiation causes the generation of vacancies or related point defects, which are essential for coloration. This is evidenced by the proton and alpha irradiated samples, which could only be colored to the thickness to which the particles can penetrate (Fig. 38.a.).

Fig. 38. a) Color center model for 5400-5500Å absorption bands, on the (100) plane in natural fluorite. \oplus represents a hole. b) Color center model for the 3900-4700Å absorption band on the same plane.



The coloration models of artificially colored synthetic fluorites

Artificially colored fluorites contain large numbers of lattice defects which are generated during the coloration processes. However, chemical impurities cannot be prevented, because the samples of synthetic fluorites appear to always contain impurities. Thus, the absorption bands and subsequent observed colors are caused primarily by lattice defects, although impurities in the crystal also play a subordinate role. Synthetic fluorite which contain fewer impurities has greater resistance to coloration by x-rays at room temperature (Gorlich et al., 1968; Bessent et al., 1969; and Roach and Senff, 1974). It is clear from spectrophotometric results that such radiation causes coloration by effecting on the impurities (see Fig. 6 and section III.1.2); they usually do not generate lattice defects in substantial quantities. However, if impurities are present in significant amounts their association with minor amounts of lattice defects may produce color and/or absorption bands.

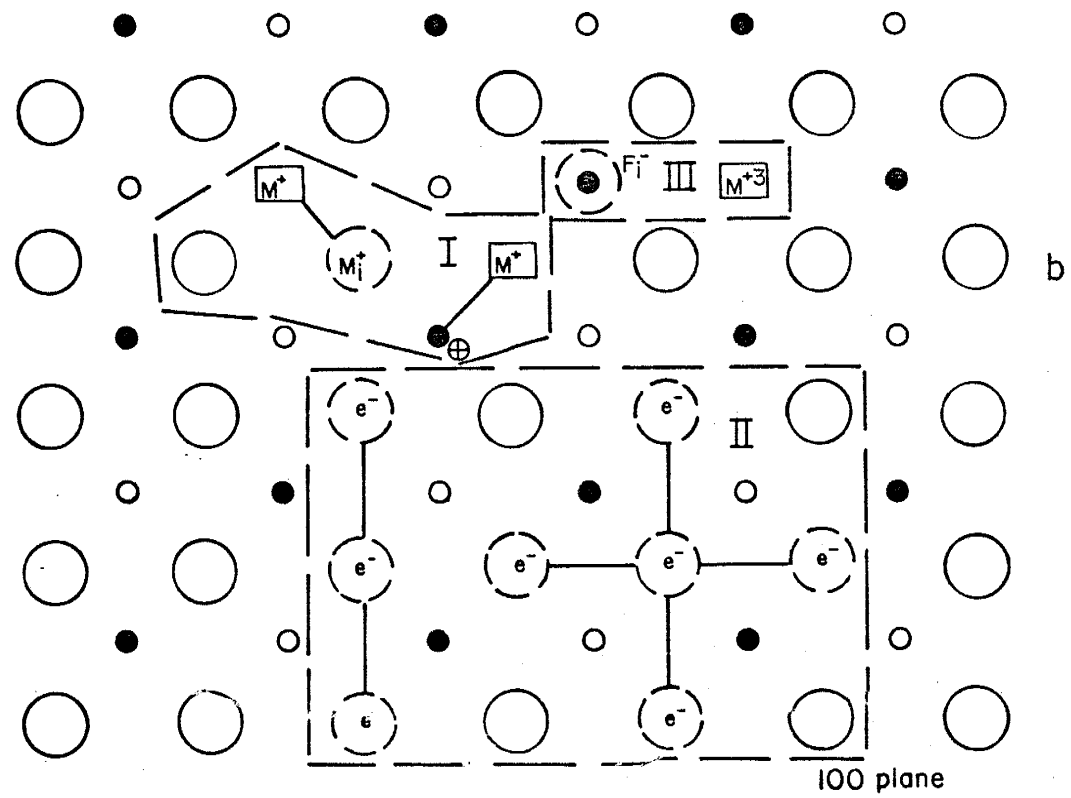
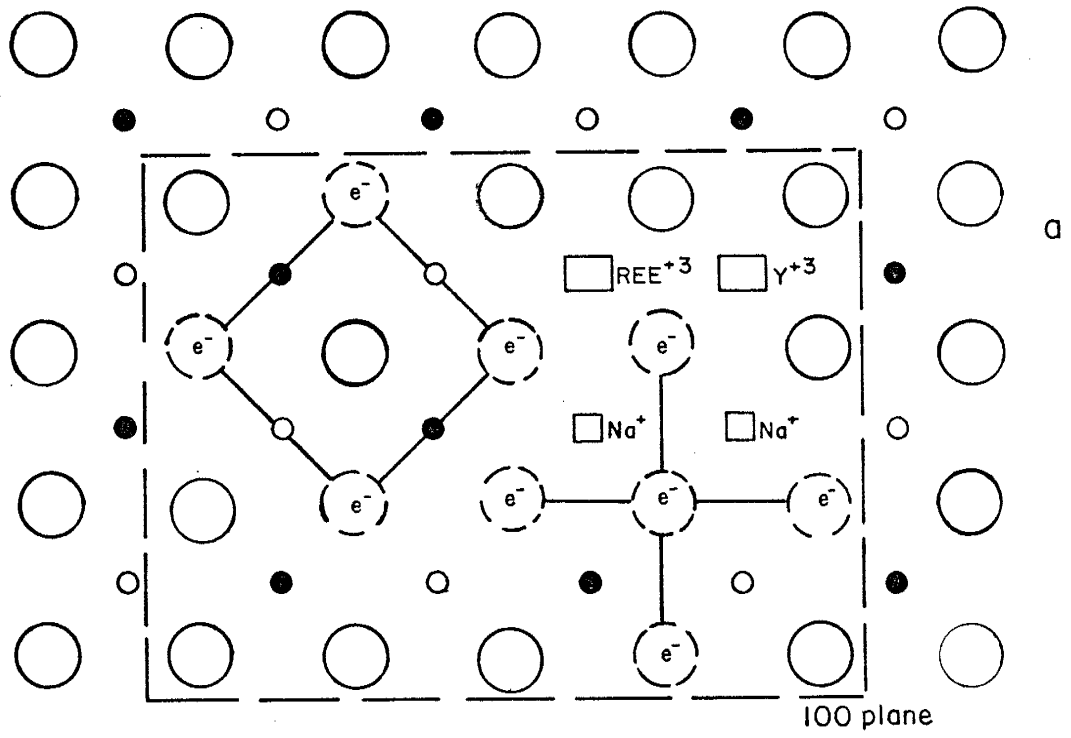
Hard gamma-irradiation is capable of producing significant lattice defects as well as effecting even very minor amounts of impurities resulting in several absorption bands and colorations. However, the position of the absorption bands are controlled by the quality and quantity of these impurities as well as the radiation dosage. Colorations by electron and neutron radiation are predominantly governed by lattice defects and aggregates of those defects, while alpha and proton irradiations accounts for the impurity related colorations. The models for synthetic fluorites colored by ionizing and particle radiation are summarized as follows:

1. The 3800Å absorption band is attributed to F-centers, M-centers (Hayes et al., 1970) and rare-earth elements, Yttrium and sodium impurities. The main contribution to coloration comes from the F-center aggregates. This is the actual basis for gamma-ray induced, and neutron induced 3800Å absorption band. In electron irradiated samples, the F-center aggregates should be the only contributing factors to the 3800Å absorption band, because the electrons cannot penetrate deep enough into the solid to effect impurities. The growth and bleaching patterns of gamma-ray, neutron and electron bombarded fluorites are consistent with this suggestion (Fig. 39.a.).

2. The 5450Å absorption band is definitely related to monovalent ion impurities and their associations with lattice defects. In the case of gamma irradiated samples the monovalent ion is sodium, and in proton bombarded samples the responsible ion is H^+ . When the size of the monovalent ion is smaller than host cation, the resulting absorption band is more resistant to bleaching (Fig. 39.b.I).

3. The 5300Å absorption band is also related to the monovalent ions, although, their contribution is less important than the 5450Å absorption band because lattice defects have such strong associations. Heating proton irradiated sample up to 400°C caused shifting of the 5450Å absorption band to 5300Å, because at high temperatures the lattice defects become mobile and begin to interact with one another (Gorlich et al, 1968). Then the position of the center which causes the 5450Å absorption band breaks away to form a different center which absorbs light at 5300Å. Consequently actual origin of this band and its position cannot be pinpointed exactly.

Fig. 39. a) Color center model for the 3800Å absorption band; the synthetic fluorites are mainly aggregates of F centers, and have little contribution from impurities. b) color center models: the 5450Å absorption band (region I), the 5050Å absorption band (region II) and the 3240Å absorption band (region III). ○ fluorine ion, ○ Ca⁺² below the plane of the paper, ● Ca⁺² above the plane of the paper.



4. The 5800-5900Å absorption band is probably related in part to monovalent and trivalent ions, because in the natural fluorites it has been found that increasing concentration of sodium increases the color center concentration of this band, however, increasing rare-earth concentration decreases the color center concentration of this band. Although aggregations of F-centers are the major contribution to the center as observed in the transmission electron microscopy portion of this study (Fig. 37.b).

5. The 5030Å absorption band probably is due largely to aggregates of F-centers, because the bleaching and growth patterns of this absorption band are very similar to those of the 3800Å absorption band (39.b.II).

6. An absorption band in the ultraviolet region occurs at 3240Å and can be generated only by hard gamma radiation. The weak intensity and different growth and bleaching pattern of this band suggested that it is probably caused by trace amounts of trivalent ions, which would produce a color center of low symmetry in which the trivalent ion occupies calcium sites; this is because the symmetry will be lowered when the compensating ion is local (Hayes, 1974). (Fig. 39.b.III). However this model is only tentative, and subject to much speculation.

IV.4. Conclusions

Analyses of whole samples and fluid inclusion free samples indicate that impurities of rare-earth elements, Yttrium and sodium are located within the structure of the fluorites. The charge compensation of trivalent ions can then be provided by different mechanisms. Trivalent

ions which are substituted for the Ca^{+2} site in the fluorite can be charge compensated by local or remote F^- interstitial ions. The compensation of the trivalent ion can also be provided by Ca^{+2} site substituted monovalent ions, when they are nearest or next nearest neighbors to the trivalent ions.

It was established that the color center concentration of the 3050A° absorption band of natural fluorites is directly related to the rare-earth element concentrations. In the visible region spectra, the color center concentration of the 5600-5900A° absorption band of natural fluorites is a direct function of the monovalent ion concentration. The presence of bands along the boundary between the ultraviolet and visible regions is a function of the total concentrations of rare-earth elements, Yttrium and sodium, with some contribution from F-center aggregates; this indicates that natural radioactivity plays a part in the generation of coloration of the natural fluorites. These findings also eliminate the use of the 3050A° absorption band and other absorption bands of natural fluorites as tools for geological age determination, because these bands are originated mainly from impurity-related color centers.

The main absorption bands of synthetic fluorites are governed for the most part by F-center aggregates generated during the radiation processes. The results of both natural and synthetic fluorite studies indicate that some of the absorption bands appearing at specific wavelengths can be originated from more than one source.

APPENDIX A: A summary of previous works on the coloration of fluorite.

Reference	Type of fluorite crystal	Coloration process or applied treatment	Experiment	Experimental results	Proposed model
Smakula (1950)	synthetic and natural	x-ray (200 K, 10 mA)	transmission is measured	bands at 3350, 4000, 5800Å°	electron traps at lattice defects
Schulman et al., (1952)	synthetic	x-ray (40 KVP, 15 mA), heated with NaF at 1500°C	absorption spectrum	bands at 3350, 4000, 5800Å°; in addition 3300 and 3800Å° bands	electron traps which increased with addition of monovalent ions
Allen (1952)	natural	x-radiation	absorption spectrum, index of refraction, unit cell dimension, chemical composition	bands at 3800, 4050, 5750 and 6500Å°	3800 to 4050 by F center, 5750 to 6500 by colloidal calcium
Barile (1952)	synthetic	x-ray (50 KV, 30 mA)	absorption spectrum	bands at 2280, 3350, 4000, 5800Å°	---
Berman (1957)	natural and synthetic	x-radiation	impurity, specific gravity, unit cell dim. index refr. x-ray diff.	color change, index of ref. increased, specific gravity decreased	nuclear particles disturb the structure
Bontinck (1958)	synthetic	x-rays (40 KV, 20 mA) neutrons (8.8 10 ¹⁷) additive coloration with Ca vapor (700°C, 1200°C)	absorption spectrum; bleaching with light; bleaching thermally	2000/2200/330/400/ 5800;2600/2200/3750/ 5200; 2000/2200/ 3750/5200	2000-2300, due Schottky defects; 3750 due to F centers; 5200,5600 due to M-center

APPENDIX A: Continued

Reference	Type of fluorite crystal	Coloration process or applied treatment	Experiment	Experimental results	Proposed model
Scouler-Smakula (1960)	synthetic	high energy electrons (2.5 MeV) at different temp. Yf ₃ and NaF doped	absorption spectrum	2250/3350/4000/5800 absorption effected by temp. and impurities	defect complexes of Yttrium, oxygne and Na along with lattice defects
Messner-Smakula (1960)	synthetic	x-ray (150 KV) high energy electrons at different temp.	absorption spectrum	2250/3350/4000/5800	2200, due to holes bound to Ca ⁺⁺ vac.; 3350 electrons bound to Ca interstitials; 4000 neutral interstitials; 5800, F center
Hayes-Twiddell (1962)	synthetic	CaF ₂ :Tn x-rays	spin resonance spec.	production of self-trapped holes	3500 in self trapped hole [F ₂ ⁻]
O'Connor-Chen (1963)	2 different kinds of synthetic	electrons (2.5 MeV)	absorption spectrum	2250/3350/4000/4800 pure crystal showed less intense	coloration due to reduction of Y ⁺³ and suppressed presence of Cm ⁺³
Arends (1964)	synthetic	additively colored with Ca vapor, tungsten cathod of RT	ESR, absorption spectrum, bleaching	3750/5200/6000/7500, 3750/5200/6000/6700/7500	3750-F center, 5200 complex lattice defects, 6000 related impurity Na ⁺ , K ⁺ 6700 M center 2F center)

APPENDIX A: Continued

Reference	Type of fluorite crystal	Coloration process or applied treatment	Experiment	Experimental results	Proposed model
Kamikawa et al. (1966)	synthetic	electrons (3 MeV) at helium T	absorption spectrum	3750/5200	3750 F center
Ratnam (1966)	synthetic	x-ray at RT; 180 to 250°C electrolytic coloration	absorption spectrum x-ray fluorescence flc. spectrum	2250/3350/4000/5800 2250/3250/3750/5000 2000/3750/3800	due to $4d^1$ transition of the Y^{+2} ion 3750 F center
Bill et al. (1967)	natural	—	EPR, absorption spectrum		Sm^{++} green coloration, yellow color (4330-2940) due to yellow center, red color due to R center (Yttrium oxygen association)
Gorlich et al. (1968)	synthetic	x-ray (180 KV, 20 mA) at RT and lower TS	absorption spectrum thermal bleaching	3750/2850 absorption bands	3750 F center, 2850 self trapped hole
Theissing et al. (1969)	synthetic	γ -ray pure and doped with Yttrium	absorption spectrum bleaching and theoretical calc.	4 band spectrum visible resian band, intensity proportional to Yttrium conc.	more than one color center (Y^{+2} and defect at remote charge comp.

APPENDIX A: Continued

Reference	Type of fluorite crystal	Coloration process or applied treatment	Experiment	Experimental results	Proposed model
Rao and Bose (1970)	synthetic	x-ray and low energy electrons at diff. temp.	absorption spectrum bleaching	4 band spectrum, no band with e at room temp., 2 band spectrum at above 180-250°C	4 band spectrum due to trace of impurity which associated with lattice defects 2 band spectrum is F centers or electron traps
Beaumont-Hayes (1969)	synthetic	additive coloration	absorption spectrum bleaching with polarized light	2 band spectrum	3750 is complex super position of bands arising from F center, 5200 M center (2 F center)
Hayes et al (1970)	synthetic	additive coloration	EPR, absorption spectrum	4 band spectrum	380: F center, 520 M center, 3840 and 5520 impurity related and arise from a single center
Staebler-Kiss (1969)	synthetic Ce doped	additive coloration	absorption spectrum UV irradiation	4 band spectrum and photochromism	rare earth and defect cents.

APPENDIX A: Continued

Reference	Type of fluorite crystal	Coloration process or applied treatment	Experiment	Experimental results	Proposed model
Staebler-Schnatterly (1971)	synthetic La, Ce, Gd, Tb, Y doped	additively colored	absorption spectrum linear and magnetic circular dichromism	4 band spectrum anisotropic	trivalent rare earth next to F center complex (REE)
Anderson-Sabisky (1971)	synthetic	additive coloration in RE doped systems	EPR at low temperatures	EPR spectra of the centers	2 types of centers $[- 2e REE^{+3}]$ $[- e REE^{+3}]$
Beaumont et al. (1972a)	synthetic	additive coloration	optical absorption and fluorescence spectrum, optical bleaching	area-phonon line observed at 6774\AA which associated with broad high energy abs. bands. F_3 complex may be re-oriented by linearly bleached light	the spectrum is caused by an F_3 complex composed of 3 nearest neighbor F center aligned along $\langle 100 \rangle$
Braithwaite et al. (1973)	natural	heated to red heat in air	organic impurity analysis; inorganic impurity analysis; absorption spectrum, thermal bleaching	no difference colored and colorless samples in both inorganic and organic cases	color zoning due to the changes in defect conc. with growth and colloidal calcium is coloring agent which these colloids produced by natural radiation

APPENDIX A: Continued

Reference	Type of fluorite crystal	Coloration process or applied treatment	Experiment	Experimental results	Proposed model
Murr (1973)	natural	electronic irradiation	transmission elec. mic.	ordered arrays of defect aggregates	color center aggregates
Sashital-Vedam (1973)	synthetic	γ -radiation	compression test Vicker's micro hardness, dislocation mobility, absorption spectrum	4 band spectrum mechanical property changes	335 is due to F_2^- rest of them complementary REF centers
Rouch-Sneff (1974)	synthetic	additively colored x-radiation	absorption spectrum fluorescence spec. optical bleaching uniaxial stress	2 band and 4 band spec., at low temp. fluorescence exhibits a pronounced phonon structure	aggregates of four F centers in tetrahedral configuration
Murr (1974a,b) (1976)	natural	electron irradiated and x-radiation	transmission elec. microscopy	observation of the hexagonal like defect structure, F aggregate (void) lattice characterization	color center aggregates producing blue coloration; natural coloration, produced by complexing with other impurity or substitutional atoms of varying valence

REFERENCES

- Allen, R. D. (1952). Variations in chemical and physical properties of fluorite. *American Min.* Vol. 37, p. 910.
- Almandinger, R. J. (1975). A model for ore genesis in Hansonburg Mining District, New Mexico. Ph.D. dissert., NMIMT.
- Anderson, C. H. and Sabisky, E. S. (1971). EPR studies of Photochromic CaF_2 . *Phys. Rev. (B)*, Vol. 3, p. 527.
- Arends, J. (1964). Color centers in additively colored CaF_2 and BaF_2 . *Phys. Stat. Sol.*, Vol. 7, p. 805.
- Barile, S. (1952). Study of x-ray induced optical absorption bands in CaF_2 . *J. Chem. Phys.*, Vol. 20, p. 297.
- Beaumont, J. H. and Hayes, W. (1969). M centers in alkaline earth fluorites. *Pro. Roy. Soc. A.*, Vol. 309, p. 41.
- Beaumont, J. H., Harmer, A. L., and Hayes, W. (1972a). The F_3 center alkaline earth fluorides: I. *J. Phy. (C). Solid. State.*, Vol. 5, p. 257.
- Beaumont, J. H., Harmer, A. L., and Hayes, W. (1972b). The F_3 center in alkaline earth fluorides: II. *J. Phys. (C) Solid State.*, Vol. 5, p. 226.
- Berman, R. (1957). Some physical properties of naturally irradiated fluorite. *Am. Min.*, Vol. 42, p. 191.
- Bessent, R. G., Hayes, W., Hodby, J. W. and Smith, P. H. S. (1969). An investigation of the effects of x-rays on undoped and on hydrogen doped alkaline earth fluorides. *Pro. Roy. Soc. A.*, Vol. 309, p. 69.

- Bill, H., Sierro, J. and Locroix, R. (1967). Origin of coloration in some fluorides. *The Am. Min.*, Vol. 52, p. 1003.
- Bontinck, W. (1958). Color centers in synthetic fluorite crystals. *Physico*, Vol. 24, p. 639.
- Braithwaite, R. S. W., Flowers, W. T., Haszeldine, R. H. and Russel, M. (1973). The cause of the color of Blue John and other purple fluorites. *Min. Mag.*, Vol. 39, p. 401.
- Dexter, D. L. (1956). Absorption of light by atoms in solids. *Phys. Rev.*, Vol. 101, p. 48.
- Gorlich, P., Karras, H., Symanowski, C. H. and Ullman, P. (1968). The color center absorption of x-ray colored alkaline earth fluoride crystals. *Phys. Stat. Sol.*, Vol. 25, p. 93.
- Hayes, W. (1974). Crystals with the fluorite structure. Electronic, vibrational, and defect properties. Clarendon, Oxford.
- Hayes, W., Lambourn, R. F. and Smith, P. H. S. (1970). The metastable triplet state of the M center in CaF_2 . *J. Phys. C. Solid. State.*, Vol. 3, p. 1797.
- Hayes, W. and Twidell, J. W. (1962). The self trapped holes in CaF_2 . *Pro. Phys. Soc.*, Vol. 79, p. 1295.
- Herman, R. and Silverman, S. (1947). The decoloration of natural fluorite crystals. *J. Optical. Soc. Am.*, Vol. 37, p. 871.
- Heyl, A. V., Brock, M. R., Jolly, J. L., and Wells, C. E. (1965). Regional structure of the southeast Missouri and Illinois-Kentucky Mineral Districts. *Geo. Sur. Bull.*, 1202-B.
- Judd, D. B. and Kelly, K. L. (1939), Method of designating colors. *J. of Research of the National Bureau of Standards*, Vol. 23, p. 355.

- Kamikawa, T., Kazumata, Y., Kikuchi, A. and Ozawa, K. (1966). The F-center in calcium fluoride. *Phys. Lett.*, Vol. 21, p. 126.
- Kiss, Z. J. and Yocom, N. P. (1964). Stable Divalent rare-earth alkaline-earth halide systems. *J. Chem. Phys.*, Vol. 41, p. 1511.
- McLaughlan, S. D. (1967). Electron paramagnetic resonance of trivalent-rare-earth-monovalent-alkaline-earth ion pairs in CaF_2 . *Phys. Rev.*, Vol. 160, p. 287.
- McLaughlin, R., Abed, U., Conway, J. G., Edelstein, N. and Huffman, E. H. (1970). Oxidation states and site symmetries of $\text{CaF}_2: \text{U}$ crystals. *J. Chem. Phys.*, Vol. 53, p. 2031.
- Messner, D. and Smakula, A. (1960). Color centers in alkaline earth fluorides. *Phys. Rev.*, Vol. 120, p. 1162.
- Munsell Book of Colors (1929). Munsell Coloration Corporation.
- Murr, L. E. (1973). Ordered lattice defects in colored fluorite: direct observations. *Science*, Vol. 183, p. 206.
- Murr, L. E. (1974a). Transmission electron microscope study of crystal defects in natural fluorite. *Phys. Stat. Sol. (A)*, Vol. 22, p. 239.
- Murr, L. E. (1974b). Void superlattices in fluorite. Diffraction studies of real atoms and real crystals. Australian Academy of Science, p. 167.
- Murr, L. E. (1976). Void-lattice formation in natural fluorite by electron irradiation. 34th Ann. Proc. Electron Microscopy Soc. Amer., p. 614.
- O'Connor, J. R. and Chen, J. H. (1963). Color centers in alkali-earth fluorides. *Phys. Rev.*, Vol. 130, p. 1790.

- Phillips, J. C. (1970). Rev. Mod. Phys., Vol. 42, p. 317 in Hayes, W. (1974). Crystals with the fluorite structure.
- Phillips, W. and Duncan, Jr., R. C. (1971). Preparation of photochromic calcium fluoride by additive coloration. Metallurgical Transactions., Vol. 2, p. 769.
- Ramachandran, G. N. (1947). Thermo-optic behavior of solids. III. Flourspar. Proc. Indian Acad. Sci., 25A, p. 286.
- Rao, D. R. and Bose, H. N. (1970). Coloration of fluorite by low energy electrons. J. Phy. Soc. Japan, Vol. 28, p. 152.
- Ratnam, V. V. (1966). On the color centers and x-ray luminescence of calcium fluoride crystals. Phys. Stat. Sol., Vol. 16, p. 559.
- Roach, R. and Senff, I. (1974). Sepctroscopic investigations of a new type of color centers in additively colored pure alkaline earth fluoride crystals. Phys. Stat. Sol. A., Vol. 26, p. 537.
- Rubloff, G. W. (1972). Far Ultraviolet reflectance spectra and the electronic structure of ionic crystals. Phys. Rev. B., Vol. 5, p. 662.
- Sashital, S. R. and Vedam, K. (1973). Growth of color centers and hardening of CaF_2 by heavy dose of γ irradiation. Phys. Stat. Sol., Vol. 19, p. 625.
- Scouler, W. J. and Smakula, A. (1960). Coloration of pure and doped calcium fluoride crystals at 20°C and -190°C . Phys. Rev., Vol. 120, p. 1154.
- Schulman, J. H., Ginther, R. J. and Kirk, R. D. (1952). Enhancement of x-ray induced absorption band in alkaline earth compounds. J. Chem. Phys., Vol. 20, p. 1966.

- Smakula, A. (1950). Color centers in calcium fluoride and barium fluoride crystals. *Phy. Rev.*, Vol. 77, p. 408.
- Smakula, A. (1953). Bleaching of CaF_2 crystals colored by x-rays. *Phys. Rev.* Vol. 91, p. 1570.
- Staebler, D. L. and Kiss, Z. J. (1969). Photo-reversible charge transfer in rare-earth doped CaF_2 . *Ap. Phys. Letters*, Vol. 14, p. 93.
- Staebler, D. L. and Schnatterly, S. E. (1971). Optical studies of a photochromic color center in rare-earth-doped CaF_2 . *Phys. Rev. B*, Vol. 3, p. 516.
- Stockbarger, D. C. (1949). Artificial fluorite. *J. Opt. Soc. Am.*, Vol. 39, p. 731.
- Theissing, H. N., Ewanizky, T. F., Caplain, P. C. and Grosse, D. W. (1969). Y^{+2} as color center in irradiated CaF_2 . *J. Chem. Phys.*, Vol. 50, p. 2657.
- Tittley, S. R. and Damon, P. E. (1962). Investigation of color centers in fluorites with application to geological time. *J. Geophy. Research*, Vol. 67, p. 4492.
- Van Alstine, R. E. (1961). Investigation of the principal fluorspar districts of Mexico U.S.G.S. proj. Pap. 424-C, G. S. Research, p. C-212.

This dissertation is accepted on behalf of the faculty of the
Institute by the following committee:

Richard E. Beane
Adviser

L. S. Moore

Carl J. Papp

10 May, 1977
Date